Spectroscopic Investigation of Alcohol-Chlorinated Methane Synergistic Binary Solvent Mixtures and its Application

A Thesis Submitted
in Partial Fulfillment of the Requirements
for the Degree of

Doctor of Philosophy

by

Shradhey Gupta

Department of Chemistry

Indian Institute of Technology Kanpur, India

October 2014

STATEMENT

I, **Shradhey Gupta**, hereby declare that the matter manifested in this thesis entitled "**Spectroscopic Investigation of Alcohol-Chlorinated Methane Synergistic Binary Solvent Mixtures and its Application**" is the result of research carried out by me in the Department of Chemistry, India Institute of Technology Kanpur, Kanpur, India under the supervision of **Dr. Pratik Sen**.

In keeping with general practice of reporting scientific observation, due acknowledgements have been made wherever the work described is based on the findings of other investigators.

Shradhey

October, 2014
IIT Kanpur

(Shradhey Gupta)

CERTIFICATE

It is certified that the work encapsulated in this thesis entitled, "**Spectroscopic Investigation of Alcohol-Chlorinated Methane Synergistic Binary Solvent Mixtures and its Application**" has been carried out by **Mr. Shradhey Gupta,** under my guidance and this work has not been submitted elsewhere for a degree.

Pratik Sen

(Dr. Pratik Sen)
Thesis Supervisor
Department of Chemistry
Indian Institute of Technology Kanpur
Kanpur - 208016, India

October, 2014
IIT Kanpur

DEPARTMENT OF CHEMISTRY
INDIAN INSTITUTE OF TECHNOLOGY

CERTIFICATE OF COURSE WORK

This is to certify that **Mr. Shradhey Gupta** has satisfactorily completed all the courses required for the Ph.D. degree. The courses include:

CHM 521	Mathematics for Chemistry
CHM 629	Principles of Physical Chemistry
CHM 636	Physical Photochemistry
CHM 650	Statistical Mechanics and its Applications to Chemistry
CHM 664	Modern Physical Methods in Chemistry
CHM 684	Computer Programming for Chemistry
CHM 799	Research
CHM 800	General Seminar
CHM 801	Graduate Seminar

Mr. Shradhey Gupta was admitted to the candidacy for the Ph.D. degree in February, 2011 after he successfully completed the written and oral qualifying examinations.

P. K. Bhattacharyya
Head
Department of Chemistry
Indian Institute of Technology Kanpur
Kanpur - 208016, India

29/11
Convener, DPGC
Department of Chemistry
Indian Institute of Technology Kanpur
Kanpur - 208016, India

P. K. Bhattacharyya
Professor & Head
Department of Chemistry
I.I.T. Kanpur-208 016 (India)

I lovingly dedicate this thesis to my Maa and family, who supported me in each step of my life....

Acknowlegements

It is my solemn pleasure to express my unpretentious, cordial and overwhelming gratitude to my thesis supervisor Dr. Pratik Sen *for being an excellent mentor, an abundant source of unstinting encouragement, inspiration and motivation. Since the moment I joined at IIT Kanpur, he hasn't only my research supervisor, but also a guardian with whom I have never experienced any hesitancy to share ideals and views in the perspectives of research. Also, his cordial mannerisms, incessant support, constant motivation and inspiration provides me perfect environment throughout my stay in the laboratory. His expertise and never ending patience taught me how to build independent research skills and deal with scientific problems. His constant encouragement motivated me to solve critical spectroscopic problem in spite of several difficulties and failures. The field of spectroscopy was a farfetched object at the moment when I joined this laboratory, but in due course of time it all looked unconcealed and clear, and this all happened because of the eager and ardent trustiness of my supervisor towards all of we labmates. To me, this journey of completion of dissertation with my mentor has been highly invigorating, filled with lots of good memories and will certainly help me in acheveing ture success in future. My special thanks are also due for Mrs. Manila Sen (Ma'am) for made a homely atmosphere while my long stay in IIT Kanpur. Lots of love is for their daughter Suchismita, whom I wish a very lovely and an incredibly bright future ahead.*

I offer my sincere thanks to Prof. P. Gupta-Bhaya, Prof. S. Manogaran, Prof. D. Goswami, Dr. M. Ranganathan and Dr. N. N. Nair for the highly informative and interesting courses they taught me as a part of my course work in the springhead of PhD program. My thanks are also due for Prof. K. Srihari, allowing me to attend his lectures whose all were very inspiring and motivating.

I express my special thanks to Prof. Keisuke Tominaga (Kobe University, Japan) for collaborative work and for letting me use his lab facilities. I also thank Prof. S. R. Gadre for fruitful discussions that is manifested in this thesis.

I extend my warm gratitude towards the Department of Chemistry, IIT Kanpur for making me an important part of it, and its student community which has always made me feel exhilarated. Thanks are due to former and present (Prof. P. K. Bharadwaj) Heads of Department. Our office staff specially Sudha madam and Geeta madam honestly deserves a whelming acknowledgement for being very cooperative and helpful whenever needed.

A sincere gratitude is due to the Department of Chemistry, Chhatrapati Shahuji Maharaj University, Kanpur from where I have earned my postgraduate degree. I would like to thank Dr. J. Daniel, Dr. Amir Srivastava, Dr. Sudha Agrawal, Dr. Nidhi Srivastava and Dr. D. K. Verma for being an excellent aspiration faculties who have always inspired me to pursue research as my career.

My life inside and out the lab has been never-to-be-forgotten experience alongside my colleagues, who have been all great companion. It was an absolute pleasure working with Shahnawaz and Rajeev who have helped me achieve the desired scrutiny and disquisition for my dissertation. Also, we enjoyed each other's accompany in all quarters while long stay especially during the lab build-up period. Likewise, my former and present lab mates Bhaswati, Gyanesh, Puspal, Vaisakh, Vipin, Naveen and Faizi have been very caring and loving and have made my long stay an unforgettable one. Due acknowledgement are to all the project students Shyamashis, Mainak, Soumen, Arghav, Nirmal, Snigdha, Sharmistha, Sunil and others who have worked in our lab since its initial phase.

Since the day I entered IIT Kanpur, my life has been adored with the presence of many caring and affectionate friends. I thank Sumit Singhal, Akhilesh, Amit, Shahnawaz, Joydeb, Nityananda, Prosenjit, Ravi, Jhasaketan, Chetan, Keshav, Basanta, Rajeev, Musheer, Chandrajeet, Dhiman, Tushar, Arwind, Asif, Ashish, Akram, Rohan, Alok, Pardeep, Sibin, Ramu, Ashu, Pankaj, Archana, Sirshendu, Sarvesh, Rahul, Ruchi, Irshad and others for making my long stay very pleasant. Also, many friends (Feng Zhang, Alvin, Minako, Naoki, Neeraj, Yuuki) from Kobe univeristy, Japan alongwith Rajiv and Thangaraj deserve a very warm acknowledgement for sharing two important months with me and being me afterwards. I express my thanks to all my schooldays colleagues, close friends and batchmates (Prashant k. Singh, Prashant Gupta, Sarahna Mishra, Omkar, Shivam, Saurabh, Sumit, Arvind, Siddharth Kumar, Ajay Vaish, and others) who always used to embolden me alot and I always miss every cherishable moments spent with them all. I extend my warm gratitude all those people who are directly or indirectly attached with me.

I'm very grateful to Council of Scientific and Industrial Research (CSIR), India for financing fellowship and also to Research and Development section IIT Kanpur for their best cooperation.

I devout my thank to my parents, my sister (Roli Gupta), my brothers-in-law (Vikas Gupta) and one loving nephew (Rishi) for their never ending support, love, encouragement, for entrusting me and wishing all the best things in world and hence making this dissertation a

success. I would like to specially thank my Maa, who always been an abundant source of unstinting encouragement, inspiration and motivation for me since my childhood. She has always been a torch bearer in supporting me for my cause and emphasized me on being a good human besides a good researcher.

Finally, I would like to express my apology for those, whose feeling, I, hurt knowingly or unknowingly.

Shradhey Gupta

SYNOPSIS

Name of the Student	:	Shradhey Gupta
Roll Number	:	Y9107082
Degree for which submitted	:	Ph.D
Department	:	Chemistry
Thesis Supervisor	:	Dr. Pratik Sen
Thesis Title	:	Spectroscopic Investigation of Alcohol-Chlorinated Methane Synergistic Binary Solvent Mixtures and its Application
Month and Year of Thesis Submission	:	October, 2014

This thesis substantially outlines the genesis of synergistic behavior in alcohol-chlorinated methane binary solvent mixtures, by using steady-state, ultrafast spectroscopic methods and analytical models. Usually, the impact of pure or mixed solvents on spectra of the chromophoric dyes is termed as solvatochromism which is by virtue of the solute/solvent nonspecific and specific interactions, comprising dipole/dipole, dipole-induced/dipole, dispersion interactions, and hydrogen bonding. An emphasis has been given here to understand the symptoms of solvent-solvent interactions which occurs in mixed solvent system, where probe molecules are used to examine their inscrutable molecular interactions, since, their solution in mixed solvent have a distinct and vivid spectroscopic evidence compare to pure solvent cases. Further, the study of the binary solvent mixture shed light on the relative importance of the solvation mechanism in different physical processes. Conclusively, the pioneer theme of this dissertation is to understand the nature of solvation and the role of molecular interactions among different solvent components along with their effects on photo-physical processes such as photo-induced electron transfer, solvation dyanmics and chemical kinetics, and also to establish that the intermolecular solvent association plays a pivotal role in mixed solvent chemistry which demonstrates improvement in product yield and affects the rate of chemical processes. This clearly is an offbeat approach in solvation chemistry and has also reasonably intensified the importance of binary solvent mixtures in green chemistry.

Summary of the Work Done

(a) Spectroscopic Evidence of Synergism in Binary Solvent Mixtures

Properties of solvent mixtures often differ from that of pure solvent systems because of the non-ideal nature of solutions. However, sometimes specific interactions amongst the different solvent components lead to strong synergistic change is the properties of the mixture, which is very different from pure solvent cases. We have studied a few such systems made of hydrogen bond donating and accepting solvent pairs. It has been observed that the static solvation of a molecule in various alcohol (e.g. methanol (MeOH), *tert*-buthanol (*t*-BuOH)) – chlorinated methane (i.e. chloroform ($CHCl_3$), dichloromethane (CH_2Cl_2 or DCM)) binary solvent mixtures show a strong synergistic behavior, which is explained in the backdrop of hydrogen bond mediated solvent–solvent interactions. Proton NMR analysis, molar refractivity, solvent exchange model and fluorescence quenching suggested that the maximum extent of hydrogen-bonding interactions prevails at different composition of the different solvent mixture. The solvation behavior of MeOH–$CHCl_3$ mixture also shows probe dependence with no synergism observed in *p*-nitroaniline. Interestingly, the strong synergistic signature observed through spectrophotometric measurement is absent when studied by fluorescence spectroscopy. Following these experiment, it has been concluded that the strength of solvent-solvent interactions are weak in nature. Analysis of ^{1}H-NMR of MeOH-$CHCl_3$ binary solvent mixture indicated the existence of solvent association in the stoichiometric ratio of 1:2.15, while in other MeOH-DCM and *t*-BuOH-DCM mixed solvent systems, the ratio has been observed to be 1:1.33 and 1:1.12 respectively. Further, the solvent exchange model has been formulated to determine the feasibility of synergistic behavior and also polarity parameter of the mixed solvent structure of alcohols-chlorinated methanes binary solvent mixtures.

(b) Dynamics in MeOH-$CHCl_3$ Binary Solvent Mixture

This work aims at elucidating the mechanism of solvation of 4-(dicyanomethylene)-2-methyl-6-(4-dimethylaminostyryl)-*4H*-pyran (pyran dye) in different composition of MeOH-$CHCl_3$ binary solvent mixture using femtosecond transient absorption pump-probe spectroscpic technique. Also, this study abundantly supplies information about the intermediary

response between the ground state and excited state. Unprecedented slowdown of solvation time of pyran dye is probably due to the slow diffusion of solvent molecules in the MeOH-$CHCl_3$ mixture-rich first solvation shell followed by hydrogen bond solvent-solvent rearrangements around the solute dipole. On the other hand, fast solvation of pyran molecule occurs by the fast reorganization dynamics of pure solvents (i.e. Methanol and chloroform) around the solute dipole. Interestingly, a remarkable solvent polarity dependency in solvation dynamics was observed in the case of MeOH-$CHCl_3$ binary solvent rather than pure solvents and achieved slower solvent dynamics at the point where E_T shift is observed highest, termed as synergistic effect. Overall interactions present within the MeOH and $CHCl_3$ binary solvent mixture furnishes a clear evidence of solvent association interplay aspect of weak hydrogen bonding.

(c) Photo-induced Electron Transfer Process in MeOH-CH_2Cl_2 Solvent Mixture

The origin of ground state synergism in MeOH-DCM binary solvent mixture is explained in the frame of solvent-solvent interactions through UV-vis absorption, ^{1}H-NMR study, molar refractivity measurement and solvent exchange model in chapter 3. The study of photo-induced electron transfer (PET) process in MeOH-DCM binary solvent mixture infers that the intermolecular solvent association is responsible for such synergistic effect in the MeOH-DCM mixture. A slow solvation in mixed solvent environment gives rise to higher degree of reorganization of reactant molecules before PET reaction. In the binary mixture with $X_{MeOH} = 0.40$, we have observed the lowest rate of PET (k_{et}) with highest reorganization energy (λ_s), as predicted from the observed highest synergistic effect. In the presence of extended hydrogen-bonding network structure, the binary solvent system enforces slowing down of the rate of diffusion of reactant molecules which hinder the formation of encounter complex and consequently lowers the rate of PET process.

(d) Facile Reaction in *t*-BuOH-CH_2Cl_2 Binary Solvent Mixture

A remark of ground state synergetic behaviour in *t*-BuOH-DCM binary solvent mixture was observed in steady state UV-visible absorption measurement by using solvatochromic probe and accounts the solvent-solvent specific interactions led by weak hydrogen bond networking, which has been confirmed by proton NMR in chapter 3. Also, the feasibility of the synergistic nature in mixed solvent system has been verified by solvent exchange model. These aspects suggested that the intermolecular association and polarity of the binary solvent

mixture must accelerate chemical reaction that goes through the polar transient state. The unique mixed solvent environment results lower rate of photo-decolourization of merocyanine compound compared to the bulk solvents, and is explained by the extended intermolecular hydrogen bond networking. Additionally, we observed that the solvent mixture of particular proportion at which maximum synergism is observed acts as an ideal medium for the efficient solubilization of TetMe-IBX reagent and increases the yield of oxidation reaction 4 times as compared to that in *t*-BuOH. Hence the binary solvent mixtures may provide platform for reactions to proceed at faster rates with higher yields. Present study apparently established that the intermolecular association plays a deciding role in the binary solvent mixture to show an improvement in product yield and effects the rate of chemical processes, which is due to the synergistic effect. This clearly is a greener approach with intensified application in chemistry.

(e) Concluding Remarks Future Outlook

In this part, we summarizes over all the work presented above and draws on the future possible research directions from this thesis.

Table of contents

Synopsis **ix**

Table of contents **xiii**

Thesis Outline **xvi**

1 Solvation: An Overview **1**

1.1 Introduction 3

1.2 Theory of Solvation 3

1.3 Theory of Solvent Effects on UV/Vis Absorption Spectra 6

1.4 The Nature of Binary Solvent Mixture 8

1.5 Behaviour of Interactive Solvents in Electronic Transition 10

1.6 Type of Solvation 12

1.6.1 Preferential Solvation 12

1.6.2 Synergistic Solvation 13

1.7 Overview of Alcohol-Chlorinated Methane Mixtures studies 14

1.8 Objective of Work 16

2 Experimental Methodologies & Analytical Models **17**

2.1 Experimental Methodologies 19

2.1.1 Steady State Measurements 19

2.1.2 Time Resolved Spectroscopic Techniques 19

2.2 Analytical Models 33

2.2.1 Proton-NMR Study of Protonated AH-BH Solvent Mixture 33

2.2.2 Solvent Exchange Model for AH-BH Binary Solvent Mixture . . . 36

3 Spectroscopic Evidence of Synergism in Binary Solvent Mixtures 43
3.1 Introduction . . . 45
3.2 Results and Discussion . . . 47
3.2.1 Absorption and Emission Study in Different Binary Solvent Mixtures 47
3.2.2 Molar Refractivity Measurements . . . 56
3.2.3 Proton-NMR Study of Binary Solvent Mixtures . . . 57
3.2.4 Solvent Exchange Model for Binary Solvent Mixtures . . . 65
3.2.5 Fluorescence Quenching in MeOH-$CHCl_3$ Binary Solvent Mixture 71
3.3 Conclusion . . . 72

4 Dynamics in MeOH-$CHCl_3$ Binary Solvent Mixture 75
4.1 Introduction . . . 77
4.2 Results and Discussion . . . 78
4.2.1 Steady State Absorption and Emission Spectra in MeOH-$CHCl_3$ Binary Solvent Mixture . . . 78
4.2.2 Solvation Dynamics Study in MeOH-$CHCl_3$ Solvent Mixture . . . 82
4.3 Conclusion . . . 86

5 Photo-induced Electron Transfer Process in MeOH-CH_2Cl_2 Solvent Mixture 89
5.1 Introduction . . . 91
5.2 Results and Discussion . . . 93
5.2.1 Electron Transfer in MeOH-DCM Binary Mixture . . . 93
5.3 Conclusion . . . 102

6 Facile Reaction in *t*-BuOH-CH_2Cl_2 Binary Solvent Mixture 103
6.1 Introduction . . . 105
6.2 Results and Discussion . . . 107
6.2.1 Photo-decolourization of BIPS-NO_2 in *t*-BuOH-DCM Binary Solvent Mixture . . . 107
6.2.2 Green Chemistry approach in *t*-BuOH-DCM Binary Solvent Mixture 109
6.3 Conclusion . . . 110

7 Concluding Remarks & Future Outlook 111
7.1 Conclusion of the Thesis chapters . . . 113
7.1.1 Chapter 1 . . . 113

7.1.2 Chapter 2 113
7.1.3 Chapter 3 114
7.1.4 Chapter 4 114
7.1.5 Chapter 5 115
7.1.6 Chapter 6 116
7.2 Discussion 117
7.2.1 Contributions of Thesis 117
7.2.2 Limitations of Thesis 117
7.3 Future outlook 118

List of Publications **139**

THESIS OUTLINE

All the details of thesis is splitted into following chapters

Chapter 1.

This chapter comprehensively describes the basic approach of solvation of solute/probe molecule in pure/binary solvent systems and also explains the consequence of solvation on the electronic transition of solvatochromic molecules. At the end of prologue is presented in detail, the appearance two distinguished solvation phenomenon in binary solvent mixture investigates through spectroscopic and analytical methods.

Chapter 2.

This chapter basically throws light on the different experimentals and also analytical methods which explore the appearance distinguished solvation in binary solvent systems and their consequence on photo-physical processes.

Chapter 3.

This chapter describes preliminary interpretation of permanence of synergistic solvation in steady state absorption study of three distinct binary solvent systems (i.e. MeOH-$CHCl_3$, MeOH-DCM, and *t*-BuOH-DCM) and also examine same phenomenon through ^{1}H-NMR analysis, solvent exchange model and fluorescence quenching study, however, such solvation phenomenon was found absent in MeOH-CCl_4 binary solvent mixture. In continuation, we also discussed the impact of other factors over synergistic solvation exclusively.

Chapter 4.

In this chapter, we have discussed, here, the solvent polarity dependent solvation dynamics of Pyran dye by using femtosecond transient absorption spectroscopy and also filled the gap between the ground state and excited state response in MeOH-$CHCl_3$ binary solvent system. An effectiveness of polarity results slower dynamics in mixture compared to pure solvent cases.

Chapter 5.

This chapter reports the spectroscopic evidence of the presence of Marcus inverted region in MeOH-DCM binary solvent mixture. The unique mixed solvent environment gives rise to higher degree of solvent reorganization energy and lower rate compared to the pure solvent case.

Chapter 6.

This chapter clearly enunciated the role of solvent polarity in *t*-BuOH-DCM mixed solvents on kinetics of photo-chemical reaction and also intensified greener application of binary solvent mixture in chemistry.

Chapter 7.

This chapter summarizes overall conclusion of all chapters and draws on the future aspects and possibilities of research outlook from this thesis.

1

Solvation: An Overview

1.1 Introduction

An enormous application of spectroscopic techniques towards the understanding of chemical, physical and biological processes has been witnessed in the last several decades.[1–11] Often, the properties of pure condensed phases were investigated spectroscopically with great details.[7–11] However, the nature of mixed solvent systems was not thoroughly studied in the literature.[12–24] Despite of thermodynamic awareness of the solvent mixtures[25–37], our understanding remains rather circumscribed in regards to the how(s) and why(s) static and dynamic properties of solvent mixture differ from their pure solvents. The static and dynamic properties of solvent mixture give an elementary insight at the molecular level and one can indeed begin to speculate the structure of network that persist in the mixed state of solvents. Additionally, it is imperative to let in time dependent behaviour of solvent mixture (solvent dynamics) into the interactive network paradigm in order to better understand how mixed solvents structures come into action. The dynamical nature of solvent mixtures is a comparatively complex process compared to pure solvent cases and evolves multidimensional distinguished interactions over a wide range of time and space. The advancement in the spectroscopic techniques has brought more attention on solvation chemistry recently, with solvent mixtures being of great concern for theoreticians and experimentalists.[38–49] Varying the solvent mixture composition immediately affects the microscopic structure of solvent mixture, causing the influence on chemical or photochemical reactivity, the reaction rate, and yield, sometimes efficaciously. Physical chemists are always inquisitive about why and how solvent mixture changes the colour of a solvatochromic/dye molecule. The spectroscopic techniques are quite auxiliary for answering such questions. Answering such substantial issues in physical chemistry requires a characterization of solvent mixtures with molecular specificity. The spectroscopic characterization of a binary solvent replies multidimensional molecular interactions and also satisfies present demands of research purposes.

1.2 Theory of Solvation

The term solvation is explicably defined in many literatures, and books in its more colloquial sense.[50–61] From the statistical thermodynamic view point, the solvation is defined as a physical process of a particle (atom, ion or molecule) moving from a fixed position of an ideal gas phase to a fixed new position in the condense or solvent state, where the moiety is being solvated by the surrounding solvent molecules.[50,51,56,59] This solute molecule may even be considered similar as solvent molecules itself, with the entire phenomenon being a condensation process from the vapor state. Mostly, solvents are pure

liquids, or a mixture of some liquids. In short, solvation may be defined the process of interactions of the solvated particle with the surrounding solvent molecules. The whole process of solvation is exempted from translational degrees of freedom of solute particle. Thus the solute particle occupies a different volume in liquid state. With this convention, we take care of different standard states and various concentration scales of solute particle in liquid or mixed solvent state.[50–56] Hence, the thermodynamics of the solvation process may completely relevant to

1. The primary interactions of solute particle with its surrounding environment in the solvent state, which is completely deprived of an ideal gas phase.
2. The initiation of solvent effects induced by the effect of solute particle on its surrounding environment.
3. The molecular interactions that occur between solute particles and surrounding solvent molecules cause the change in its internal degree of freedom.

Under the thought process, the solvation of a particle (atom, ion or molecule) in any solvent or solvent mixture may proceed in the following virtual steps.[50–56]

1. The solute particle generates the cavity of an appropriate size and shape to accommodate it in the solvent environment.
2. The cavity is occupied by the solute particle, without having any interaction with its surroundings.
3. In the cavity, solute particle reaches its equilibrium state in the solution by mean of change in polarization and molecular configuration.
4. The surrounding solvent molecules around the solute particle commutates through dispersion and dipole-induced dipole or dipole-dipole interactions.
5. The molecules of solvent or solvent mixture adjacent to the solute particle, in their midst start adjusting themselves.

Indeed, all these steps occur simultaneously, but thermodynamically, it may be thought of as being separated and considered to be additive, as shown in Fig. 1.1.

Most common factor of solvent effects depends upon the distance between the solute and solvent molecules.[50–56,58–61] Some interactions or effects are considered to be long range, if the solvent is a solution containing ions. The columbic interactions generally act on longer ranges and admit as a stronger in nature than those developing from dispersion alone. The energies of columbic interactions (ion-ion and ion-dipole interactions) depend on $\frac{1}{r}$ and $\frac{1}{r^2}$,

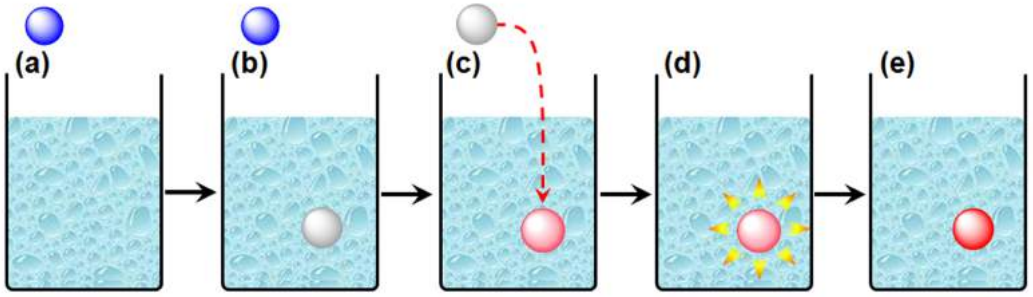

Fig. 1.1

Schematic representation of process of solvation, (a) solute particle (blue circle) present in an ideal gas phase, (b) solute shaped cavity in gas phase is induced in the solvent, (c) the solute charge density is placed in the solute cavity, (d) solvent molecules start to reorient and polarize in response to the solute charge density, (e) the solute particle is solvated by solvent molecules.

respectively. On the other hand, there are number of interactions (like dipole-dipole, dipole-induced dipole and dispersive interactions), which actually work at very short distances with energies expected to be a function of $\frac{1}{r^3}$, $\frac{1}{r^4}$, and $\frac{1}{r^6}$ respectively.

Plenteous models, theories and computational strategies have been developed by theoretical chemists over many years.[50–61] Most studies furnish better understanding to the complex phenomenon of solvation. Altogether, there are three common approaches available which may be used for the theoretical descriptions of solute-solvent interactions;

1. When the solvent is dealt as a continuous and homogeneous medium (or structureless). The solute particle is surrounded by structureless media, characterized solely by its relative permittivity(ε_r). The solvated solute (ion, atom or molecule) induces polarization effects on the environment of surrounding continuous media that successively furnish an additional electric field in the vicinity of the solute, which is recognized by quantum-chemical continuum models and also called (Onsager) reaction fields.[61–63]
2. Supramolecular models treat solvent media and solute, both as discrete particle in an ensemble of solute and solvent molecules by using Monte Carlo statistical mechanics or molecular dynamics methods.[61,64,65]
3. When the direct electrostatic solute/solvent interactions are calculated quantum mechanically within the first solvation shell and remaining position or part of solvent media retains the reaction field contribution, such a model underlies semicontinuum quantum-chemical models.[61,66–68]

From last few decades, much progress has been consecrated to remove their limitations and flaws in the theoretical description of solvation by introducing new ideas and views. The recent computational compilation approaches are (a) implicit solvation models, (b) micro-solvation models and (c) hybrid solvation models.[61,69]

1.3 Theory of Solvent Effects on UV/Vis Absorption Spectra

The process of solvation in liquid medium has been well established, where the solute particles dissolved in any solvent experiences intermolecular force/interactions with the surrounding solvent molecules. Consequently, the electronic absorption transition of the solute molecules will change more or less, depending on the type of molecular interaction with the surrounding environment. Hence, the electronic transition of solutes in solvent media is somewhat unlike that of solutes in the gas phase state.

It is obvious now that the characteristics of the molecular electronic state such as electron distribution, dipole moment, and spatial configuration changes when electronic transition occurs between two electronic states. In general say, the solute-solvent interaction efficiency must bring the change in the molecular electronic transition between the two electronic states. As a consequence of solvent effect on electronic transition, the band position, band shape, and intensity of spectra in solution is not the same as those of a free solute in the vapor phase. Therefore, effect of solvents on the spectra of a solute molecule was thoroughly discussed in the details by former studies.[70–79] Most of the research groups have adopted the fundamental ideas of Onsager reaction field, which can be used in order to shed light on molecular interactions due to solvation.[72–79] Under this reaction field, the solute particle is reduced to a point dipole at the centre of a spherical cavity dissolved in a homogenous solvent media which acts as an effective electric field on the solute particles.[70,73,74] McRae[73,74] has defined this electric field in terms of the reaction field (R) and the magnitude of the reaction field relates to inductive and orientation polarizations of homogenous solvent dielectric owing to the solute dipole (μ). The polarizing molecule generates the reaction field (R) in solvent dielectric, is formulated as

$$R = \frac{2\mu}{a^3}\left(\frac{\varepsilon - 1}{\varepsilon + 2}\right) \tag{1.1}$$

where μ, ε and a are the dipole moment, static dielectric constant, and cavity radius of the solute molecule, respectively. Additionally, the reaction field also arises due to the inductive polarization, expressed similar as equation 1.1, but the term ε replaced by n^2, which is the

optical dielectric constant.

$$R = \frac{2\mu}{a^3}\left(\frac{n^2-1}{n^2+2}\right) \tag{1.2}$$

In the case of polar solvent, there involves an extra reaction field term owing to both the electrostatic (ε) and inductive (n^2) polarizations, called orientation polarization (R_{or}) and is expressed as

$$R = \frac{2\mu}{a^3}\left(\frac{\varepsilon-1}{\varepsilon+2} - \frac{n^2-1}{n^2+2}\right) \tag{1.3}$$

It is important to note that solvent orientation around the solute molecule at excited state (Franck-Condon state) is assumed to be the same contribution as that in the ground equilibrium state in the case of absorption spectra.

In the presence of radiation field, the transition dipole induced in the molecule and is stabilized by the reaction field of solvent molecules which sieges the solute, as a result, induced the change in absorption spectrum of free solute in the vapor phase. As a consequence, the solvent effect causes a shift in absorption band towards the red side of spectrum, which strongly depends on polarity of the solvent as shown in Fig. 1.2. In other words, the favorable intermolecular interaction between the solute and solvent media leads the low energy transition induced in the solute molecule and appear as a red shifted absorption spectrum. Therefore, the sensitivity of solute molecule depends on the polarity of the solvent. It is expressed in term of energy of absorption, and is given by

$$\begin{aligned}\Delta E - \Delta E_{ref} = {} & \frac{(\mu_{00})^2 - (\mu_{ii})^2}{a^3}\left[\frac{n^2-1}{2n^2+2}\right] \\ & + 2\frac{((\mu_{00}) - (\mu_{ii}))\mu_{ii}}{a^3}\left[\frac{\varepsilon-1}{\varepsilon+2} - \frac{n^2-1}{n^2+2}\right]\end{aligned} \tag{1.4}$$

where ΔE_{ref}, μ_{00} and μ_{ii} represent the energy or frequency shift induced by a non-polar reference solvent or vacuum, ground and excited state dipole moment of solute molecule solvated by solvent molecules, respectively. Other terms have usual meaning described earlier.

In short, it is commonly stated in the literatures[70,75–79] that solvent molecules near the dipolar solute molecules are organized, and as a result, brought the shift in the absorption spectra of solute molecules which indicates that this phenomenon could possibly be used to quantitative measurement of the solvent or solvent mixture polarity.

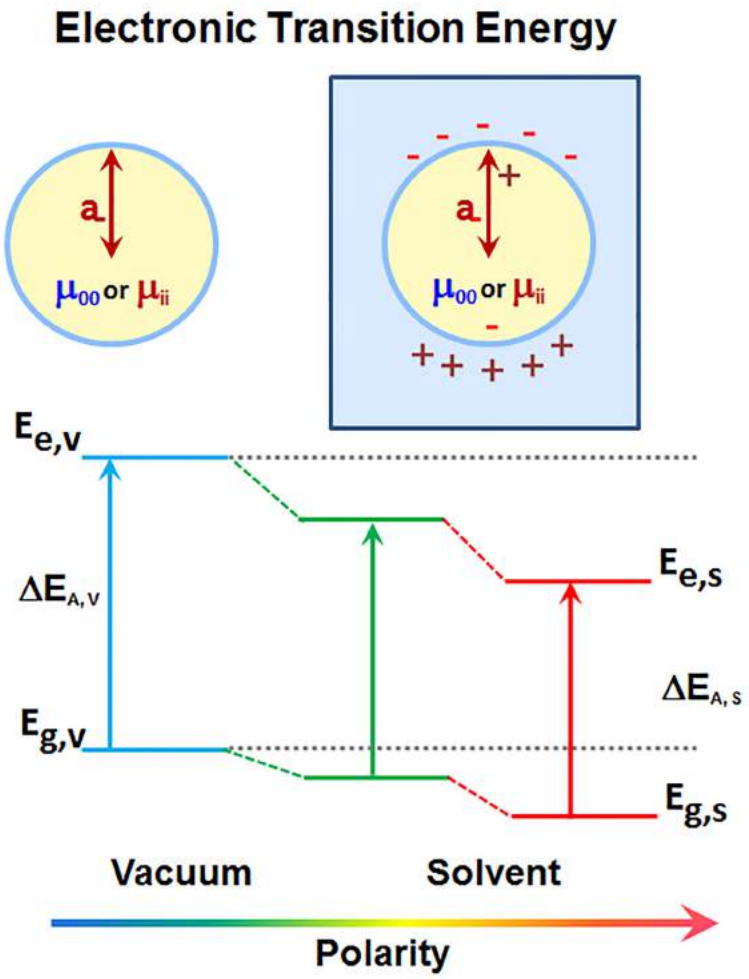

Fig. 1.2

Schematic qualitative representation of solvent effects on the electronic transition energy of dipolar solute in vacuum and solvents with increasing polarity. μ_{00} and μ_{ii}, are the dipole of the ground state and excited of the solute. E_{gs} and E_{es} are the energies of molecule in ground and excited states (in case of vacuum and solvent) and $\Delta E_{A,v}$ and $\Delta E_{A,s}$ are the absorption transition energies in vacuum and solvents, respectively.

1.4 The Nature of Binary Solvent Mixture

It has been briefly discussed in literature how the nature of solvents influence the physical properties of solute molecules.[60,61,70,80–84] At the same time, there have been many instances in the past where many groups looked into the nature of binary mixture, as a solution. Conversely, major challenges in the study of binary solvent mixture have always been the determination of mutual intermolecular interactions, association or aggregation and specific solvent structuring amongst different solvent pairs and remains as a current research interest.

Binary mixtures of different solvent pairs have been extensively studied in the past and motivated to discuss the equilibrium properties of liquid mixtures. In several experiments on liquid mixtures, it has established that the ideal or non-ideal behavior of liquid mixture in term of partial vapor pressure. The ratio of the partial vapor pressure of each component to its vapor pressure as a pure liquid is approximately equal to the mole function of the liquid mixture is termed as an ideal solution, and this is established as rule recognized as Raoult's law.[80–90]

$$p_{S_2} = X_{S_2} p^*_{S_2} \tag{1.5}$$

where p_{S_2} and $p^*_{S_2}$ are, respectively, the partial and total vapor pressure of solvent S_2 and X_{S_2} is the mole fraction of solvent in liquid mixture.

There are some solutions that departed noticeably from the Raoult's law as shown in Fig. 1.3, called non-ideal solution or real solution. In other words, if the measured property of

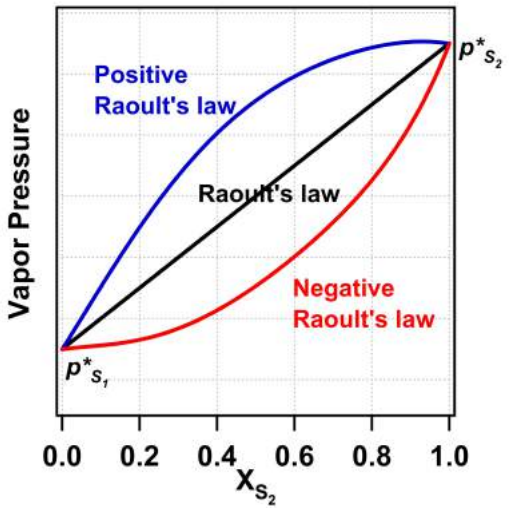

Fig. 1.3

Schematic representation of positive and negative deviation from Raoult's law.

liquids mixture depends nonlinearly on the local composition of solvent component, such nonlinearity behavior is known as Non-Raoult's variation and is of two types. When the vapor pressure of a solvent mixture is lower than that predicted by Raoult's law, this is known to be a negative deviation. Such nonlinearity behavior is a property of mixture composition and degree of association. This testifies that the adhesive forces between different components of mixed liquid are expected to be stronger than the average cohesive forces among the same components of liquid. In the wake of this, each component is held in the liquid phase

by attractive forces which are found to be stronger than in the pure solvent case so that its partial vapor pressure is lower. On the contrary, if the average cohesive forces amongst same molecules of solvent are expected to be greater than the adhesive forces, the dissimilar nature makes both solvent components immiscible in a mixed state. Hence, the vapor pressure would be higher than expected from the Raoult's law, exhibiting the positive deviation. Nonlinearity in liquid mixture is evidence to distinct molecular environments in the mixture compared to its pure case. This detailed study has been extended to explain the solvent mixture properties like the degree of molecular association or aggregation and specific solvent structure.

1.5 Behaviour of Interactive Solvents in Electronic Transition

The physical and thermodynamical properties of many solvent have been well known and extensively studied. Such a particular knowledge suggests that the organization of solvent molecules around the solute constitutes low entropy structures or cages. Under such circumstances, the adjustment of solvent structure changes the physical properties of the solute (such as electronic transition probability), sometime, to a greater degree than expected. Although, there are many studies on the effect of pure solvent structure around the solute cage, as far as we know, the composition in the neighborhood of the indicator solute in binary solvent mixture may, however differ from the pure solvent cases and the proper awareness of the microscopic solvent structure of a binary solvent system being involved in solvation has been found delimited. In this part, we setup equations that relate the behavior of solute or solvatochromic indicators with the composition of binary solvent mixtures. These equations take into account the effect of solvent-solvent interaction on the electronic transition probability of solvatochromic indicator. In other words, the equilibrium composition of binary solvent mixture in the immediate vicinity of indicator solute molecule will be determined by the criterion of modification in electronic transition probability of the solute molecule. In a mixing of molecules of solvent A and B, the interactions amongst unlike neighbors (U_{AB}) and like neighbors U_{AA} and U_{BB} must be of the same average strength and the longer-range interactions must be considered almost zero. If the intermolecular forces are considered to be same between AA, AB and BB, i.e. $U_{AB} = U_{AA} = U_{BB}$, then the mixture is automatically known as ideal mixture. For an ideal behaved solvation, the electronic transition probability of solute indicator in a binary solvent mixture is not only the function of inductive and orientation polarizations of a particular solvent as earlier discussed, but also depends on the mole fraction of solvent used in binary solvent system. Thus, the sensitivity of a solute molecule depends linearly on the polarity of the binary solvent mixture

where the mean strength of the interactions is the same between all the molecules of the mixture, is expressed in term of energy of absorption, is given by

$$\begin{aligned}\Delta E_{abs} = &\left[P\left(\frac{n^2-1}{2n^2+2}\right)+R\left(\frac{\varepsilon-1}{\varepsilon+2}-\frac{n^2-1}{n^2+2}\right)\right]X_A \\ &+\left[P\left(\frac{n^2-1}{2n^2+2}\right)+R\left(\frac{\varepsilon-1}{\varepsilon+2}-\frac{n^2-1}{n^2+2}\right)\right]X_B\end{aligned} \tag{1.6}$$

where $P=\frac{(\mu_{00})^2-(\mu_{ii})^2}{a^3}$ and $R=2\frac{((\mu_{00})-(\mu_{ii}))\mu_{ii}}{a^3}$ terms involved are discussed earlier. All terms involved in equation have their usual meaning as already described. X_A and X_B are a mole fraction of solvent A and B respectively. From this equation, it follows that in an ideal binary solvent mixture, the variation of as a function of mole fraction of any component should always be a linear dependence.

However, generally in most of the cases, the variation are not linear, which points toward the existence of some specific/nonspecific interactions between both components of solvent mixture. In other words, if the enthalpy of the mixture (or enthalpy of mixing) is nonzero, the nonzero enthalpy turns the solution to a non-ideal behaved mixture. More formally, for mingling of molecules of solvent A and B, the interactions amongst unlike neighbors (U_{AB}) must be different from average strength of like neighbors U_{AA} and U_{BB}. Additionally, the dissimilar behavior of solvent A and B cause the expected deviation from the ideality. Hence, the sensitivity of a solute molecule depends on the behavior of the binary solvent mixture and also involved the average interaction strength between all the molecules of the mixture, is expressed in term of energy of absorption, is given as

$$\begin{aligned}\Delta E_{abs} = &\left[P\left(\frac{n^2-1}{2n^2+2}\right)+R\left(\frac{\varepsilon-1}{\varepsilon+2}-\frac{n^2-1}{n^2+2}\right)\right]X_A \\ &+\left[P\left(\frac{n^2-1}{2n^2+2}\right)+R\left(\frac{\varepsilon-1}{\varepsilon+2}-\frac{n^2-1}{n^2+2}\right)\right]X_B \\ &+\left[P\left(\frac{n^2-1}{2n^2+2}\right)+R\left(\frac{\varepsilon-1}{\varepsilon+2}-\frac{n^2-1}{n^2+2}\right)\right]X_{AB}\end{aligned} \tag{1.7}$$

All terms have their usual meaning as described earlier. X_{AB} is the mole fraction of two different interactive solvent pairs. From the above equation, the variation of ΔE_{abs} as a function of mole fraction of any component of binary mixture may adopt a nonlinear nature. This reflects that solvent-solvent interactions in binary solvent mixtures are the main major factor based on the fact that one solvent component in a binary solvent mixture interacts with

another component either by specific interactions such as hydrogen bonding or nonspecific interactions. Such interactive solvent system or network alters the electronic structure and dipole moment of solute indicator.

1.6 Type of Solvation

In spite of considerable study into the nature of solvent-solvent interactions in binary solvent mixture at the molecular level, it still seems to be more intricate subject compared to the pure solvent. In a pure solvent case, the composition of the microsphere of solvation of a solute indicator called cybotactic region. However, the composition of the binary solvent mixture in this microsphere can be expected more complex. The degree of solvent-solvent interactions in solvent mixture may strongly or weakly affect the physical properties of a solute molecule, and this effect is directly reflected in the modification of the microsphere of solvation. Since, the solvatochromic solute indicator is used to study the solvent-solvent interactions, and the electron transition energy of the solute indicator counts on the microsphere of solvation composition and properties. Such a method is much more efficient to probe the information about mixed solvent properties like polarity and hydrogen bonding capabilities. The modification in solvent-solvent interactions by varying the composition of mixture of neat solvent to microsphere of solvation of a solute is therefore categorized into two parts.

1.6.1 Preferential Solvation

A prognostic description of solvation of solute indicator in solvent mixture is always found challenging and more complicated. In addition, the interactions amongst unlike solvent molecules play substantial role in the microsphere of solvation. This contributes to deviation from the ideal behaviour as predicted by Raoult's law of partial vapor pressure of the binary solvent mixture. Hence, the physical properties of solvent mixture can exhibit adequate and noticeable distinct when compared with their respective pure solvent components. From investigations, in some cases, there is an excess of one solvent component, leading to an inadequacy of the other solvent component in a binary solvent mixture in microsphere of solvation shell relative to the bulk composition, or one solvent component solvates the solute predominantly than the other. This is designated as "preferential solvation" or "selective solvation" as shown in Fig. 1.4a.[23] This is generally accompanied by more negative entropy of solvation.

Consider a solute molecule has some extent of similar characteristics to one component

of a solvent mixture. In normal condition, a molecule requires (a) a cavity to fit inside the mixed solvent atmosphere, (b) accommodating its configuration to have neighboring solvent molecules, (c) organize around a solvation shell and (d) affect interactions between the solvent molecules in its surroundings. The microscopic local environment of solute generates inhomogeneity in a multi-component solvent mixture, which is generally described as (i) specific solute/solvent interactions caused by hydrogen bonding (ii) nonspecific interaction such as dielectric enrichment in the solvation shell of a solute molecule. Besides, the redundancies and deficiencies of solvent molecules in a certain region of microsphere of solvation around a given solute indicator can be distinguished by structure determination methods such as X-ray or neutron diffraction, or the complete picture may be discerned by molecular dynamic (MD) simulation.

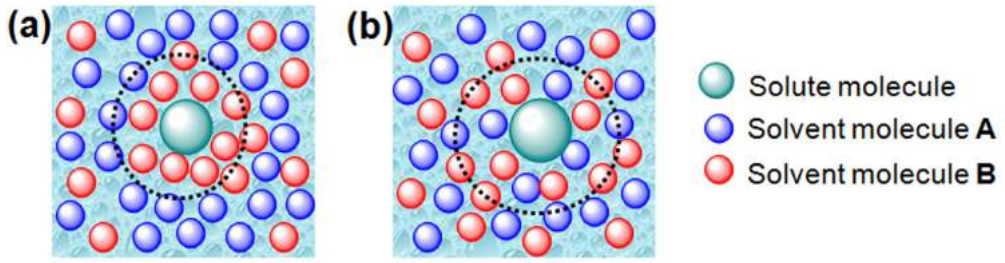

Fig. 1.4

Schematic representation of (a) preferential and (b) synergistic solvation in binary solvent system.

1.6.2 Synergistic Solvation

The modification of free energy of a solute molecule in the vicinity of solvent molecules is more chronic and cardinal problem in physical chemistry. As a result of most studies, the characterization of several modes of interactions of pure solvent with a solute molecule has been established, and the modifications in free energy of microscopic solvation shell reveals a linear dependence on the parameters being involved in different modes.[91–95] It has been cleared from studies that the solvent-solvent interactions play underlying role in the collective process of solvation. Moreover, there may be some possibilities of distinction in the characteristic of interactions of a solute molecule with two solvent components. These sophisticated possibilities may lead to preferential solvation of the solute molecule where the local composition of the solvation shell surrounding the solute molecule is distinct from the average solvent composition. In other words, there are always some possibilities

of a combined interaction of mixed solvent providing entirely distinct solvation, which is recognized as "synergistic solvation" or "cooperative solvation", as shown in Fig. 1.4b. The objective of the latest researches is to study solute-solvent and solvent-solvent interactions in a solution by mean of solute solubility.[91–95] Moreover, solvation in binary solvent mixture attributes to non-ideal behavior and solvent-solvent interaction plays a critical and a deterministic role in the solubility and the microscopic solvent structure situated around the solute molecule.[95]

For an interactive solvent mixtures, probing specific/nonspecific interactions are decisive for structural and dynamical aspects and also shed light on the nature of intermolecular association, which has not been well characterized and brought as a subject of research interest.

1.7 Overview of Alcohol-Chlorinated Methane Mixtures studies

The different binary solvent pairs of alcohols and chlorinated methanes have been widely and exclusively discussed often many times in many literatures. It exhibits a distinct microscopic environment in a solution resulting from specific interactions e.g. hydrogen bonding or from nonspecific interaction, such as dipole-dipole, dipole-induced dipole interactions leading to a unique property.

The nature of the environment and degree of associations in different solvent pairs has been investigated into a large extend through various thermodynamic and spectroscopic method. Singh *et al.*[96] determined the excess Gibbs free energy of mixing, G_E values, and excess enthaly of mixing, H_E values, which have been obtained from the measured vapor pressure of methanol-chloroform binary mixture. Additionally, the ideal associated model has been found to be suitable approach to describe the general behavior of H_E over the entire range of chloroform mole fraction in methanol-chloroform binary mixture. According to the analysis, the mixture has been characterized by the occurrence of different molecular associative species in solution state. Since, Tkadlecova *et al.*[97] gave tetramerization model and the reasonable agreement of this model accord with experiment data of ^{1}H NMR and the excess thermodynamic function of methanol-chloroform binary mixture and pointed to the high degree of organization that results from the formation of associated species in solution via H-bonding between acidic hydrogen in chloroform and the oxygen atom of methanol. The excess viscosities of a mixture of chloroform with different alcohols were measured at different temperature by Crabtree *et al.*[98] On the other hand, the endothermic heat of mixing at region of large chloroform mole fraction has been explained by break-

ing of hydrogen bonds between the alcohol molecules. Besides, in a low mole fraction of chloroform, the exothermic heat of mixing is due to the formation of ROH-$CHCl_3$ interaction. Sameti *et al.*[99] and Orchilles *et al.*[100] determined the excess thermodynamic parameters (the expansion coefficients ,and their excess values E, and isothermal coefficient of pressure excess molar enthalpy) and isobaric vapor-liquid and liquid-liquid equilibrium for alcohols-chlroform binary mixture. This study renders appropriate and reasonable agreement between theory and experiment. Also, some experimental observations of NMR and IR studies[101–103] in methanol-chlorinated methane solvent mixture were briefly discussed in terms of the predominance of hydrogen-bonded cluster or association of methanol molecules with chlorinated methane molecules. Interestingly, the estimated value of reorientation relaxation time and dispersion amplitudes in methanol-tetrachloromethane mixture indicates the strong hydrogen bonding interaction between the methanol molecules persisting even at low concentration of methanol, which were studied by dielectric relaxation spectra.[104] Similarly, the ultrafast infrared pump probe spectroscopy has been used to study hydroxyl stretch spectral diffusion, hydrogen bond dissociation, reformation, and vibrational relaxation in a mixed solution of methanol-h and methanol-d in CCl_4 by Fayer and coworkers.[105–107] The observed dynamics have been compared with the predictions of dielectric continuum theory. The direct relaxation of a vibrationally excited -OH stretch into H-bond stretch is responsible for H-bond breaking. From this study, it identified that both direct and indirect mechanisms for the H-bond dissociation give significant pathways for H-bond breaking and, as well as, both mechanisms take place after vibrational relaxation of the initially excited hydroxyl stretch. Also, it is clarified that the variety of H-bond breaking and reformation processes and time scales, which provides a significant understanding of the nature of molecular motion and couplings caused the H-bond breaking and reformation. Besides, the fluorescence dynamics of styrylthiazoloquinoxaline (STQ) in methanol-dichloromethane mixture shows an anomalous feature of an increasing fluorescence lifetime and silently points to the interaction between methanol and dichloromethane solvent molecules. Moreover, the solvent exchange model suggests changes in solvent composition around dye in the excited state study.[108] The carbon 1s photoelectron spectroscopy has been used to confirm the formation of mixed methanol-chloroform cluster in adiabatic expansion of the mixture azeotrope.[109] Lately, Bhattacharyya *et al.*[110] observed the thermal-lens signals as a function of relative proportions of binary solvent mixtures and suggested its dependence on the extent of interaction between different molecules present in a solvent mixture.

Additionally, a lot of work has also been carried out using simulation studies[109,111,112] and ab-initio calculations.[103,113] Kessler and coworkers,[111] on the basis of molecular dynamic simulations comfirmed molecular clustering effect or association in the methanol-chloroform solvent mixture. They also certified that such a mixture preferentially solvates the hydrophilic and hydrophobic parts of ampiphilic solutes. Durov *et al.*[113] figured out the excess thermo-dynamic functions and dielectric permittivity of methanol-chloroform mixture in the frame of the quasichemical model of non-ideal association solution and procreated the physicochemcial properties of the mixture to an extact precision. The framework of this model, based on supramolecular aggregate formation, suggested that deviation from ideality is preponderantly due to parallel orientation of dipoles in the methanol aggregates and in the complexes with chloroform. Bloch *et al.*[112] verified two simulation models and probed the structure and dynamics of methanol-carbon tetrachloride mixtures. These models were efficient to reproduce the experimental observation of a maximum in the rotational correlation time. The slow rotations at an intermediate methanol concentration led to an increase in the average lifetime of H-bonds which indicates the enhancement in H-bond strength inducing loose connection or network to the structure of the H-bonded liquid.

1.8 Objective of Work

Alcohols have its own importance in many chemical and biological systems and, in turn, their behaviour gives insight into H-bonding dynamics as found in water. A series of experiments[105–107] have been preformed lately to investigate the characteristics of the hydrogen bond network in the range of different systems, nevertheless, some of important features, like how the directionality or rotational mechanism of hydrogen bonds in liquid media remain elusive.

The following chapter will shed light on the nature of intermolecular interaction of different interacting solvent mixtures, which has not been characterized before and persisted as a subject of interest in this thesis. Exclusive role of syergistic solvation in deciding the fate of physical and the subsequent photochemical processes will be dicussed thoroughly throughout this thesis.

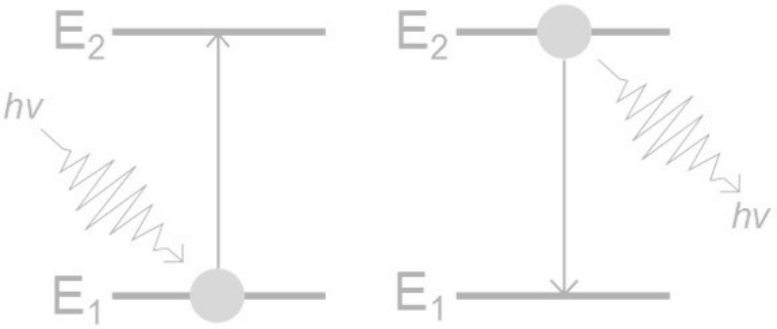

$$I(t) = \sum_i \alpha_i \exp(-t/\tau_i)$$

$$\frac{dx(t)}{dt} = Ax(t) + Bu(t) + Ew(t)$$

$$A = \log\left(\frac{I_0}{I}\right) = \ln 10 \ln\left(\frac{I_0}{I}\right) = \frac{x}{D} = x\frac{c}{\delta}$$

2

Experimental Methodologies & Analytical Models

This chapter drafts the experimental and analytical methods which have been used in carrying out the research work presented in this thesis. I will mainly focus to describe the fundamental theory, basic principles and the instrumental details of time resolved spectroscopic technique namely millisecond flash photolysis, time correlated single photon counting (TCSPC) and transient absorption. In this chapter, an analytical model for ^1H NMR measurements and different solvent exchange models are also discussed in detail.

2.1 Experimental Methodologies

2.1.1 Steady State Measurements

The steady state absorption spectra of solvatochromic dye in pure and mixed solvents were recorded in Schimadzu 2450 spectrophotometer. Steady state emission spectra were recorded in Shimadzu RF5301, FluoroLog 3-21, Jobin Yvon, and Fluoromax-4, Jobin Yvon spectrofluorimeter. The proton NMR spectra of all liquid samples were recorded by commercial spectrometer (JEOL ECX-500, Japan) operating at 500MHz. Tetramethylsilane was used as reference.

2.1.2 Time Resolved Spectroscopic Techniques

Time resolved spectroscopy (TRS) is the most exceptional physical method to study the dynamic processes in chemical substance or materials by means of spectroscopic techniques. In essence, the TRS techniques can be applied to map any physical or chemical process that leads to a change in properties of a sample. With the help of appropriate laser source, it is possible to trace distinct processes that occur in different time scales as femto to millisecond region. There are several TRS techniques such as millisecond flash photolysis, time-correlated single photon counting (TCSPC), fluorescence up-conversion, Streak camera, and transient absorption that can be used to monitor for different physical or photochemical ultrashort processes. These all TRS techniques often work at different time resolutions, time window and sensitivity. For a case, TCSPC has the time-resolution of the order of some few picoseconds (ps) to microsecond, Streak camera has the time-resolution of $\sim 1-5$ picoseconds (ps), fluorescence up-conversion and transient absorption has the similar order of time resolution i.e. the order of hundreds of femtoseconds (fs) which depends on type pulse laser used. For the present work, I have used millisecond flash photolysis, TCSPC and transient absorption technique.

(a) Millisecond Flash-Photolysis Measurements

In 1967, the Nobel Prize in chemistry was shared amongst Manfred Eigen, Ronald George, George Porter and Wreyford Norrish for their co-discovery of Flash Photolysis. Flash Photolysis is a time-resolved technique in which an absorption change is measured in response to an intense pulse of radiation, and used extensively to study photochemical processes that occur extremely straightaway.[114–117] It is the one of the most effective methods for studying by direct measurement the reactions of transient species, excited states or ions, in chemical and biological systems. Recently, flash photolysis has been

used progressively in the field of bioinorganic reaction mechanisms, such as, studies on electron transport in cytochromes or ligand binding by haem containing proteins.[118–120] More contemporary approaches demanding the flash photolysis technique have indulged in the studies on the conformational changes of functional proteins that occur during the mean of their activity.[121] The instrumental methodology of flash photolysis is very simple. A short pulse of radiation is used to interact with a sample that has been placed in the optical path of a detector. As a result of such light-matter interaction can be either a transient absorption or an emission process. The changes in detector signal occur following excitation source may be caused by variety of processes such as electronic excitation producing a triplet state, cleavage of a molecule producing radicals, electron transfer, molecular rearrangement etc.

In our setup, the rate constant of first order transient specie was measured by millisecond flash-photolysis setup in Fig. 2.1. The time dependent absorbance of sample is a quantitative measured by millisecond flash-photolysis setup and expressed in term of logarithmic ratio between laser intensity before and after flashing through a sample

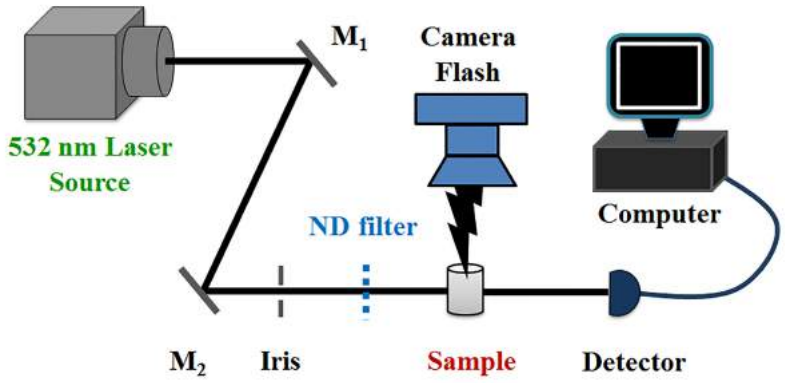

Fig. 2.1

A schematic representation of millisecond photolysis setup.

$$A_\lambda(t) = \log\left[\frac{I_0}{I(t)}\right] \tag{2.1}$$

where, $A_\lambda(t)$ is time dependent absorbance at a certain wavelength beam (λ) and recorded at every 50 millisecond time intervals. I_0 and $I(t)$ are intensity of laser light measured before and after flashing through sample. Although, the time dependent absorbance decay, $A_\lambda(t)$, was fitted by first order rate formula

$$A_\lambda(t) = A_0 exp(-kt) \tag{2.2}$$

(a.i) Millisecond Flash Photolysis Setup

In millisecond flash-photolysis setup, the sample was excited by flash using digital flash (Nissin Digital, Mark II Di622) and flash timing was controlled by using 5 volt electrical relay (Ningbo Tianbo ganglian electronics Co. Ltd), and voltage is supplied by National Instrument data card (NI USB-6008). The laser produces 532 nm continuous green light of power 5 mW, purchased from Shanghai Dream Laser Technology Co. Ltd (SDL-532-LN-002T). The fundamental 532 nm continuous beam was employed to measure the change in samples which were excited by flash light and the laser spot size was taken approximately 1 mm. To avoid higher power, the power of green laser was reduced to 50 μW by introducing variable circular neutral density filter before the sample holder, and sample was placed in a quartz corvette of path length 5 mm and continuous stirred by magnetic stirrer (2 ML, Remi Laboratory Instruments, India). The absorbance change in the sample has been recorded by Fujitsu FIDO8T13TX silicon photodiode (Japan) and this recorded signal has been amplified by using combination of 9014B silicon NPN epitaxial transistor and 500 ohm resistance, and further transferred this amplified signals to data card, where it communicates with lab view programming. The concentration of sample has been maintained at $5x10^{-4}$ M and all measurements were performed at 300 K.

(b) Time Correlated Single Photon Counting (TCSPC) Measurement

At the most of occasions, the time resolved measurements are commonly performed by using time correlated single-photon counting method to examine the relaxation process of molecules from an excited state to a lower energy state. Importantly, TCSPC method functions on simple principle of detection of a single photon followed by excitation pulse and measuring its arrival time with respect to a reference pulse. Since, it is well known that fluorescent sample emit photons at different times followed by their excitation pulse. Hence, the general methodology basically laid on the probability distribution of a single fluorescent photon after an excitation instance occur the actual intensity against time distribution of all the photons emitted as a consequence of the excitation. By accumulating the single fluorescent photon at larger extent followed by each excitation pulses, the experiment reconstructs actually probability distribution profile.

(b.i) Time Correlated Single Photon Counting (TCSPC) Setup

This technique examines the first emitted photon from the fluorescent sample is being monitored with respect to the pulse exciting the fluorescent sample molecule.[122–126] To examine such measurement, the samples were excited by high repetition rate low intensity picosecond diode laser or nano LED excitation source. A schematic diagram of TCSPC setup is represented in Fig. 2.2. In this setup, a trigger pulse initiates from the diode laser or nano LED synchronous with excitation laser pulse is utilized as a start pulse in TAC (time to amplitude converter) to produce a voltage ramp, which increases linearly against time. The emitted radiation from the sample is collected by an optical filter and the collected fluorescence signal is dispersed to the monochromator. The selected fluorescence transient is detected at magic angle polarization (i.e. 54.7°) from vertical excitation polarization employing micro-channel plate photomultiplier tube (MCP-PMT). The final outcome of the PMT is utilized as stop pulse to the TAC after going through constant faction discriminator (CFD), which accurately monitors the arrival time of pulse. The TAC produces voltage which is linearly proportional to the time difference between the excitation of the sample and detected photon. Later, this voltage is amplified and converted to numerical value using programmable gain amplifier (PGA) and analog-to-digital convertor (ADC), respectively. Repeating this process many times and by continuing detection of fluorescence event lower compare to the number of excitation pulses (2% or less), the fluorescent decay profile of the sample is constructed. This decay profiles are best fitted by deconvolution method using commercial softwares such as DAS6 and FAST. To estimation the lamp profile, we use a

scattering solution (Ludox) in place of the sample.

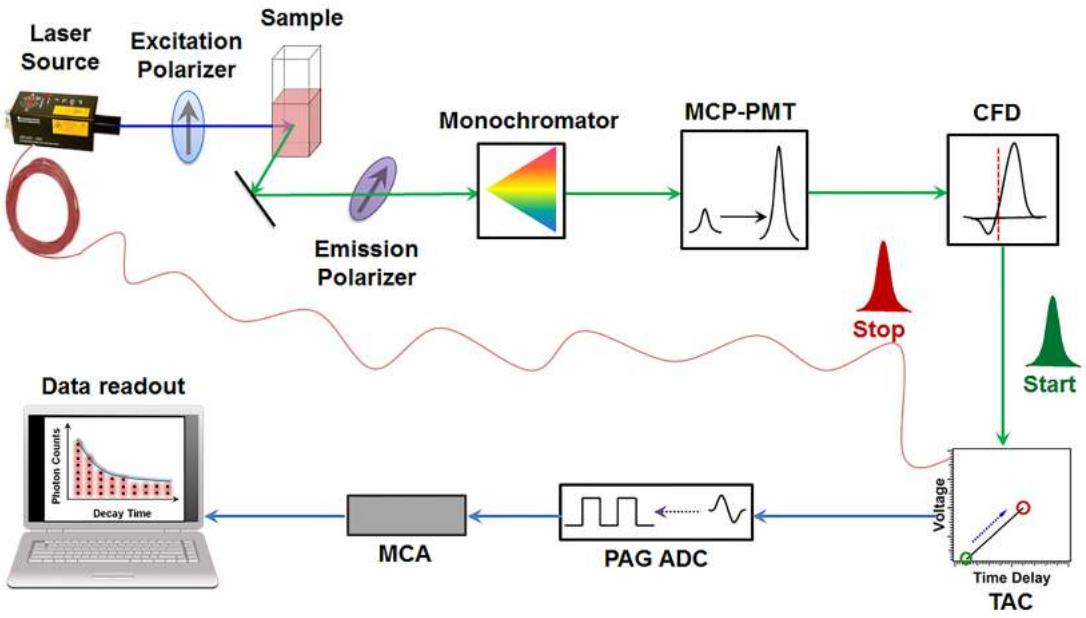

Fig. 2.2

A schematic representation of time correlated single photon counting (TCSPC) setup.

The prime role of CFD is intended to evaluate the exact arrival time of photoelectron pulse with precise resolution time. It is the most obligatory component which faces with photoelectron pulse. Generally, CFD is used to reduce the time jitter grew from the amplitude jitter, detected by the PMT. To achieve minimum pulse amplitude in the arrival time of the signal, CFD eliminates the pulses which has lower amplitude than a given threshold (voltage) and allows filtering through only those pulses with higher amplitude for next signal processing. Further, it splits the incoming pulse into two parts; first one third part of the pulse is inverted and the rest part is delayed by the half of the pulse width. In subsequent step, the time jitter is minimized dramatically at crossing point where above two parts is recombined.

Since the time jitter has been reduced by using the CFD, the photoelectron pulse is further encountered with time to amplitude convertor (TAC), which is a most substantive part of TCSPC. The exclusive function of TAC is to produce the voltage ramp by charging the capacitor inside TAC is linearly proportional to the time difference between the excitation and first arriving of photon event. As the start pulse (first arriving photon event pulse) hits to the TAC, the capacitor inside TAC starts creating to voltage charge from 0 to 10 volts over an order of picosecond to microsecond time scale and stopped by the stop pulse. The

TAC voltage starts increasing linearly with time perfectly depends on the arrival time of the stop pulse. At that moment, the increment in voltage is being stopped, the final voltage inside the TAC is linearly proportional to the time difference between the excitation and the fluorescent photon event. The resultant pulse of TAC can further be amplified and converted to numerical value using programmable gain amplifier (PGA) and analog-to-digital convertor (ADC), respectively. Multichannel analyzer (MCA) now assesses the voltage signal from the TAC and modified it according to the counts at each particular voltage (time); and hence place into different time bins in the MCA. The width of the time bins (i.e. time per channel) is the ratio of the full time-range of the TAC and the number of channels in MCA decided by the resolution of ADC. In the present study, we have made all measurement through two commercial TCSPC setups, Life Spec II from Edinburgh Instruments, UK and FluoroLog 3-21 fom Jobin Yvon, USA.

(b.ii) Method of Data Processing

In general, the average decay time is much larger compared to that of excitation pulse, the excitation event may be ascribed as a δ function. For some instance, if the excitation pulse is larger compared to decay time, the measured data may resolved from the actual fluorescence response owing to a finite decay time of the pump pulse, response time of the photomultiplier tube along with associated electronic devices. However, the measured fluorescence decay profile by the TCSPC system is a convolution of the fluorescence from the molecule and the instrument response function. In order to retrieve actual fluorescence lifetime from measured fluorescence lifetime decay, it is most important to deconvolute the measured data collected during the experiment. The measured fluorescence decay is mathematically expressed in term of convolution integral part fluorescence intensity $F(t)$ at any time t,[122–125]

$$F(t) = \int_0^t I(t')P(t-t')dt' \tag{2.3}$$

where, $I(t')$ is the intensity of the exciting light at time t' and $P(t-t')$ is the response function of the experimental system. t' denotes variable time delays (channel numbers) of infinitesimally small time-widths, dt' (channel widths). For single exponential decays, $P(t-t')$ can be written as $P(t-t') = exp[-(t-t')/\tau]$. Hence, the observed fluorescence decay $F(t)$ in equation (3) reformulates as,[122–125]

$$F(t) = exp(-t/\tau)\int_0^t I(t')exp(-t'/\tau)dt' \tag{2.4}$$

Here, $I(t')$ is the instrument response function, which are measured experimentally by fluorescence decays of sample and Rayleigh scattering from a LUDOX solution in water, respectively.

The methodology of deconvolution analysis is basically based on an iterative least square regenerative convolution method.[122–127] An excitation pulse profile (i.e., IRF) and fluorescence lifetime decay are both measured experimentally. On other side, the deconvolution analysis starts combining IRF and a projected decay to develop a new reconvoluted function. Now, newly developed function is fitted over the experimentally obtained fluorescence data and the difference is summed, producing the χ^2 function for the fit. The procedure of deconvolution continues via a series of such iterations until a significant change in χ^2 obtains between two successive iterations. χ^2 tells preference of fitting and can be expressed as

$$\chi^2 = \sum_{j=1}^{n} \frac{1}{\sigma_j^2}[F(t_j) - F_p(t_j)]^2 \tag{2.5}$$

where, $F(t_j)$ and $F_p(t_j)$ are respectively the measured and projected data at different time-points. n is the number of data points or channels utilized in a particular analysis and σ_j is the standard deviation of each data point, which is the square root of the number of photon counts since TCSPC operates on Poisson statistics, i.e. $\sigma_j = [N(t_j)]^{\frac{1}{2}}$.

Ordinarily, the quality of fit is estimated by measuring the reduced χ^2, the plot of the weighted residuals and the autocorrelation function of residuals. The reduced χ^2 is explained following as

$$\begin{aligned} \chi_r^2 &= \frac{\chi^2}{n-p} \\ &= \frac{\chi^2}{v} \end{aligned} \tag{2.6}$$

Here, n, p and $v = n - p$ are respectively the number of data points, floating parameters and the number of degree of freedom.

It is most essential to take care the fitting of multi-exponential function, particularly where the difference between lamp and decay profile is comparatively small. The different multi-exponential functions require unless the data quality of fitting will satisfactory not improve. The large number of multi-exponential terms gets significant meaning only when fitting is inappropriate with fewer numbers. Therefore, there is certain some probability of reaching to a local minimum during deconvolution procedure.

(c) Femtosecond Transient Absorption Spectroscopy

Transient absorption (TA) spectroscopy is one of most distinguished pump-probe technique in ultrashort time domains which probes the ultrafast dynamics of photo-chemical and photo-physical phenomena.[128–137] It is a very sensitive spectroscopic technique for investigating the time evolution of energetic states and the lifetimes of short-lived intermediates by detecting the time dependent transient absorption responses.[136,137] The basic methodology of TA spectroscopy adopts the fundamental idea of flash photolysis technique since the introduction of ultrafast laser source. The technical principles of TA are essentially identical though more much sensitive compare to flash photolysis in order to carry out experiments with higher time resolution. By applying pulse width of approx. 100 fs, it is possible to capture most of the ultrafast dynamics owning in the excited states such as internal conversion, intramolecular vibrational relaxation, intersystem crossing, excited state reactions like charge transfer, proton transfer, and also many other processes occurring to reactive pathways.

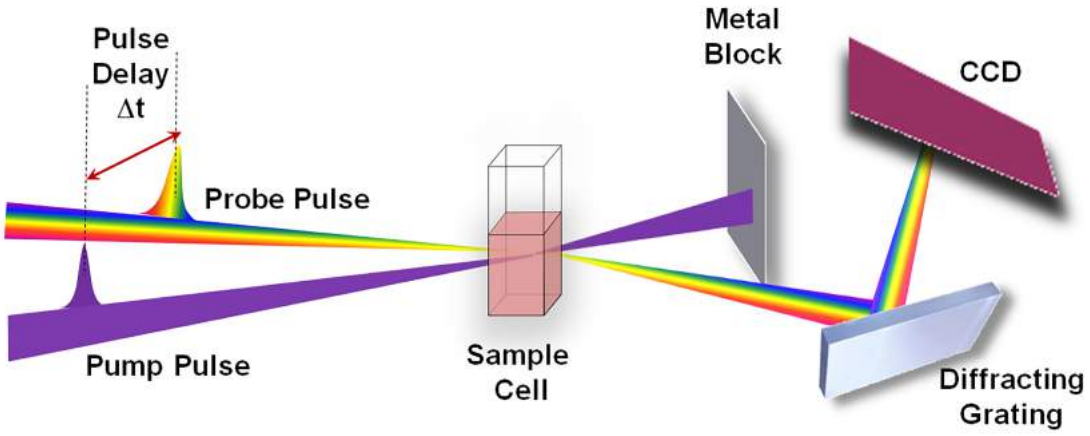

Fig. 2.3

A schematic illustration of the transient absorption spectroscopy principle.

A schematic diagram of TA presents in Fig. 2.3. In Fig. 2.3, the TA techniques involves two ultrashort laser pulses, where first monochromatic strong pump pulse (I_{pump}) which is used here to resonant the photochemical reaction, however, a weak probe pulse (broad or monochromatic, I_{probe}) employ to examine such photo processes. In brief, the pump pulse induces an electronic or vibrational transition in the photo-system of interest as passes through a sample solution. Therefore, the pump pulse triggers transition in molecules to their

higher energy levels by vertical Franck-Condon transition and the strength of the transition indeed depends on the strength of pump power and absorption cross-section of molecules. On the contrary, the probe pulse goes through the same intersection volume of liquid sample, where pump pulse was being focused, after a different particular time (t) with respect to pump pulse. The absorption intensities of the probe pulse with and without pump pulse (I^{pump}_{probe} & I^{0}_{probe}) are measured for each particular delay time between the pump and the probe pulses. In this manner, the difference absorption spectra, $\triangle A(\lambda,t)$ is computed to monitor the signal related to the energetic states and the evolution of product states.[136]

$$\triangle A = log\left[\frac{I^{0}_{probe}}{I^{pump}_{probe}}\right] \tag{2.7}$$

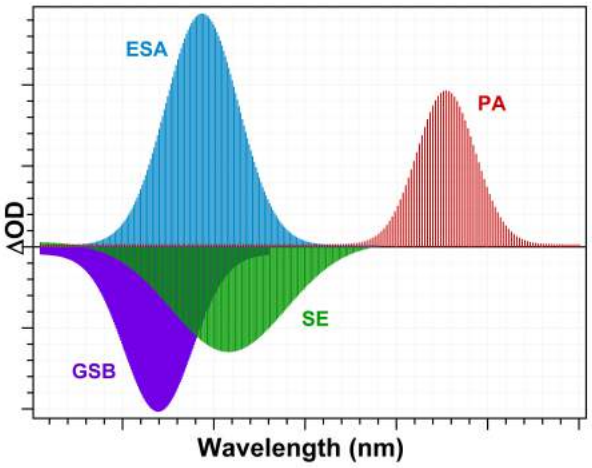

Fig. 2.4

The distribution of various processes involved in difference absorption spectrum: ground state bleaching (GSB), excited state absorption (ESA), stimulated emission (SE), and product state absorption (PA).

In case of broad probe pulse, the obtained $\triangle A(\lambda,t)$ is quite straightforward by dispersing the white light continuum onto a Charge-Coupled Devices (CCD). Upon energetic pulse excitation, there is various types of photo-processes occurred in system. However, the possibilities to underlie susceptible processes depend on the nature of the molecular system. Hence, the contributions of different photo-processes in TA spectra (Fig. 2.4) are discussed briefly below.

1. **Ground State Bleaching or Depopulation signal**

By means of a ultrashort pump pulse, a fraction of the molecular population within the excitation volume has been pushed to excited states and thus, the population in ground state is reduced. Therefore, only small molecular population will absorb the probe light and rest will be just transmitted through it. In such manner, the amount of probe light arrive at CCD and will be found more in the case of pump on compared to pump off and consequently calculated absorption difference will be obtained negative in the wavelength region see in Fig. 2.4.

2. **Stimulated Emission**

   For a two level molecular system, the electronic transitions are bound between two energy states, where Einstein coefficients for absorption phenomenon originate from ground state to excited state denotes as A_{12} and whereas stimulated emission from the excited state (A_{21}) are identical almost. The process of stimulated emission is possible only once transitions are optically feasible, and probe light of particular frequency exposes to the sample while molecule stays in excited state. Additionally, the spectra profile of stimulated emission is similar to the steady state fluorescence spectrum of the chromophore molecule and it shifts to the ground state, termed as stokes shift. In other words, a photon of particular frequency from the probe pulse stimulates emission of another photon from the excited molecular state and forces to back molecular ground state. Under induced process, a new photon is produced which follows same direction as that of probe photon and finally both will be detected. Thus stimulated emission contributes in increased light intensity on the CCD, corresponding to a negative $\triangle A$ response, see in Fig. 2.4. Under specific circumstance, the stokes shift might have a possibility to be so little that the stimulated emission band spectrally convergences with the ground state bleaching process and emerge efficiently as a single band.

3. **Excited state Absorption**

   Upon photo-excitation of pump pulse, the molecules are promoted to excited states, and occur only if transitions are feasibly allowed in certain wavelength regions, and subsequently absorption of the probe pulse in particular wavelength region will cause another transition. Therefore, the intensity of the probe pulse in these particular wavelength regions is comparable higher on pump off situation rather in pump on and consequently a positive response in the $\triangle A$ is observed in the wavelength region of the excited state absorption.

4. **Product Absorption**

By introduction of a pump pulse, photo-reaction after pulse excitation of sample may occur that leads in the generation of a transient or some long lived intermediate species in higher excited state such as charge transfer species, proton transfer species, isomerisation and triplet state species etc. The absorption of such intermediate species is displayed positive response in the $\triangle A$ spectrum.

(c.i) Artifacts in Femtosecond Transient Absorption Spectroscopy

Most of the troublesome appears during the femtosecond transient absorption experiment are those originating from the sample cells. Those possible undesired signals or artifacts might result ambiguously in femtosecond transient absorption data. The most significant reason of their appearance follows,[136,137]

1. Introduction of ultrashort pulses train (less than 100 fs) which prompt extremely high pump power density, which easily triggers two photon absorption (TPA) and stimulated Raman amplication (SRA).
2. Usage of a spectrally broad probe pulse, the ordinarily white light continuum in a wide range (i.e., 300–1100 nm), which mutually temporal chirp in the continuum and high pulse intensities unintentionally supplies worthy conditions for efficient cross-phase modulation.
3. The sensitivity of detecting device may obscure undesired signal of relative low intensity become comparable with weak transient responses.

It is noteworthy that undesired responses are potential to be prompt both in the liquid state studied and also common in fused silica cell sample windows.

(c.ii) Transient Absorption Setup

The amplified pulsed light used for the propose of transient absorption (TA) experiments irradiated from a Ti:sapphire regenerative amplifier (Spectra Physics, Spitfire Pro XP) producing 50 fs pulse trains, centred at 800 nm, at a 1 kHz repetition rate with energy of 4 mJ per pulse. The generation of amplified pulse has been accomplished by introducing seed laser i.e. a mode locked oscillator (Spectra Physics, *Mai Tai SP*) and a 20 W Q-switched Nd:YLF Laser (Spectra Physics, Empower) is here used to pump the Ti:sapphire regenerative amplifier. A schematic illustration of our transient absorption setup is shown in Fig. 2.5. The fundamental amplified pulse was directed to the setup by some series of mirrors 'M_{A1}' and 'M_{A2}' and was divided into two part by introduction of a beam splitter 'M_{A4}' with large fraction being used to produce the pump pulse, whereas, remained part was employed to

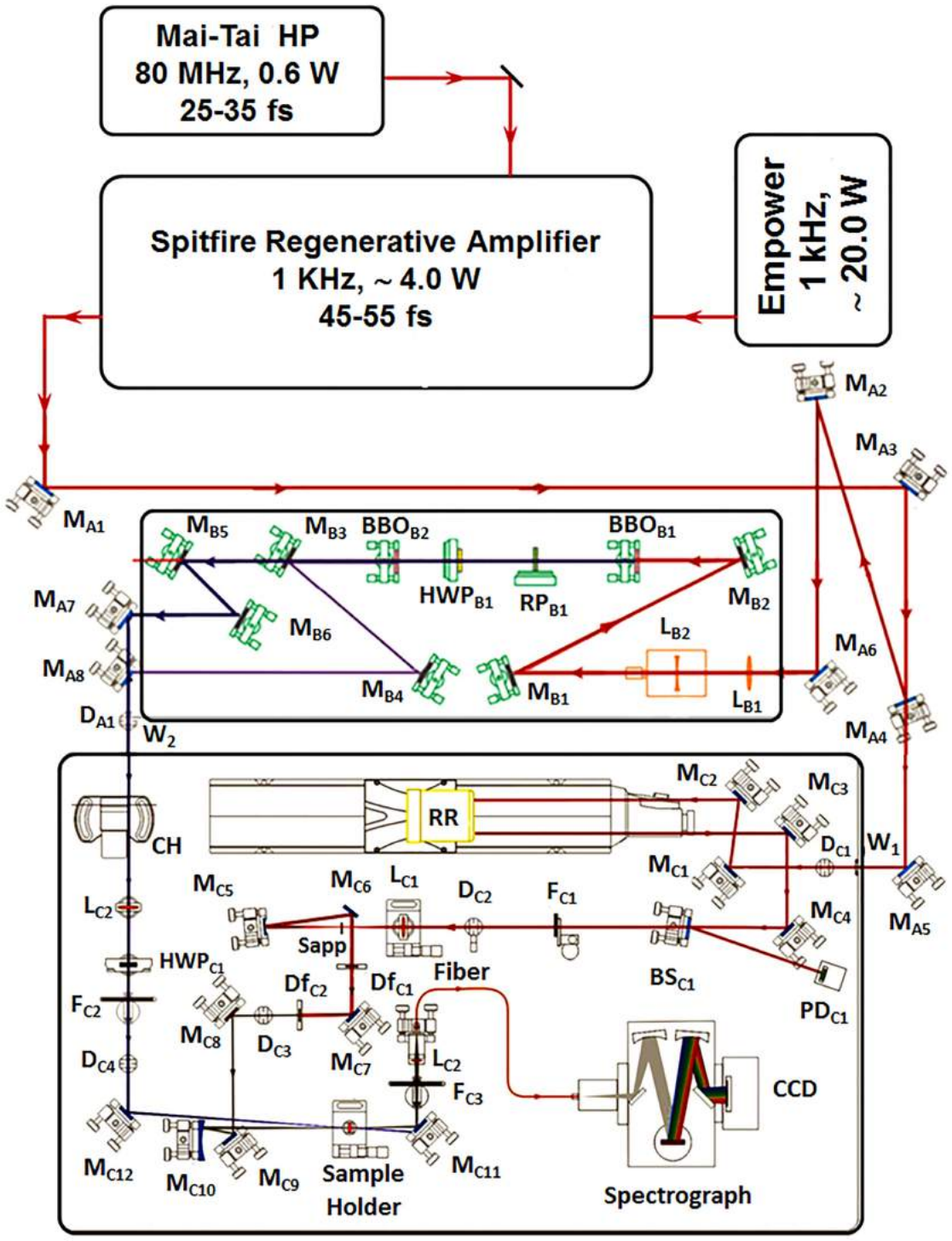

Fig. 2.5

Schematic depiction of a femtosecond transient absorption (FTA) setup in our laboratory.

probe the sample. Majority of the photochemical and photophysical processes in molecular systems were controlled by exposing light in the UV-vis region, therefore, in reality the frequency doubling or tripling of the fundamental pulse light has been essentially demanded. The process of frequency doubling was achieved by using a 0.2 mm BBO crystal (BBO_{B1}), and in next step, the fundamental (800 nm) and the second order harmonic beam light (400 nm) were fetched collinearly in another 0.2 mm BBO crystal (BBO_{B2}) to produce third harmonic light (266 nm). To generate third harmonic light successfully, it was in principle required a temporal overlap between the 800 nm and 400 nm light, 800 nm light was delayed in time by introduction of CaF_2 crystal (RP_{B1}). Subsequently, the 2^{nd} and 3^{rd} order harmonic light beam are further handled by some sets of mirrors 'M_{A7}' and 'M_{A8}'. The remaining proportion of fundamental pulse light was let to pass through a window 'W_1' in the FemtoFrame-II and fell onto the retro-reflector '*RR*' through use of mirrors 'M_{C1}' and 'M_{C2}' and intensity of light was controlled by iris 'D_{C1}'. The retro-reflector is hold onto a computer controlled motorized translation stage, which can control the time of arrival of probe pulses relative to pump pulses onto the sample cell. The reflected light beam from the retro-reflector is focused onto the beam splitter 'BS_{C1}' by use of mirrors 'M_{C3}' and 'M_{C4}'. The large proportion of light passes through the beam splitter and traverses through a variable linear neutral density filter 'F_{C1}', an iris 'D_{C2}'. After lens 'L_{C1}', light is focused onto the 0.3 mm sapphire crystal plate where it generates the white light continuum. The generation of white light continuum is optimized by controlling the neutral density filter 'F_{C1}', an iris 'D_{C2}'. The remaining part of beam from the beam splitter 'BS_{C1}' is permitted to reach a photodiode 'PD_{C1}'placed just behind the 'BS_{C1}'. The wide spectral bandwidth (450 to 770 nm) of white light continuum originated from the sapphire crystal plate is reflected by using a series of mirrors from 'M_{C5}' to 'M_{C9}' onto a concave mirror 'M_{C10}' mediated by two dielectric notch filters 'Df_{C1}' and 'Df_{C2}' and the white light intensity is controlled by an iris 'D_{C3}'. The main propose of dielectric notch filters are get rid of the fundamental part of light from the white light continuum. The concave mirror 'M_{C10}' is being used to incline the probe white light continuum into the optical fibre cable by using a plane mirror 'M_{C11}' and a small focal length lens 'F_{C3}'. The intensity of white light continuum after mirror 'M_{C11}' is controlled by a variable circular neutral density filter. The intensity of white continuum light is further passed by a diffraction grating onto a multichannel charged coupled device (CCD). On another side, 2^{nd} or 3^{rd} order harmonic part of pump light bean from the JANOS tripler are focused inside the FemtoFrame–II by use of mirror 'M_{A7}' or 'M_{A8}' through a window

'W_2'. The pump beam again passes through electronically controlled chopper 'CH', a 50 cm focal length lens 'L_{C2}', a half waveplate 'HWP_{C1}', a rotatable circular neutral density filter 'F_{C2}' and an iris 'D_{C4}' onto the mirror 'M_{C12}'. The mirror 'M_{C12}' reflects the pump beam into the sample cell keeping a small angle of divergence with respect to probe light beam. After passing through sample cell, the pump beam is ceased by using metallic blocker. The alignment of the pump and the probe beams is keeping in such a manner to provide a spatial and a temporal overlaps between the two pulses with the observation volume. The repetition rate of pump pulse is reduced by used electronically controlled chopper and its rotations are synchronized with the photodiode placed behind the beam splitter in the path of probe. The spectral and temporal data is recorded by charge-coupled device (CCD) which is also synchronized by the photodiode. The half waveplate is intended to control the pump pulse polarization relative to the probe pulse and for the present experiments is set at 54.7° (magic angle) to avoid any contribution from the rotational diffusion of the molecules. The beam waist of the pump light beam is generally taken larger than that of the probe light, observed data is recorded in FemtoFrame 2.4.6 software based on LabVeiw and also such experiments are performed with pump energy of approx. 1 μJ. At end, the recorded data is analyzed by using Femtosuite software.

2.2 Analytical Models

The basic idea of evolution of analytical models is used to calculate the distinct mutual properties of the binary solvent mixture (such as solvation nature and interaction pattern or strength) which may not be possible to evidently figure out from physical or spectroscopic measurements. This way all the molecular level information about the binary solvent mixture can be substantially squeeze out from the experiments data. In this part the fundamentals of these analytical models are discussed in more detail.

2.2.1 Proton-NMR Study of Protonated AH-BH Solvent Mixture

To furnish a deeper and more relevant understanding about the microscopic structure of binary solvent mixture, proton-nuclear magnetic resonance (^{1}H-NMR) measurements were performed. There is certainly a kind of interaction persisting between molecules of different solvents which is distinct than the intra-molecular interactions leading to the deviation from ideality. In protonated AH-BH binary mixture, the solvent molecules interact through the formation of hydrogen bonding network and therefore as the proportion of either of the components is changed, the local electronic cloud around the hydrogen bonded hydrogen atoms of each solvent feels intermolecular forces/attractions and was directly observed as a change in the chemical shift. This change in chemical shift of proton of AH and BH in the binary mixture supplies a direct evidence of two solvent (AH and BH) network formation. The nature of network between AH and BH molecules is explained by proposing the following models.[138]

(a) Model for AH Proton in AH-BH Solvent Mixture

The observed chemical shift (δ_{obs}) of AH proton in binary mixture was found shifted toward either the up-field or down-field region with increase in proportion of BH solvent concentration. In case of pure AH, the AH molecules exist as self-aggregate. It is assumed that the increasing the proportion of BH solvent in the binary mixture results in the loss of self-association of AH molecules and leads to the formation of H-bond between AH and BH. In AH-BH binary mixture, the observed chemical shift of AH proton is brought as a linear combination of chemical shift of self-associated AH molecules (δ_{AA}) and chemical shift of AH proton hydrogen-bonded to BH (δ_{AB}) and can be formulated as

$$\delta_{obs} = \frac{X^I_{AA}}{X_A}\delta^{AA} + \frac{X^I_{AB}}{X_A}\delta^{AB} \tag{2.8}$$

Here, X^I_{AA}, X^I_{AB} and are portion of AH self-aggregated, fraction of AH interacted to BH. X_A is total mole fraction of AH in the mixture ($X_A = X^I_{AA} + X^I_{AB}$). At highest concentration of AH, i.e. when $X_A \rightarrow 1$,

$$\lim_{X_A \rightarrow 1} \delta_{obs} \equiv \delta^{AA} \tag{2.9}$$

At infinite dilution condition ($X_A \rightarrow 0$), AH molecules solely interact with the surrounding BH molecules through the hydrogen bonding network in the binary mixture. In this regime, the observed chemical shift of AH proton is therefore equal to that of AH interacted to BH molecules.

$$\lim_{X_A \rightarrow 1} \delta_{obs} \equiv \delta^{AB} \tag{2.10}$$

Now, the equation could be reformulated as

$$\delta_{obs} = \delta^{AB} + \frac{X^I_{AA}}{X_A}(\delta_{AA} - \delta_{AB}) \tag{2.11}$$

Substituting $\frac{X^I_{AA}}{X_A}$ by a normalized fitting function as given below

$$\frac{X^I_{AA}}{X_A} = \frac{[-a_1 exp(-b_1 X_A) - a_2 exp(-b_2 X_A) + a_1 + a_2]}{[-a_1 exp(-b_1) - a_2 exp(-b_2) + a_1 + a_2]} \tag{2.12}$$

The corresponding chemical shift of AH solvent proton ^{1}H-NMR data set in AH-BH mixture is fitted to obtain the unknown parameters a_1, a_2, b_1, b_2 and δ^{AB}. By substituting the value of fitting parameters in equation 2.12, we calculate the portion of AH interacted to AH in binary mixture of the particular concentration. Consecutively, the portion of AH interacted to BH has been calculated from the following equation

$$X^I_{AB} = X^I_{AA} - X_A \tag{2.13}$$

(b) Model for BH Proton in AH-BH Solvent Mixture

In the same set of binary mixture, there is not only a shift in the chemical shift position of AH proton but also the position of BH proton is also getting influenced. It is found that the observed chemical shift (δ_{obs}) of BH proton in binary solvent mixture is shifted toward either up-field or downfield region with decreasing BH proportion. Increasing he proportion of AH induces the self-aggregation of BH molecules to minimize and the interactions with the added AH molecules to initiate, resulting in the shielding or deshielding of BH proton. The theory to describe this model is based on the same model proposed earlier for AH proton

and the terms have their usual meanings. The main equation relating the observed NMR chemical shift values with the chemical shift values of BH-BH self-aggregated and AH-BH interactions is

$$\delta_{obs} = \frac{X^I_{BB}}{X_B}\delta^{BB} + \frac{X^I_{BA}}{X_B}\delta^{BA} \tag{2.14}$$

where, X^I_{BB} and X^I_{BA} are portion of BH self-aggregated, fraction of BH interacted to AH. X_B is total mole fraction of BH in the mixture ($X_B = X^I_{BB} + X^I_{BA}$). The equation 2.14 is rewritten again following as

$$\delta_{obs} = \delta^{BA} + \frac{X^{BB}_I}{X_B}(\delta_{BB} - \delta_{BA}) \tag{2.15}$$

The equation 2.15 is used to fit the observed chemical shift (δ_{obs}) of BH proton data in binary solvent mixture. Using equation $X^I_{BA} = X^I_{BB} - X_B$, by substituting the value of X^I_{BB} corresponding to every mole fraction of BH, calculate the portion of BH at which strongest interaction between BH and AH molecules exist.

On the basis of the above analysis, it is proposed that in a binary mixture of AH-BH, AH molecule is associated with BH molecules through hydrogen bonding. The total interaction may be simply calculated by summing both interactive terms X^I_{AB} and X^I_{BA} as

$$X^I_{tot} = X^I_{AB} + X^I_{BA} \tag{2.16}$$

A plot X^I_{tot} against mole function any solvent depicts corresponding to strongest hydrogen bond networking in the AH-BH binary mixture. Additionally, the ratio between maximum position of both X^I_{AB} and X^I_{BA} is represented in terms of relative aggregation of AH with BH and BH with AH and it turns out to be an extended hydrogen bond network is being present between AH and BH and also easy to explain the stoichiometric proportion of two solvents involved in interactions.

2.2.2 Solvent Exchange Model for AH-BH Binary Solvent Mixture

To build this model, we brought some essential ingredient from the ^{1}H NMR as evident from the stoichiometric ratio between two AH and BH solvent in binary solvent mixture. The basic idea of such models have been used to develop a correlation between the nature of solvation sphere around the solvatochromatic indicator and transition energy (E_T) of that in AH-BH solvent mixture. All solvation exchange models discuss here consider that the transition energy (E_T) of a solvatochromic indicator is mean or average transition energies in the mixed solvents that compile the solvation microsphere of the solvatochromatic indicator.[138–142]

(a) Solvent Exchange Model 1

The solvent exchange model assumes solvent exchange (1:1) equilibrium prevails between solvent AH (A) and solvent BH (B) which produces the hydrogen bonded complex specie between A and B (i.e. AB). The proposed equilibrium of 1:1 complex species can be written as

$$A + B \leftrightharpoons 2AB \tag{2.17}$$

Equilibrium constant for this process,

$$k = \frac{X_{AB}^2}{X_A X_B} \tag{2.18}$$

where, X_{AB}, X_A and X_B are respective mole fraction of the solvent aggregate, pure solvent AH and BH. These are related to the mole fractions of the mixed solvent (X_A^0), (X_B^0) as

$$X_A^0 = X_A + \frac{X_{AB}}{2} \tag{2.19}$$

$$X_B^0 = X_B + \frac{X_{AB}}{2} \tag{2.20}$$

and

$$\begin{aligned} X_A^0 + X_B^0 &= X_A + X_B + X_{AB} \\ &= 1 \end{aligned} \tag{2.21}$$

By using above equation, we reformulate equation 2.18 in the quadratic form as

$$X_{AB}^2 \left(\frac{(4-k)}{4}\right) + X_{AB}\left(\frac{k}{2}\right) + X_B^0(X_B^0 - 1)k = 0 \tag{2.22}$$

The final solution of quadratic form is given as

$$X_{AB} = \alpha - \sqrt{\alpha^2 + 4\alpha X_B^0 (X_B^0 - 1)} \tag{2.23}$$

here, $\alpha = \left(\frac{4-k}{4}\right)$

Consider, any solvatochromic molecule (P) dissolves in the mixture then the molar transition energy (E_T) of the solvatochromic probe is being effected by all three entities pure solvent AH (A), solvent BH (B) and the hydrogen bonded complex specie between A and B (i.e. AB). The total molar transition energy can be formulated in binary mixture as

$$E_T = \frac{E_{TA}X_A^S + E_{TB}X_B^S + E_{TAB}X_{AB}^S}{X_A^S + X_B^S + X_{AB}^S} \tag{2.24}$$

where, X_{AB}^S, X_A^S and X_B^S are mole fraction of the solvent aggregate, pure solvent A, and B in the solvation sphere of the probe molecule, respectively and also assumed as $X_A^S + X_B^S + X_{AB}^S = 1$, E_{TA}, E_{TB} and E_{TAB} are the transition energies of solvatochromic probe molecule in pure solvent A, B and solvent aggregate AB. Now, equation 2.24 is rewritten as

$$E_T = E_{TA} + \frac{(E_{TB} - E_{TA})X_B^S + (E_{TAB} - E_{TA})X_{AB}^S}{X_A^S + X_B^S + X_{AB}^S} \tag{2.25}$$

Hence, there are two possible solvent exchange processes in the solvation sphere, determined as

$$P(A) + B \leftrightharpoons P(B) + A \tag{2.26}$$

$$P(A) + AB \leftrightharpoons P(AB) + A \tag{2.27}$$

The equilibrium constants of the above process can be written as

$$f_{B/A} = \frac{X_B^S / X_A^S}{X_B^0 / X_A^0} \tag{2.28}$$

$$f_{AB/A} = \frac{X_{AB}^S / X_A^S}{X_{AB}^0 / X_A^0} \tag{2.29}$$

where, all terms are of their usual meaning. This is to note that $f_{B/A}$ is a measure of the probe to be more preferentially solvated by BH solvent to AH, while $f_{AB/A}$ quantified the efficacy of the indicator to be synergistically solvated by solvent aggregate rather than the pure solvent components. In this case, E_T of mixed solvent system can be expressed as

$$E_T = E_{TA} + \frac{aX_B^0 + cX_{AB}}{1 + bX_B^0 + dX_{AB}} \tag{2.30}$$

$$a = (E_{TB} - E_{TA}) f_{B/A} \tag{2.31}$$

where,

$$b = f_{B/A} - 1 \tag{2.32}$$

$$c = (E_{TAB} - E_{TA}) f_{AB/A} - \frac{(E_{TB} - E_{TA}) f_{B/A}}{2} \tag{2.33}$$

$$d = f_{AB/A} - \frac{f_{B/A} + 1}{2} \tag{2.34}$$

Equation 2.30 has been brought under limitation by the choice of equilibrium constant k. The sensitivity of E_T is controlled by pure solvent AH, BH, and mixed solvent structure in the microsphere solvation shell. Finally, a direct estimation of k from the E_T value of mixture solvent system is problematic. The estimation of both parameters (k and $f_{AB/A}$) at same time is extremely dangerous and may generate error in results.

If we consider formation of AB solvent structure on the microsphere of solvation shell, the m model of solvent exchange processes are given as

$$P(A)_m + mB \leftrightharpoons P(B)_m + mA \tag{2.35}$$

$$P(A)_m + \frac{m}{2}B \leftrightharpoons P(AB)_m + \frac{m}{2}A \tag{2.36}$$

The equilibrium constants of the earlier two processes can be written as

$$f_{B/A} = \frac{X_B^S / X_A^S}{\sqrt{(X_B^0 / X_A^0)^m}} \tag{2.37}$$

$$f_{AB/A} = \frac{X_{AB}^S / X_A^S}{\sqrt{(X_{AB}^0 / X_A^0)^m}} \tag{2.38}$$

Finally, the value of E_T in microsphere of solvation shell of AH-BH solvent aggregate can be expressed as

$$E_T = E_{TA} + \left[\frac{(E_{TB} - E_{TA})(X_B^0)^m f_{B/A} + (E_{TAB} - E_{TA})(X_B^0)^{m/2}(X_A^0)^{m/2} f_{AB/A}}{(X_A^0)^m + (X_B^0)^m f_{B/A} + (X_B^0)^{m/2}(X_A^0)^{m/2} f_{AB/A}} \right] \tag{2.39}$$

Present model clearly suggests possible nature of solvation around the solvatochromic probe molecule in mixed interactive solvents.

(b) Solvent Exchange Model 2

In the modified form of solvent exchange model, it adopts two solvent exchange (1:2) equilibrium persists between solvent AH (A) and solvent BH (B), and produces the hydrogen bonded intermediated species between AH and BH (i.e. AB), thus, newly intermediated complex again undergoes in equilibrium with BH and produces resultant species (i.e. AB_2). The proposed equilibria of 1:2 complex species can be written as

$$A + B \leftrightharpoons 2AB \tag{2.40}$$

Equilibrium constant for this process,

$$k_1 = \frac{X_{AB}^2}{X_A X_B} \tag{2.41}$$

The newly generated intermediated complex undergoes in equilibrium with solvent BH as

$$AB + B \leftrightharpoons 2AB_2 \tag{2.42}$$

Equilibrium constant for this step,

$$k_2 = \frac{X_{AB_2}^2}{\left(X_A - \frac{X_{AB_2}}{2}\right)\left(X_B - \frac{X_{AB_2}}{2}\right)} \tag{2.43}$$

where, X_{AB_2}, X_{AB}, X_A and X_B are mole fraction of the resultant solvent aggregate, intermediate species, pure solvent AH and BH respectively. These are related to the mole fractions of the mixed solvent (X_A^0, X_B^0) as

$$X_A^0 = X_A + \frac{1}{3}X_{AB_2} \tag{2.44}$$

$$X_B^0 = X_B + \frac{2}{3}X_{AB_2} \tag{2.45}$$

and

$$\begin{aligned} X_A^0 + X_B^0 &= X_A + X_B + X_{AB_2} \\ &= X_A^S + X_B^S + X_{AB_2}^S \\ &= 1 \end{aligned} \tag{2.46}$$

where all terms have usual meaning and discussed earlier. Herein, the term X_{AB} exclude from equation, because it is considered as intermediate product and considered playing not major role in molecular interactions. This quantity has taken under assumption such as

$$X_{AB} = \sqrt{X_A^0 X_B^0}\beta \tag{2.47}$$

where $\beta$is a constant. The mole fraction of solvent aggregate X_{AB_2} can be written as

$$X_{AB_2}^2\left(\frac{k_2-4}{2k_2}\right)-\left(\frac{X_{AB_2}}{2}\right)(X_{AB}-X_B^0)+X_{AB}X_B^0=0 \tag{2.48}$$

Substituting $\alpha=\left(\frac{4k_2}{k_2-4}\right)$ The final solution of the equation 2.48 is given as

$$\begin{aligned}X_{AB_2}=&\left[(X_B^0)^{1/2}(X_A^0)^{1/2}\beta+(X_B^0)^{1/2}\right]\alpha\\&-\sqrt{\left[(X_B^0)^{1/2}(X_A^0)^{1/2}\beta+(X_B^0)^{1/2}\right]^2\alpha^2-4\alpha\beta(X_B^0)^{3/2}(X_A^0)^{1/2}}\end{aligned} \tag{2.49}$$

The E_T value of the mixed solvent system is written as

$$E_T=\frac{E_{TA}X_A^S+E_{TB}X_B^S+E_{TAB_2}X_{AB_2}^S}{X_A^S+X_B^S+X_{AB_2}^S} \tag{2.50}$$

where, $X_{AB_2}^S$, X_A^S and X_B are mole fraction of the solvent aggregate, pure solvent A and B in the solvation sphere of the probe molecule, respectively. E_{TA}, E_{TB}, and E_{TAB_2} are the transition energies of solvatochromic probe molecule in pure solvent A, B and solvent aggregate AB_2. Now, equation 2.50 is again rewritten as

$$E_T=E_{TB}+\frac{(E_{TA}-E_{TB})X_B^S+(E_{TAB_2}-E_{TB})X_{AB_2}^S}{X_A^S+X_B^S+X_{AB_2}^S} \tag{2.51}$$

There are two possible solvent exchange processes in the solvation sphere, expressed as

$$P(A)+B\leftrightharpoons P(B)+A \tag{2.52}$$

$$P(A)+AB_2\leftrightharpoons P(AB_2)+A \tag{2.53}$$

The equilibrium constants of the above process can be written as

$$f_{B/A}=\frac{X_B^S/X_A^S}{X_B^0/X_A^0} \tag{2.54}$$

$$f_{AB_2/A}=\frac{X_{AB_2}^S/X_A^S}{X_{AB_2}^0/X_A^0} \tag{2.55}$$

where, all terms involved in equations are of their usual meaning. In this case, E_T of mixed solvent system can be expressed as

$$E_T=E_{TB}+\frac{aX_A^0+\left[(E_{TAB_2}-E_{TB})f_{AB_2/A}-\frac{(E_{TA}-E_{TB})}{3}f_{B/A}\right]X_{AB_2}}{1+bX_A^0+dX_{AB_2}} \tag{2.56}$$

where,

$$a = (E_{TA} - E_{TB}) f_{B/A} \tag{2.57}$$

$$b = f_{B/A} - 1 \tag{2.58}$$

$$d = f_{AB_2/A} - \left(\frac{f_{B/A}}{3} + \frac{2}{3} \right) \tag{2.59}$$

Equation 2.56 has been taken under limitation by the choice of equilibrium constant k_2. The sensitivity of E_T is guided by pure solvent AH, BH, and mixed solvent structure in the microsphere solvation shell, not by bulk. Hence, a direct estimation of k_2 from E_T the value of mixture solvent system is dangerous. The estimation of both parameters (k_2 and $f_{AB_2/A}$) at same instant is extremely difficult and may grow enormous error in results.

If we assume formation of AB_2 solvent structure on the microsphere of solvation shell, the m model of solvent exchange processes are formulated as

$$P(B)_{3m} + 3mA \leftrightharpoons P(A)_{3m} + 3mB \tag{2.60}$$

$$P(B)_3 m + mA \leftrightharpoons P(AB_2)_m + mB \tag{2.61}$$

For this process, the equilibrium constants are defined as

$$f_{A/B} = \frac{X_A^S / X_B^S}{(X_A^0 / X_B^0)^{3m}} \tag{2.62}$$

$$f_{AB_2/B} = \frac{X_{AB_2}^S / X_B^S}{(X_A^0 / X_B^0)^m} \tag{2.63}$$

At end, the value of E_T in microsphere of solvation shell of solvent aggregate can be expressed as

$$E_T = E_{TB} + \frac{(E_{TA} - E_{TB}) f_{A/B} (X_A^0)^{3m} + f_{AB_2/B} (E_{TAB_2} - E_{TB}) (X_A^0)^m (1 - X_A^0)^{2m}}{(1 - X_A^0)^{3m} + f_{A/B} (X_A^0)^m + f_{AB_2/B} (X_A^0)^m (1 - X_A^0)^{2m}} \tag{2.64}$$

The m value indicates the number of solvent molecules in microsphere of solvation shell of the probe molecule affecting its transition energy. The proper trial and validation of these models have been briefly discussed in chapter 3. A different solvent exchange model has been used to determine the feasibility of solvation behavior and polarity parameter of the mixed solvent structure. The final result of fitting depicts that the close look about H-bonding network between hydrogen donor and hydrogen acceptor solvent contributed more polar environment in binary solvent system around the solvatochromic probe.

3

Spectroscopic Evidence of Synergism in Binary Solvent Mixtures

[1]*A strong synergistic solvation was observed for the mixtures of different hydrogen bond donating and accepting solvent pairs. The nature of the interactions between two solvent pairs were investigated with different dye molecules viz. coumarin 480, coumarin 153, 4-(dicyanomethylene)-2-methyl-6-(4-dimethylaminostyryl)-4H-pyran, 4-aminophthalimide, and p-nitroaniline. Coumarin dyes in different alcohol-chlorinated methane (alcohols: MeOH, t-BuOH and chlorinated methanes: CH_2Cl_2, $CHCl_3$) binary mixtures show a strong synergism, which is explained in the backdrop of solvent-solvent interactions. The solvation behavior of MeOH-$CHCl_3$ mixture shows strong probe dependence with no synergism observed in p-nitroaniline, which is ascribed to its higher ground state dipole moment (8.8 D) relative to C480 (6.3 D). Interestingly, the strong synergistic signature observed through spectrophotometric measurement of solvatochromic molecules in alcohol-chlorinated methane binary mixtures is absent when studied by fluorescence measurement. The higher excited state dipole moment of coumarin 480 (13.1 D) is considered to be the driving force for the absence of synergism in the excited state. In such strongly perturbed systems (due to high dipole moment values) the dominant phenomenon is preferential solvation. Analysis of proton NMR of alcohol-chlorinated methane binary solvent mixtures indicate the existence of alcohols-chlorinated methanes binary molecular association in the different stoichiometric ratio. Refractive index measurement also infers the existence of hydrogen bonded network structure between alcohols and chlorinated methanes. The solvent exchange model has been used to determine the feasibility of synergistic behavior and polarity parameter of the mixed solvent structure of alcohol-chlorinated methane binary solvent mixtures. Fluorescence quenching of C480 by 1,2-phenylenediamine in the MeOH-$CHCl_3$ binary solvent mixture displays the maximum deviation in quenching constant corresponding to $\sim$0.45 mol fraction of MeOH in MeOH-$CHCl_3$ binary mixture and hence suggested the maximum extent of hydrogen-bonding interactions prevailing at this proportion of mixture.*

---

[1]Published: *J. Phys. Chem. B.* **2012**, *116*, 1346.

3.1 Introduction

The spectroscopic studies of molecules and clusters have crossed the boundaries of homogeneous medium and a lot of concern is being devoted to understand the behavior in micro heterogeneous systems.[143–146] Recently, solvent mixtures made a lot of attention because of its unique behavior compared to its constituent counterparts which can be explained in terms of differential interaction leading to the formation of micro heterogeneous environment.[143–154] The use of solvent mixtures provide the means of modification of solute-solvent interactions by virtue of its composition. The solute-solvent interaction is generally monitored in terms of the stabilization of its electronic energy level and this interaction depends on the proportion of either of the constituting solvents and is known for several years.[155–163] The behavior of a molecules in binary solvent mixture depends on either one or both solvents component by specific interactions e.g., hydrogen bonding, self-association or by nonspecific interactions such as dipole-dipole, dipole-induced dipole interactions.[145,146,154–162] In binary solvent mixtures, the deviation from ideality is believed to originate from the nature and extent of solute-solvent interactions, locally developed in the immediate vicinity of the solute molecules, which has an impact on the spectroscopic properties of the molecules. Generally, solvent polarizability, H-bond donating ability (HBD) and H-bond accepting ability (HBA) or solvent basicity are three parameters which have been characterized to represent the variation of solute-solvent interactions.[164,165] All these parameters are solvatochromic parameter (represented like as π^*, α and β respectively, the Kamlet-Taft parameters) and provide information about the different modes of solvent interaction with the probe molecules in pure solvents and also in solvent mixtures.[164–171] Characterization of solvation behavior has been done employing various methods like conductance or transfer measurements,[172] NMR chemical shifts,[173–176] vibrational spectroscopy,[145,146,154] UV-vis spectroscopy,[160–163] solvation dynamics,[143,150] etc. Refractive index measurements of binary solvent mixtures have also been used to determine the quantitative information about the solvent-solvent interactions.[177,178]

In solvent mixtures the proportion of constituting solvents may substantially differ around the solute compared to that in bulk resulting the change in Gibbs energy of solvation. This would be the resultant of probe being solvated preferentially by one of the solvents in the mixture.[149,179] The phenomenon, where one solvent solvates the solute predominantly than the other, through specific or nonspecific solute-solvent interactions, is known as "preferential solvation". It has been studied both experimentally,[156–163,169–171,180–182] and

theoretically[155,183–186] to a great deal. Apart from preferential solvation, there is always some probability where both the constituent solvents can solvate the molecules together by mutual interaction and giving rise to a completely different solvation environment. Such a phenomenon is observed for some specific solvent pairs and is termed as "Synergism".[166] In synergism, the solvent mixture constituting the solvation shell around the probe acts as a completely different entity and behaves distinctly than either of the bulk solvents. Mancini *et al.*[166] proposed that the combination of dipolarity and hydrogen bond donating and accepting capacity of solvents leads synergistic effect in binary solvent mixtures, which clearly reflects through the empirical solvent polarity parameter, $E_T(30)$. They measured the kinetics of 1-fluoro-2,4-nitrobenzene with morpholine and piperidine in several binary mixtures of polar aprotic H-bond accepting solvents like acetonitrile and chloroform and observed that the binary solvent mixture exhibited synergism. Gratias *et al.*[187] on the basis of molecular dynamic simulations revealed clustering effect in the MeOH-$CHCl_3$ solvent mixture. They also demonstrated that such a mixture preferentially solvates the hydrophilic and hydrophoblic parts of ampiphilic solutes. Durov *et al.*[188] calculated the excess thermodynamic functions and dielectric permittivity of MeOH-$CHCl_3$ mixture in the framework of quasichemical model of nonideal association solution and reproduced the physicochemcial properties of the mixture to a good accuracy. This model, based on supramolecular aggregate formation, proposes that deviation from ideality is predominantly due to parallel orientation of dipoles in the methanol aggregates and in the complexes with chloroform. The deviations from ideality can also be explained in terms of the heterogeneity at a microscopic level[187,188] and the self association of alcohol molecules.[189] This homonuclear or heteronuclear clustering of molecules has been attributed to large negative excess entropy of MeOH-$CHCl_3$ mixture.[179] Recently Bhattacharyya *et al.*[190] measured the thermal-lens signals as a function of relative proportion of binary solvent mixtures and proposed its dependence on the extent of interaction between the molecules of the solvent mixtures.

In spite of the large number of studies, the experimental determination of the nature of solvation cage in the binary solvent mixture has not yet been well established. In the present contribution, we throw light on the origin of synergism in MeOH-$CHCl_3$, MeOH-CH_2Cl_2, and *t*-BuOH-CH_2Cl_2 binary solvent mixtures using electronic spectroscopy, refractive index measurements, proton NMR measurements and fluorescence quenching study. The probe dependent behavior of the solvation shell was also studied and its impact was discussed.

3.2 Results and Discussion

3.2.1 Absorption and Emission Study in Different Binary Solvent Mixtures

The absorption spectra of organic dyes viz. Coumarin 480 (C480), Coumarin 153 (C153), 4-(dicyanomethylene)-2-methyl-6-(4-dimethylaminostyryl)-*4H*-pyran (Pyran), 4-aminophthalmide (4-AP), and *p*-nitroaniline (*p*NA) (see in Fig. 3.1) were measured in

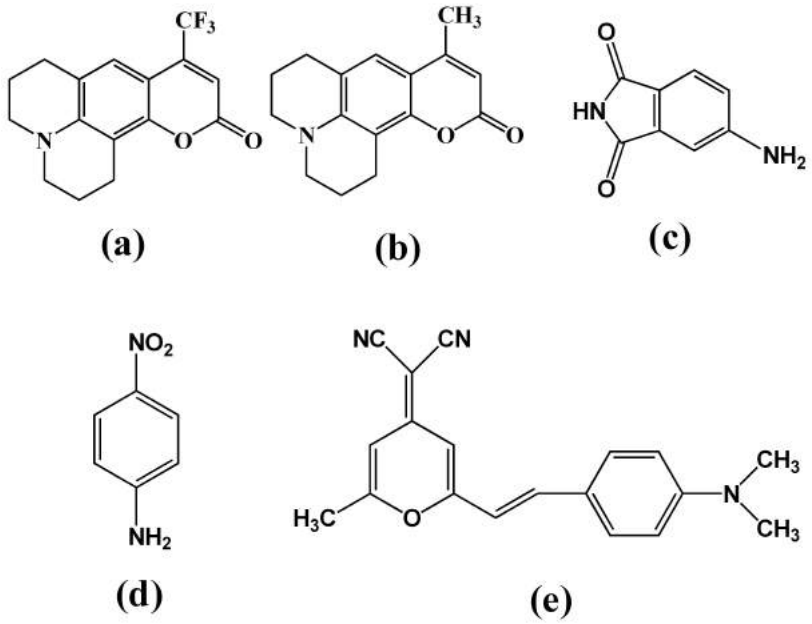

Fig. 3.1

Molecular structures of (a) Coumarin 153 (C153), (b) Coumarin 480 (C480), (c) 4-aminophthalmide (4-AP), (d) *p*-nitroaniline (*p*NA) and (e) 4-(dicyanomethylene)-2-methyl-6-(4-dimethylaminostyryl)-*4H*-pyran (Pyran) used this study.

several binary solvent mixtures of different compositions. In the present work, we studied different binary solvent mixtures of alcohols and chlorinated methanes (alcohol = methanol (MeOH), tert-butanol (*t*-BuOH); chlorinated methane = carbon tetrachloride (CCl_4), chloroform ($CHCl_3$), Dichloromethane (CH_2Cl_2)). The concentration of dyes was maintained at $\sim 10^{-5}$ M to suffice very negligible solute-solute interactions such that intersolute effect makes no significant contribution to the solvent-solvent interactions. In order to portray the stability of different dyes in the corresponding binary mixtures, we invoke the concept of molar electronic transition energy, E_T (kcal mol^{-1}) whose relationship with absorption

maximum (λ_{max}) is given as[191,192]

$$E_T = \frac{28591}{\lambda_{max}} \tag{3.1}$$

In an ideal case, where all solvent-solvent interactions are considered to be equal, the dyes are characterized by maximum value of molar electronic transition energy given by[153,163]

$$E_T(ideal) = X_{S_1} E_{T(S_1)} + X_{S_2} E_{T(S_2)} \tag{3.2}$$

where X_{S_1} and X_{S_2} are mole fractions of solvent 1 and solvent 2 respectively and $E_{T(S_1)}$ and $E_{T(S_2)}$ are E_T values of a dye or indicator solute in pure solvents 1 and 2. From this equation, it follows that in an ideal binary solvent mixture, the variation of E_T as a function of mole fraction of any component should always be linear. However generally the variation is not linear, which points toward the existence of some specic/nonspecic interactions between the dye molecule and one of the components of the mixture, which is known as preferential solvation. Apart from this, the deviation from the ideal behavior may also arise from the interaction between the solvent counterparts in the binary solvent mixture, showing a synergistic effect. The absorption spectra of C480 in MeOH, CCl_4, and various

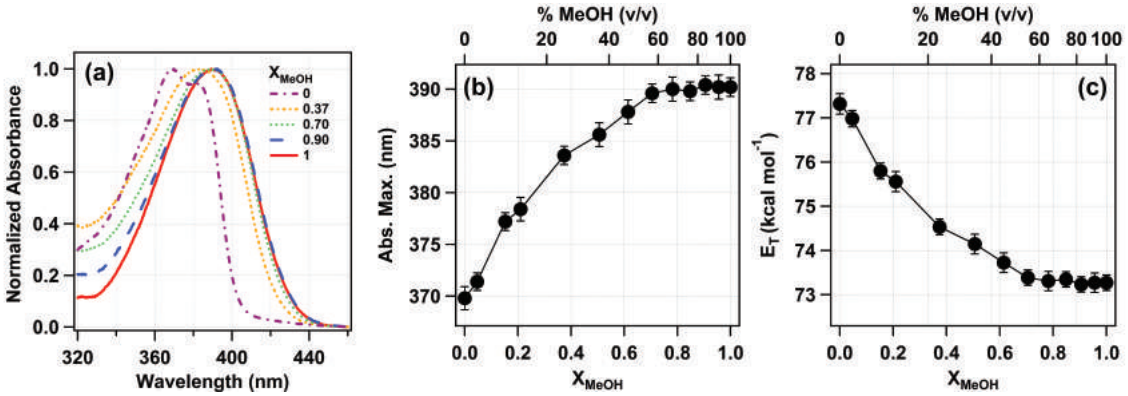

Fig. 3.2

(a) Normalized steady state absorption spectra of C480 in bulk carbon tetrachloride, bulk methanol, and with increasing proportion of MeOH in MeOH-CCl_4 binary solvent mixture. (b) Absorption maxima of C480 plotted against mole/volume fraction of MeOH in MeOH-CCl_4 binary mixture. (c) Molar electronic transition energy, E_T (kcal mol^{-1}) represented against the mole/volume fraction of MeOH in MeOH-CCl_4 binary solvent mixture.

proportions of MeOH-CCl_4 binary mixtures are shown in Fig. 3.2a. C480 is characterized by an absorption maximum of 369.8, 389.6, and 390.2 nm in pure CCl_4, 0.70 mole fraction of MeOH in MeOH-CCl_4 mixture and in pure MeOH. The variation of absorption maxima

and molar electronic transition energy of C480 as a function of mole fraction of methanol in MeOH-CCl_4 binary mixture is shown in Fig. 3.2b and 3.2c. The plot clearly shows that, as the methanol proportion is increased, the absorption maximum keeps on shifting toward the longer wavelength region. The variation of (λ_{max}) with MeOH mole fraction clearly suggests that MeOH molecules are solvating C480 preferentially. In this case, the absorption maxima of C480 in all the mixtures are in between the pure MeOH and CCl_4 with no signature of synergism.

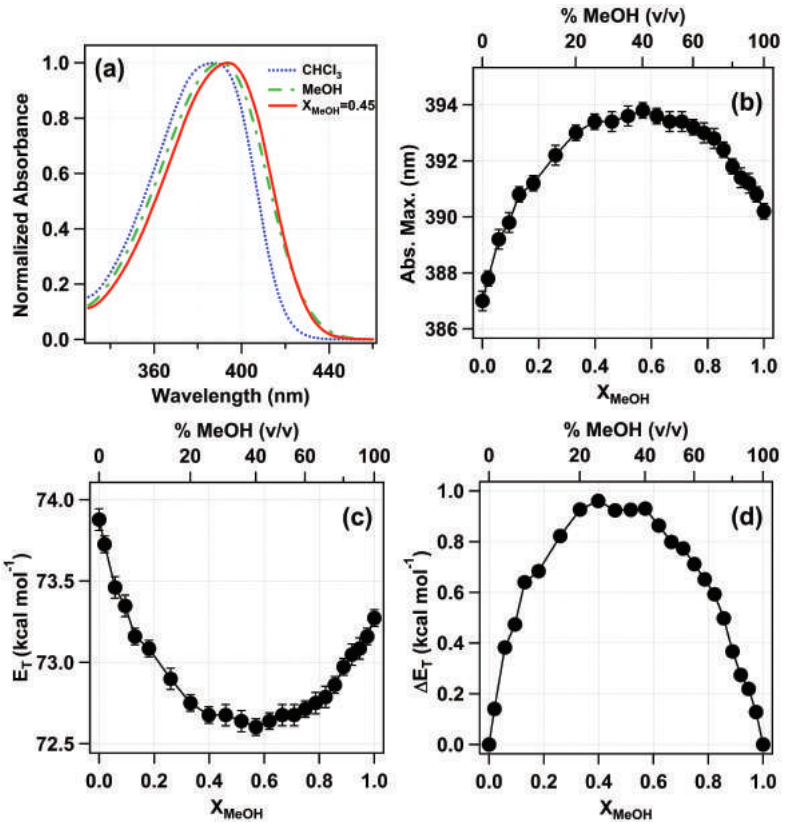

Fig. 3.3

(a) Normalized steady state absorption spectra of C480 in bulk chloroform, bulk methanol, and 0.45 mole fraction of MeOH in MeOH-$CHCl_3$ binary solvent mixture. The respective absorption maxima are 387, 390.2, and 393.4 nm. (b) Absorption maxima of C480 plotted against mole/volume fraction of MeOH in MeOH-$CHCl_3$ binary mixture. (c) Molar transition energy (E_T) of C480 plotted as a function of MeOH mole/volume fraction in MeOH-$CHCl_3$ binary mixture. (d) The difference in molar electronic transition energy ($\triangle E_T$) of C480 in different composition of MeOH-$CHCl_3$ binary solvent mixture as a function of mole/volume fraction of MeOH in MeOH-$CHCl_3$ solvent mixture.

However, once the CCl_4 is being replaced by $CHCl_3$, the variation of absorption maxima as a function of MeOH mole fraction changed unexpectedly. Fig. 3.3a shows the absorption spectra of C480 in MeOH-$CHCl_3$ binary mixture for few different MeOH mole fractions (0.00, 0.45, 1.00). The absorption maximum of C480 in pure $CHCl_3$ and pure MeOH are observed at 387 and 390.2 nm, respectively. However, 0.45 mole fraction of MeOH, the absorption maximum is found at 393.4 nm. This clearly indicates that the MeOH-$CHCl_3$ mixture provides more polar environment and hence solvate C480 more efficiently compared to pure MeOH or $CHCl_3$. The dependence of absorption maximum of C480 as MeOH mole fraction in MeOH-$CHCl_3$ binary solvent mixture is shown in Fig. 3.3b. In terms of molar transition energy, E_T, which gives the direct measure of stabilization energy on account of solvation, the variation is shown as a function of mole fraction of MeOH in MeOH-$CHCl_3$ binary mixture (Fig. 3.3c). It is shown that, maximum stabilization in terms of solvation is obtained at ca. 0.45 mole fraction of MeOH, after deducting the ideal behaviour of the dye in the binary mixture as $E_T(ideal) = X_{S_1}E_{T(S_1)} + X_{S_2}E_{T(S_2)}$ (see in Fig. 3.3d). The efficient solvation carried out by mixed solvent inferences toward the prevalence of mutual solvation around the solvatochromic probe molecule and such a phenomenon is called synergism. This suggests that the binary mixture acts as a different entity than either of the bulk solvents, and its mutual interaction seems to be stronger than the pure bulk solvents. Similar observations were found for C153 and C480 dye in respective MeOH-CH_2Cl_2 and *t*-BuOH-CH_2Cl_2 binary mixture. The dependence of molar transition energy on the mole fraction of MeOH and *t*-BuOH in respective MeOH-CH_2Cl_2 and *t*-BuOH-CH_2Cl_2 binary mixtures are shown in Fig. 3.4a and 3.5a respectively. In both other solvent mixtures cases, the solvatochromic dye is achieved the highest stabilization at near 0.40 mole fraction of MeOH and *t*-BuOH in respective MeOH-CH_2Cl_2 and *t*-BuOH-CH_2Cl_2 binary mixtures, see in Fig. 3.4b and 3.5b. In order to discuss the solvatochromic shifts observed in MeOH-$CHCl_3$ binary solvent mixture quantitatively, we analyzed the data using $E_T^N(30)$ polarity scale with water polarity defined as unity.[191] The aim is to find the total stabilization energy gained by solute molecule from the solvation environment in the MeOH-$CHCl_3$ mixture with strongest interactions, which is $\sim$0.45 mole fraction of MeOH. The absorption maxima of C480 obtained in ten different solvents are plotted against solvent $E_T^N(30)$ values. The data was best fitted by a straight line (Fig. 3.6a). The absorption maxima of C480 in $\sim$0.45 mol fraction MeOH-$CHCl_3$ binary mixture was appended on the line of best linear fit and the observed $E_T^N(30)$ value of this binary mixture was found to be 0.87. This value quantifies the

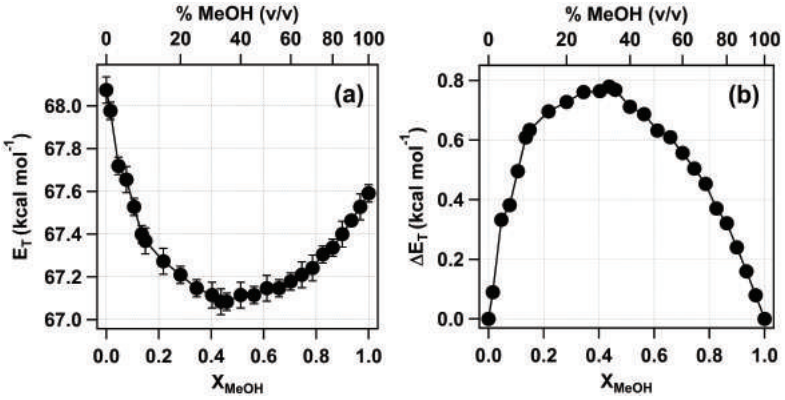

Fig. 3.4

(a) Molar transition energy (E_T) of C153 plotted as a function of MeOH mole/volume fraction in MeOH-CH_2Cl_2 binary mixture. (b) The difference in molar electronic transition energy ($\triangle E_T$) of C153 in different composition of MeOH-CH_2Cl_2 binary solvent mixture as a function of mole/volume fraction of MeOH in MeOH-CH_2Cl_2 solvent mixture.

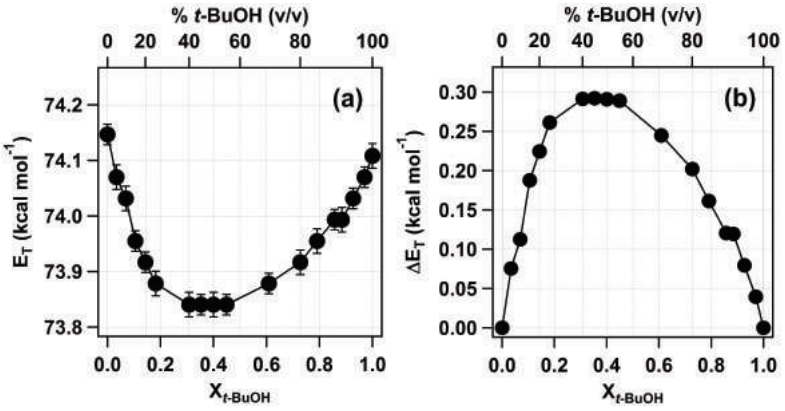

Fig. 3.5

(a) Molar transition energy (E_T) of C480 plotted as a function of *t*-BuOH mole/volume fraction in *t*-BuOH-CH_2Cl_2 binary mixture. (b) The difference in molar electronic transition energy ($\triangle E_T$) of C480 in different composition of *t*-BuOH-CH_2Cl_2 binary solvent mixture as a function of mole/volume fraction of *t*-BuOH in *t*-BuOH-CH_2Cl_2 solvent mixture.

different polarity sensed by C480 in the MeOH-$CHCl_3$ binary mixture and also the different stabilization energy, which is higher than that in pure methanol and chloroform. Similar type of quantitative investigation has been done for other two solvent mixtures (i.e. MeOH-DCM and *t*-BuOH-DCM). From the quantitative analysis, it is observed that maximum stabilization achieved by the solvatochromic dye (i.e. $E_T^N(30)$ value) in MeOH-DCM and *t*-BuOH-DCM binary solvent mixtures was found to be 0.89 and 0.41 respectively (in Fig.

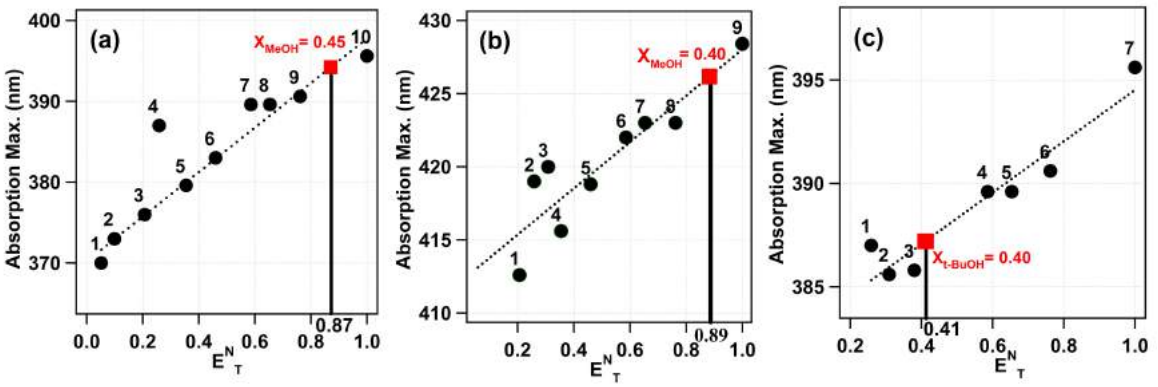

Fig. 3.6

a) Plot of absorption maxima of coumarin 480 in 10 solvents against the solvent E_T^N values (solid black circle). The solvents plotted are carbon tetrachloride (1), toluene (2), THF (3), $CHCl_3$ (4), acetone (5), ACN (6), *n*-butanol (7), ethanol (8), methanol (9), and water (10). The absorption maximum of C480 in $\sim$ 0.45 mol fraction of MeOH in MeOH-$CHCl_3$ binary mixture is appended on the best fit line designated by a solid red square. (b) Similar plot of absorption maxima of C153 in nine different solvents against the solvent E_T^N values (solid black circle). The solvents plotted are THF (1), chloroform (2), DCM (3), acetone (4), ACN (5), *n*-butanol (6), EtOH (7), MeOH (8), and water (9). The absorption maximum of C153 in 0.40 mole fraction of MeOH in respective MeOH-DCM binary mixture is appended on the best fit line designated by a solid red square. (c) The plot of absorption maxima of C480 in seven different solvents against the solvent E_T^N values (solid black circle). The solvents plotted are chloroform (1), DCM (2), *tert*-butyl alcohol (3), *n*-butanol (4), EtOH (5), MeOH (6), and water (7). The absorption maximum of C480 in 0.40 mole fraction of *t*-BuOH in *t*-BuOH-DCM binary mixture is appended on the best fit line designated by a solid red square. Solid black dash line in all plots represents the best fit of the data. Vertical solid black line represents the corresponding value experienced by solvatochromic dye in the (a) $\sim$ 0.45 mole fraction of MeOH in the MeOH-$CHCl_3$ binary mixture, (b) 0.40 mole fraction of MeOH in MeOH-DCM binary mixture and (c) 0.40 mole fraction of *t*-BuOH in *t*-BuOH-DCM binary mixture.

3.6b and 3.6c). This study strongly refers that the maximum stabilization energy achieved by solvatochromic dye from the solvation environment in the binary mixture with strongest interactions, which is same as analyzed by absorption studies. To ensure whether the type of solvation occurring in the binary system (preferential or synergistic) is purely a function of intra/intersolvent interactions or it as well shows some dependence on the probe molecule, probe dependent spectrophotometric measurements were pursued in the MeOH-$CHCl_3$ binary mixtures with Pyran, 4-AP, and *p*NA as the corresponding probe molecules. The variation of molar transition energy of all the probe molecules mentioned above are plotted against

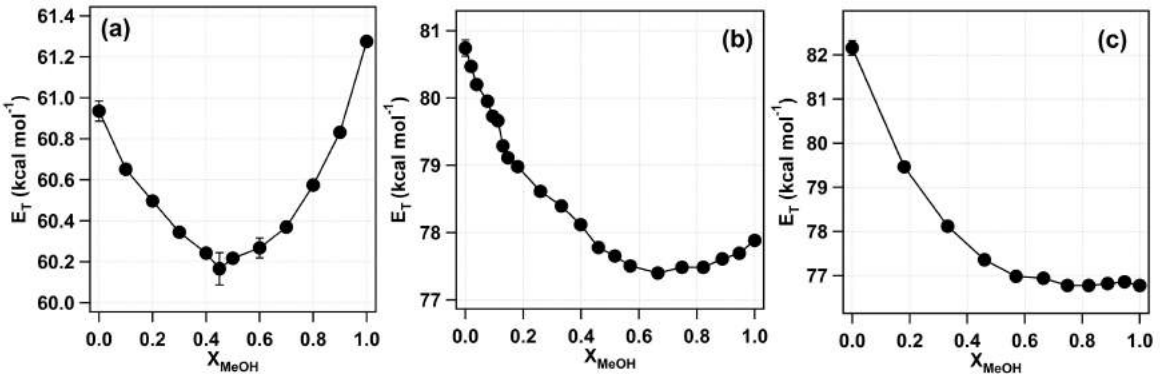

Fig. 3.7

Molar transition energy (E_T) plotted of different probe molecules; (a) Pyran, (b) 4-AP, and (c) *p*NA against the mole fraction of MeOH in MeOH-$CHCl_3$ binary mixture. In graphs (a) and (b), maximum solvatochromic stabilization to the dye in the ground state is provided by binary mixture instead of either of bulk solvents and is thus a representation of synergistic solvation. While as in case of *p*NA, MeOH molecules are solvating the probe preferentially, as the stabilization provided by binary mixture is same as that provided by bulk methanol.

the mole fraction of MeOH as shown in Fig. 3.7. It is observed that, for Pyran and 4-AP (like C480) the large solvatochromic stabilization is deciphered by the MeOH-$CHCl_3$ binary mixture instead of pure solvent counterparts. However, this is the not the case with *p*NA. In *p*NA, the ground state solvatochromic stabilization offered by the binary solvent mixture does not exceed than the bulk counterpart. This intriguing result enunciates that the types of solvation not only depends on intra/inter solvent interactions, but also on the property of the probe molecules. The plots shown in Fig. 3.8 represent the dependence of emission maxima of C480, Pyran and 4-AP in MeOH-$CHCl_3$ binary mixture of different compositions. In all cases, it is well evident that the excited state solvatochromic stabilization provided by the binary mixture does not exceed than the bulk $CHCl_3$ and MeOH. Similar excited state observation has been noticed for both MeOH-DCM and *t*-BuOH-DCM binary solvent mixtures (depicted in Fig. 3.9).

The prevalence or absence of synergism is credited to the feasibility of hydrogen bonding network formation. The components of a binary mixture which are capable of forming hydrogen bonding network with each other tend to solvate the probe molecules synergistically, while as if the solvent molecules fail to create any hydrogen bonding network, then under those conditions either of the two solvents will solvate the probe molecule preferentially and hence no synergism is being observed. This is the reason that we do not observe any

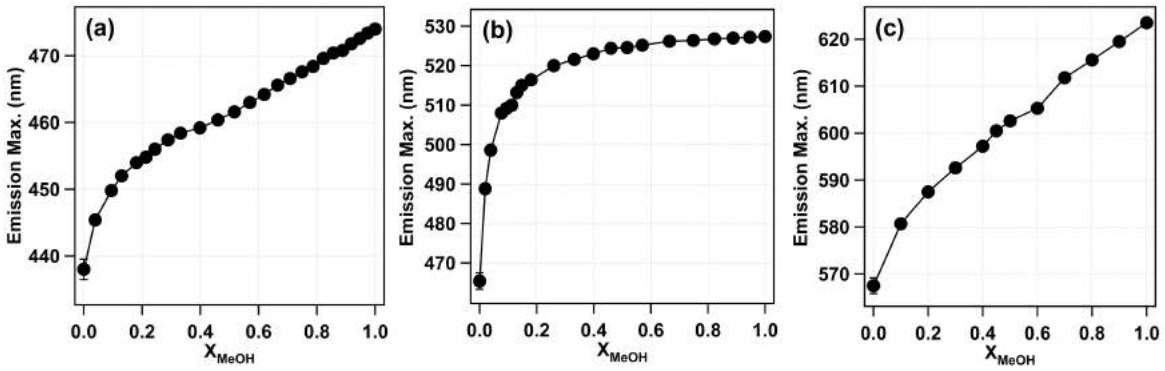

Fig. 3.8

Emission maxima of (a) C480 and (b) 4-AP (c) Pyran dyes plotted against mole fraction of MeOH in MeOH-$CHCl_3$ binary mixture. It is clearly evident that, in all cases, the excited state is being solvated preferentially.

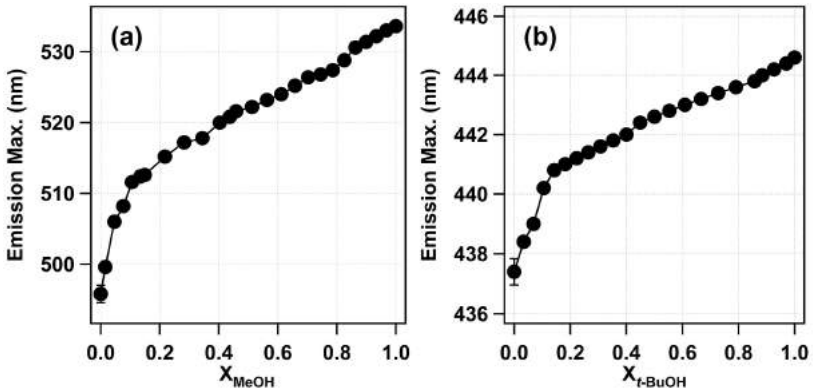

Fig. 3.9

(a) Fluorescence maxima of C153 dye plotted against mole fraction of MeOH in MeOH-DCM binary mixture. (b) Emission maxima of C480 probe molecule drawn against the mole fraction of *t*-BuOH in *t*-BuOH-DCM binary mixture.

synergism in the case of the MeOH-CCl_4 binary mixture, as CCl_4 tends to have zero hydrogen bond donating ability, and hence the formation of a hydrogen bonding network is absent. Once CCl_4 is replaced by $CHCl_3$ or DCM, due to the presence of hydrogen, this molecule acts as a potential hydrogen donor for the formation of hydrogen bond with the oxygen of alcohol molecules results in the formation of Alcohol-Chlorinated methane molecular association. Hence Alcohol-Chlorinate methane binary mixture exists as a continuous network held by hydrogen bonds and the clusters of the binary mixture incline to solvate probe molecules synergistically.

Compounds	μ_g (D)	μ_e (D)
***p*NA**	8.80	
C480	6.38	13.10
Pyran	5.60	26.30
4-AP	5.00	10.60

Table 3.1
Ground and Excited state dipole moments of different probe molecules used in the study.[193–196]

Solvent	α	β	π^*
Methanol	93	62	60
***tert*-Butanol**	68	101	41
Chloroform	44	00	58
Dichloromethane	30	00	82
Carbon tetrachloride	00	00	28

Table 3.2
Kamlet-Taft parameters of organic solvents used in the measurements; HBD ability (α), HBA ability (β), polarity/polarization (π^*).[164,165]

In addition to hydrogen bonding network formation in the binary mixture, the dipole moment of probe molecules also plays an important role in deciding the nature of solvation. Generally, the nature of solvation around a probe molecule is decided by the structure of solvation sphere around it, when the dipole moment of probe molecule is small, as in the case of ground state of solvatochromic molecules (Table 3.1), the structure of binary solvent mixture held intact by hydrogen bonding network, remains rigid in the solvation sphere. The intersolvent clusters are no longer perturbed, which consequently provides enough stabilization to the system with the resulting synergism as the main form of solvation. In case of *p*NA, the ground state dipole moment being comparatively large, will create enough perturbation in its immediate surroundings. These induced perturbations destabilize the binary solvent MeOH-$CHCl_3$ molecular association in such a way that, it doesn't permit the formation of binary solvation layer and hence instead of solvating the *p*NA synergistically, only one solvent among the two components will solvate the probe preferentially. This phenomenon is also supported by the absence of any synergism observed through fluorescence study for all probe molecules under consideration. The excited state dipole moment of C480,

Pyran and 4-AP is larger than the ground state, which is eventually characterized by the generation of large perturbation in the excited state, and consequently, either of the solvents will preferentially solvate the excited state and thus no synergism is observed.

3.2.2 Molar Refractivity Measurements

Refractive index measurements were carried out in order to confirm the intercomponent interactions in the binary mixture. The molar refractivity is a characteristic of the molecular structure of binary solvent mixture and is both an additive and a constitutive property. The molar refractivity ($cm^3\ mol^{-1}$) of a binary mixture is given by[197]

$$R_{exp} = \frac{(n^2-1)}{(n^2+2)}\left(\frac{X_{S_1}M_{S_1} + X_{S_2}M_{S_2}}{\rho}\right) \tag{3.3}$$

where n, X_{S_1}, X_{S_2}, M_{S_1}, M_{S_2} and ρ are the refractive index of solvent mixture, mole fraction of solvent 1 and 2, molar masses of solvent 1 and 2 and the density of mixed solvents, respectively. If we consider that the two solvent components interact ideally with each other, then their molar refractivity, called as ideal molar refractivity ($cm^3\ mol^{-1}$) is given by following equation

$$R_{ideal} = \frac{(n_{S_1}^2-1)}{(n_{S_1}^2+2)}\left(\frac{X_{S_1}M_{S_1}}{\rho_{S_1}}\right) + \frac{(n_{S_2}^2-1)}{(n_{S_2}^2+2)}\left(\frac{X_{S_2}M_{S_2}}{\rho_{S_2}}\right) \tag{3.4}$$

where the symbols have their usual meaning. The difference between the experimentally obtained molar refractivity values and ideal refractivity will give us the magnitude of interactions between the two solvent components:

$$\triangle R = R_{Exp} - R_{ideal} \tag{3.5}$$

Since molar refractivity is a direct measure of electron polarization induced by the influence of constituent solvent molecules on each other in the binary mixture, as the value of $\triangle R$ exceeds $\sim$0.1, it will direct us towards the molecular interactions shared by solvent molecules with respect to each other. Fig. 3.10 shows the variation of $\triangle R$ against the mole fraction of MeOH in respective MeOH-$CHCl_3$ and MeOH-DCM binary mixtures with maximum deviation being observed at ca. X_{MeOH} = 0.45 and 0.40 in their respective mixtures. This comprehends that the electronic clouds of the constituent binary molecules interact to the maximum extent at $\sim$0.45 mole fraction of MeOH in the MeOH-$CHCl_3$ binary mixture. Similar behavior is as well observed for MeOH-DCM binary mixtures where the maximum extent is at $\sim$0.40 mole fraction of MeOH in MeOH-DCM binary solvent mixture. These

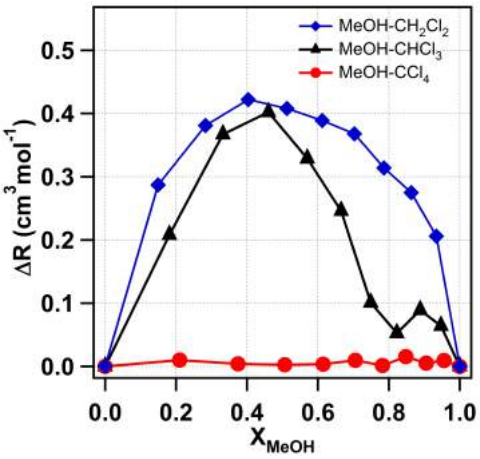

Fig. 3.10

Molar refractivity difference ($\triangle R$) between the experimental and theoretical values in MeOH-$CHCl_3$, MeOH-DCM and MeOH-CCl_4.

varied electronic polarizations generated by the differential proportions of the components of binary mixtures interact with the solute molecules to a varied extent and hence result in shift of the absorption maxima. However, such kind of behavior was not experienced by the dye molecules in MeOH-CCl_4 binary mixture, where preferential solvation of the dye molecule by MeOH is observed in the binary mixture. Thus, molar refractivity measurements act as a deterministic tool to probe the interaction of solvent binary mixtures with the solute molecules, especially in terms of the nature of solvation. From refractivity data, as mentioned earlier the maximum interactions between the solvent components in the binary mixture occurs and from absorption measurements, the maximum deviation is also observed at the same mole fraction and hence supports the involvement of synergistic nature of solvation.

3.2.3 Proton-NMR Study of Binary Solvent Mixtures

To furnish a deeper and more relevant understanding about the microscopic structure of binary solvent mixture, proton-nuclear magnetic resonance (^{1}H-NMR) measurements were carried out. As observed in the absorption spectroscopic and molar refractivity measurements, there is definitely a kind of interaction prevailing between molecules of different solvents which is distinct than the intrasolvent interactions leading to the deviation of molar refractivity from ideality. In alcohol-chlorinated methane binary mixture, the solvent molecules interact through the formation of hydrogen bonding network and hence as the proportion of either of the components is changed, the local electronic cloud around the hydrogen bonded hydrogen

atoms of each solvent changes and was directly observed as a change in the chemical shift. This change in chemical shift of proton of alcohol and chlorinated methane in the binary mixture provides a direct evidence of alcohol-chlorinated methane network formation. The nature of network between alcohol and chlorinated methane molecules is estimated by ^{1}H-NMR models and already briefly discussed in chapter 2.

(a) Proton-NMR Study of MeOH-$CHCl_3$ Binary Solvent Mixture

(a.i) Model for Chloroform Proton in MeOH-$CHCl_3$ Binary Mixture

The observed chemical shift (δ_{obs}) of $CHCl_3$ proton in binary mixture was found to shift toward the upfield region with increase in proportion of $CHCl_3$ as shown in Fig. 3.11b. In pure chloroform, the $CHCl_3$ molecules exist as self-aggregate.[198] It is presumed that the increasing the proportion of MeOH in the binary mixture results in the loss of self-association of $CHCl_3$ molecules and leads to the formation of H-bond between $CHCl_3$ and MeOH. In MeOH-$CHCl_3$ binary mixture, the observed chemical shift of $CHCl_3$ proton is taken as a linear combination of chemical shift of self-associated chloroform molecules (δ^{CC}) and chemical shift of $CHCl_3$ proton hydrogen-bonded to MeOH (δ^{CM}) (the equation for chemical shift of proton position thoroughly is discussed in chapter 2) and can be written as

$$\delta_{obs} = \delta^{CM} + \frac{X^I_{CC}}{X_C}(\delta^{CC} - \delta^{CM}) \tag{3.6}$$

The mole fraction of $CHCl_3$ can be describe as

$$X_C = X^I_{CC} + X^I_{CM} \tag{3.7}$$

where X^I_{CC}, X^I_{CM}, and X_C are the mole fraction of $CHCl_3$ in the self-aggregate form, fraction of chloroform interacts to MeOH and total mole fraction of $CHCl_3$ in the mixture respectively.

The NMR data set corresponding to the chemical shift of chloroform proton in the MeOH-$CHCl_3$ binary mixture was fitted by equation 3.6 and the fitting of NMR data of $CHCl_3$ proton shown in Fig. 3.11b. After fitting, we calculate the fraction of chloroform interacted to chloroform in the binary mixture of particular composition. Consecutively, the fraction of chloroform interacted to methanol has been calculated from equation 3.7. The calculated value of fraction of chloroform interacted to methanol is plotted against MeOH mole fraction as shown in Fig. 3.11c. The maximum value is found to be 0.56 mol fraction of MeOH.

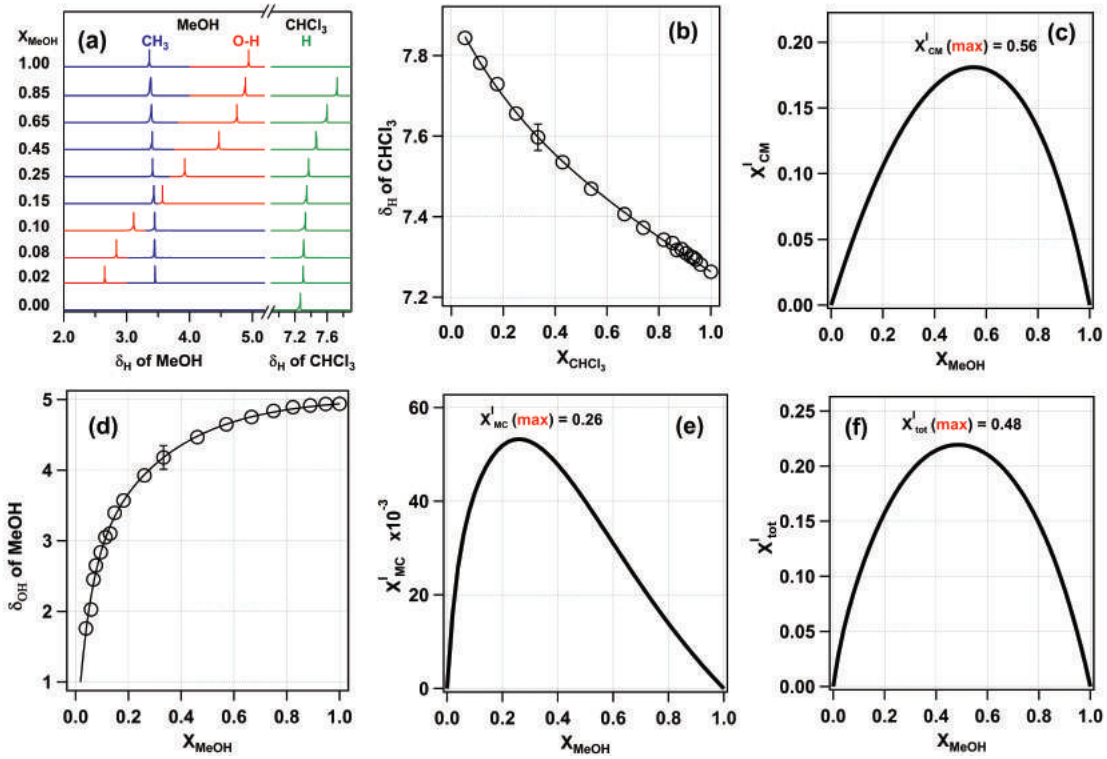

Fig. 3.11

(a) Proton NMR spectra of MeOH-$CHCl_3$ binary mixture. (b) Chemical shift of $CHCl_3$ proton in different proposition of $CHCl_3$. (c) Plot between fraction of $CHCl_3$ interacted to MeOH vs mole fraction of MeOH. (d) Chemical shift of MeOH hydroxy proton in different proposition of MeOH. (e) A plot between fractions of MeOH interacted to $CHCl_3$ vs mole fraction of MeOH. (f) Plot showing total fraction of hydrogen bonding interaction of MeOH-$CHCl_3$ mixture (X^I_{tot}) as a function of mole fraction of MeOH in MeOH-$CHCl_3$ binary mixture. The light black line in graph (b) and (d) are the best fitted lines.

(a.ii) Model for Methanol OH Proton in a MeOH-$CHCl_3$ Binary Mixture

In the same set of binary mixture, not only is there a shift in the chemical shift position of $CHCl_3$ proton but the position of MeOH proton is also getting affected. It is found that the observed chemical shift (δ_{obs}) of MeOH proton in binary solvent mixture is shifted toward the downfield region with increasing MeOH mole fraction. Increasing the proportion of $CHCl_3$ causes the self-aggregation of MeOH molecules to minimize and the interactions with the added $CHCl_3$ molecules to initiate, resulting in the shielding of MeOH proton. The theory to describe this model is based on the same model proposed earlier for chapter 2

and the terms have their usual meanings. The main equation relating the observed NMR chemical shift values with the chemical shift values of MeOH-MeOH self-aggregated and MeOH-$CHCl_3$ interactions is

$$\delta_{obs} = \delta^{MC} + \frac{X^I_{MM}}{X_M}(\delta^{MM} - \delta^{MC}) \tag{3.8}$$

The mole fraction of MeOH can be describe as

$$X_M = X^I_{MM} + X^I_{MC} \tag{3.9}$$

where X^I_{MM}, X^I_{MC}, and X_M are the mole fraction of MeOH in the self-aggregate form, fraction of MeOH interacted to $CHCl_3$, and total mole fraction of MeOH in the mixture.

The fitting of the NMR data by the equation 3.8 is shown in Fig. 3.11d and by substituting the value of X^I_{MM} corresponding to every mole fraction of MeOH, the fraction of MeOH at which strongest interaction between MeOH and $CHCl_3$ molecules exist is furnished as shown in Fig. 3.11e. The maximum in the plot representing the strong hydrogen bonding between $CHCl_3$ and MeOH molecules corresponds to 0.26 mol fraction of MeOH.

Proton NMR analysis suggests that the proportion of MeOH hydrogen interacted to $CHCl_3$ is different from fraction of $CHCl_3$ interacted to MeOH at a particular mole fraction of MeOH in the mixture. The difference in the maximum position of both X^I_{MC} and X^I_{CM} is interpreted in terms of relative aggregation of MeOH with $CHCl_3$ and $CHCl_3$ with MeOH and it turns out to be an extended hydrogen bond network is being formed between MeOH and $CHCl_3$ with a ratio of MeOH:$CHCl_3$ = 1:2.15. On the basis of the above analysis, it is proposed that in a binary mixture of MeOH-$CHCl_3$, one MeOH molecule is associated with ca. two $CHCl_3$ molecules through hydrogen bonding and one $CHCl_3$ molecule is hydrogen bonded to one MeOH molecule. The total interaction may be simply calculated by summing X^I_{MC} and X^I_{CM} as

$$X^I_{tot} = X^I_{MC} + X^I_{CM} \tag{3.10}$$

A plot of X^I_{tot} as a function of X_{MeOH} will eventually determine the mole fraction of MeOH corresponding to strongest hydrogen bond networking in the MeOH-$CHCl_3$ binary mixture, and the value is found to be 0.48 (as shown in Fig. 3.11f), which is the approximately the same value obtained from refractivity measurements $[X_{MeOH}(\triangle R^{max}) = 0.45]$, and from the UV-vis absorption study of a solvatochromic dye $[X_{MeOH}(\triangle E^{min}_T) = 0.45]$. Thus, we propound that the addition of MeOH to $CHCl_3$ introduces microscopic heterogeneity in the resulting binary solvent mixture.

(b) Proton-NMR Study of MeOH-DCM Binary Solvent Mixture

(b.i) Model for Dichloromethane Proton in MeOH-DCM Binary Mixture

The position of the observed chemical shift (δ_{obs}) of DCM protons in the binary mixture was found to shift towards the down-field region with increase in proportion of MeOH as shown in Fig. 3.12a. In MeOH-DCM binary mixture, the observed chemical shift of DCM proton has been taken as a linear combination of chemical shift of DCM non-interacting with MeOH (δ_{obs}) and chemical shift of DCM proton interacting to MeOH (δ_{obs}). As described in chapter 2, δ_{obs} can be written as

$$\delta_{obs} = \delta^{DM} + \frac{X^I_{DD}}{X_D}(\delta^{DD} - \delta^{DM}) \tag{3.11}$$

The mole fraction of DCM in the mixture can be written as

$$X_D = X^I_{DD} + X^I_{DM} \tag{3.12}$$

where X^I_{DD}, X^I_{DM} and X_D are respectively the mole fraction of DCM interacting with DCM, fraction of DCM interacting with MeOH and total mole fraction of DCM in the mixture.

The NMR data set corresponding to the chemical shift of DCM proton in the MeOH-DCM binary mixture was fitted by equation 3.11 and the fitting of NMR data of DCM proton shown in Fig. 3.12a. The fraction of DCM interacted to MeOH is plotted against MeOH mole fraction as shown in Fig. 3.12b. It is observed that the maximum value is found near 0.44 mole fraction of MeOH.

(b.ii) Model for Methanol -OH Proton in a MeOH-DCM Binary Mixture

It is observed that chemical shift (δ_{obs}) of MeOH hydroxyl proton in binary solvent mixture was shifted towards the down field region with increasing MeOH mole fraction. Same as before, increasing proportion of DCM possibly ruptures the aggregation of MeOH molecules and the interactions start between the added DCM molecules with MeOH, resulting in the shielding of MeOH hydroxyl proton. The basic theory to describe this model is based on the same argument, which has been proposed in chapter 2. The main equation is relating the observed chemical shift values of MeOH hydroxyl proton can be written as

$$\delta_{obs} = \delta^{MD} + \frac{X^I_{MM}}{X_M}(\delta^{MM} - \delta^{MD}) \tag{3.13}$$

The mole fraction of MeOH can be described as

$$X_M = X^I_{MM} + X^I_{MD} \tag{3.14}$$

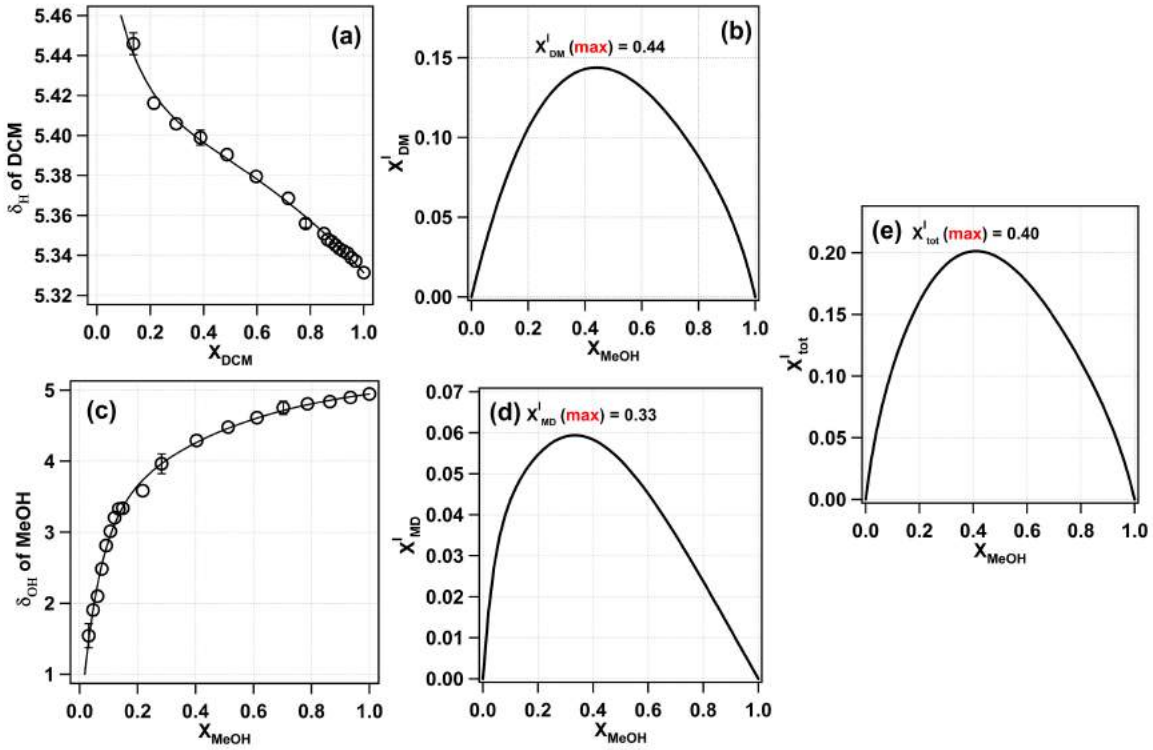

Fig. 3.12

^{1}H-NMR data of DCM in MeOH-DCM binary mixtures (a) Chemical shift of DCM protons in different proposition of MeOH (b) plot between fractions of DCM interacted to MeOH vs. mole fraction of MeOH. (c) Chemical shift of MeOH hydroxyl proton in different proposition of MeOH (d) A plot between fractions of MeOH interacted to DCM vs. mole fraction of MeOH. (e) Plot showing total hydrogen bonding interaction between MeOH-DCM molecules in mixture (X^I_{tot}) as function of mole fraction of MeOH in MeOH-DCM binary mixture. The light black line in graph (a) and (c) are the best fitted lines.

where all terms have usual meaning described in chapter 2. The fitting of the NMR data by the equation 3.13 is shown in Fig. 3.12c. From the fitting, it is evident that the position of δ^{MD} maxima is found approximately at 0.33 mole fractions of MeOH. (See in Fig. 3.12d)

It is very clear from these fitting models that the fraction of MeOH interacted to DCM is different from fraction of DCM interacted to MOH and the ratio between δ^{DM} and δ^{MD} is approximately 1:1.33. Above analysis proposed that in MeOH-DCM binary mixture on an average one MeOH molecule is associated with 1.33 DCM molecules through hydrogen bonding network. The total interaction may be simply calculated by summing δ^{DM} and δ^{MD} as

$$X^I_{tot} = X^I_{DM} + X^I_{MD} \tag{3.15}$$

A plot of X^I_{tot} as a function of X_{MeOH} will finally determine the mole fraction of MeOH corresponding to strongest hydrogen bond networking in the MeOH-DCM binary mixture, and the value is found to be 0.40 (as shown in Fig. 3.12e), which is same value obtained from UV-vis absorption study of the solvatochromic dye (C153) $[X_{MeOH}(\triangle E^{min}_T) = 0.40]$. To reconfirm the observed data, the difference between the experimentally obtained molar refractivity values and ideal refractivity ($\triangle R$) has been calculated. The plot of $\triangle R$ vs. the mole fraction of MeOH is shown in Fig. 3.10. The maximum value of the change in molar refractivity is found to be at 0.40 mole fraction of MeOH $[X_{MeOH}(\triangle R^{min}) = 0.40]$.

(c) Proton-NMR Study of *t*-BuOH-DCM Binary Solvent Mixture

(c.i) Model for Dichloromethane Proton in *t*-BuOH-DCM Binary Mixture

The position of the observed chemical shift (δ_{obs}) of DCM protons in the binary mixture was found to shift towards the downfield region with increase in composition of *t*-BuOH as shown in Fig. 3.13a. Here, the observed chemical shift of DCM proton were taken as a linear addition of chemical shift of DCM non-interacting with *t*-BuOH (δ^{DD}) and chemical shift of DCM proton hydrogen-interacted to *t*-BuOH (δ^{DB}) as (already explained in chapter 2)

$$\delta_{obs} = \delta^{DB} + \frac{X^I_{DD}}{X_D}(\delta^{DD} - \delta^{DB}) \tag{3.16}$$

The mole fraction of DCM in *t*-BuOH-DCM binary mixture can be describe as

$$X_D = X^I_{DD} + X^I_{DB} \tag{3.17}$$

where, X^I_{DD}, X^I_{DB}, and X_D are respectively the mole fraction of DCM interacting with DCM, mole fraction of DCM interacting with *t*-BuOH and total mole fraction of DCM in the mixture.

The NMR data set corresponding to the chemical shift of DCM proton in the *t*-BuOH-DCM binary mixture was fitted by equation 3.16 and the fitting of NMR data of DCM proton shown in Fig. 3.13a. The fraction of DCM interacted to *t*-BuOH is plotted against *t*-BuOH mole fraction as shown in Fig. 3.13b. It is observed that the highest value is found near 0.48 mole fraction of *t*-BuOH.

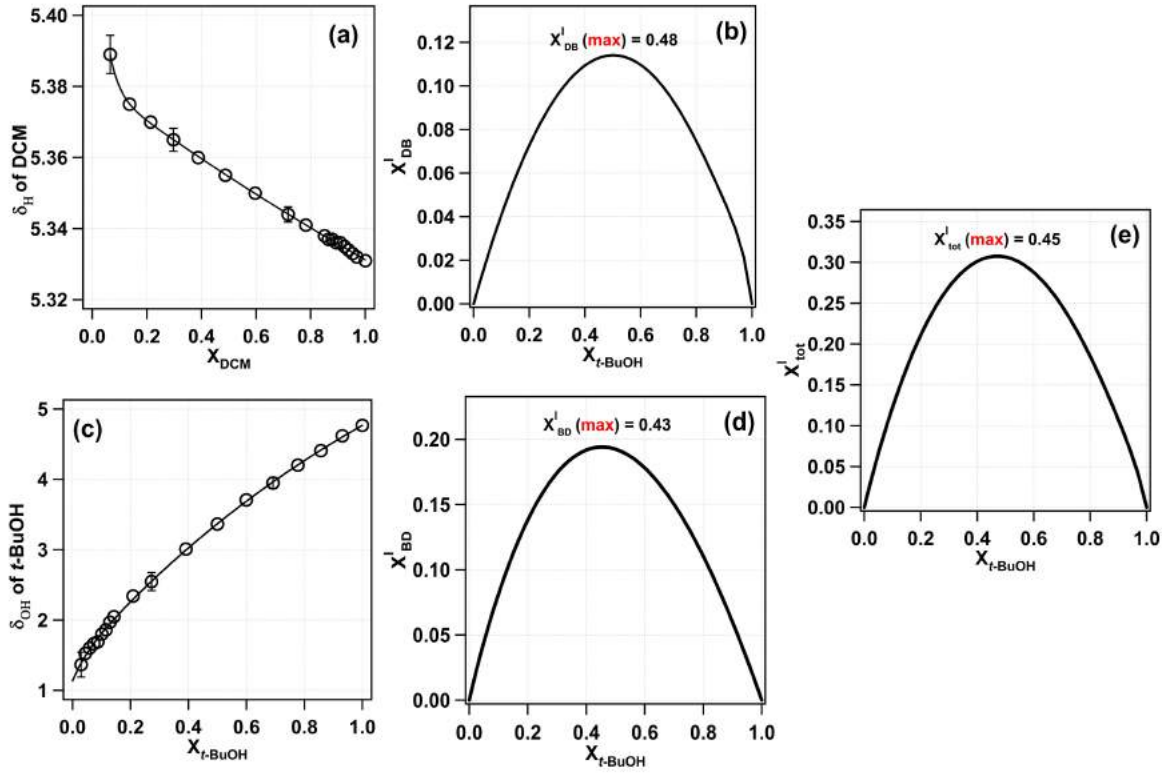

Fig. 3.13

^{1}H-NMR data of DCM in *t*-BuOH-DCM binary mixtures (a) Chemical shift of DCM protons in different composition of *t*-BuOH (b) plot between fractions of DCM interacted to *t*-BuOH vs. mole fraction of *t*-BuOH. (c) Chemical shift of *t*-BuOH hydroxy proton in different proposition of *t*-BuOH (d) A plot between fractions of *t*-BuOH interacted to DCM vs. mole fraction of *t*-BuOH. (e) Plot showing total hydrogen bonding interaction between *t*-BuOH-DCM molecules in mixture (X^I_{tot}) as function of mole fractions of *t*-BuOH in *t*-BuOH-DCM binary mixture. The light black line in graph (a) and (c) are the best fitted lines.

(c.ii) Model for tert-Butyl alcohol Hydroxyl Proton in *t*-BuOH-DCM Binary Mixture

The similar observations have been viewed with hydroxyl proton of tert-butyl alcohol with increasing proposition of *t*-BuOH in *t*-BuOH-DCM. The chemical shift (δ_{obs}) of *t*-BuOH hydroxyl proton in binary solvent mixture has been found to shift towards the down field region with increasing *t*-BuOH mole fraction. Same as earlier, increasing proportion of DCM possibly break off the accumulation of *t*-BuOH molecules and the interactions start between the added DCM molecules with *t*-BuOH, resulting in the shielding of *t*-BuOH hydroxyl proton. The main concept to describe this model is based on the same argument which has

been suggested for DCM protons and chapter 2. The basic form of equation which pertaining the observed chemical shift values of *t*-BuOH hydroxyl proton can be written as

$$\delta_{obs} = \delta^{BD} + \frac{X^I_{BB}}{X_B}(\delta^{BB} - \delta^{BD}) \tag{3.18}$$

where all the terms have usual sense as before described. The measured values of chemical shifts is fitted by equation 3.18 and is shown in Fig. 3.13c. It is clearly evident from fitting that the position of maxima is found ca. at 0.43 mole fractions of *t*-BuOH (see Fig. 3.13d).

It has been elucidated from these analytical models that the fraction of *t*-BuOH interacted to DCM is unlike from fraction of DCM interacted to *t*-BuOH and the ratio between X^I_{DB} and X^I_{BD} is approximately 1:1.12. From above analysis, we proposed that in *t*-BuOH-DCM binary mixture on an average one *t*-BuOH molecule is associated with 1.12 DCM molecules through weak hydrogen bonding network. The total interaction may be simply calculated by adding X^I_{DB} and X^I_{BD} as

$$X^I_{tot} = X^I_{DB} + X^I_{BD} \tag{3.19}$$

The total interaction X^I_{tot} appears in the *t*-BuOH-DCM binary mixture as a function of X_{t-BuOH} determines the mole fraction of *t*-BuOH corresponding to highest hydrogen bond networking in the *t*-BuOH-DCM binary mixture, and the value is found to be 0.45 (as shown in Fig. 3.13e), which is approximately near from UV-vis absorption study of a solvatochromic dye $[X_{t-BuOH}(\triangle E^{min}_T) = 0.40]$. Thus we suggested that the mixing of DCM to *t*-BuOH brings microscopic heterogeneity in the resulting binary solvent mixture.

3.2.4 Solvent Exchange Model for Binary Solvent Mixtures

A solvent exchange model has been developed to correlate the transition energy of solvatochromatic indicator in the solvent mixture.[156–159] In other words, the nature of solvation of the binary solvent mixture towards a solvatochromic probe molecule in the solvation sphere has been characterized by the solvent exchange model (discussed concisely in chapter 2). Solvent exchange model believes two equilibria exist between the solvatochromic probe (P) and solvent molecules (i.e. more polar pure solvent, less polar pure solvent and the interacting solvents complex). This model applies to settle conclusively the behavior of solvation of different binary solvent mixtures used in present study.

(a) Solvent Exchange Model for MeOH-$CHCl_3$ Binary Solvent Mixture

In this case, we have taken a 1:2 stoichiometry ratio for MeOH (M) and $CHCl_3$ (C) (as evident from the ^{1}H-NMR measurement) to construct the solvent exchange model, see in

chapter 2. If we consider formation of MC_2 solvent structure on the microsphere of solvation shell, the *m* model of solvent exchange processes are given as

$$P(C)_{3m} + 3mM \leftrightharpoons P(M)_{3m} + C \tag{3.20}$$

$$P(C)_3m + mM \leftrightharpoons P(MC_2)_m + mC \tag{3.21}$$

For this process, the equilibrium constants are defined as

$$f_{M/C} = \frac{X_M^S/X_C^S}{(X_M^0/X_C^0)^{3m}} \tag{3.22}$$

$$f_{MC_2/C} = \frac{X_{MC_2}^S/X_C^S}{(X_M^0/X_C^0)^m} \tag{3.23}$$

At end, the value of E_T in microsphere of solvation shell of solvent aggregate can be expressed as

$$E_T = E_{TC} + \frac{(E_{TM} - E_{TC}) f_{M/C}(X_M^0)^{3m} + f_{MC_2/C}(E_{TMC_2} - E_{TC})(X_M^0)^m(1 - X_M^0)^{2m}}{(1 - X_M^0)^{3m} + f_{M/C}(X_M^0)^m + f_{MC_2/C}(X_M^0)^m(1 - X_M^0)^{2m}} \tag{3.24}$$

where, X_{MC_2}, X_M and X_C are mole fraction of the resultant solvent aggregate pure solvent MeOH and $CHCl_3$ respectively. $X_{MC_2}^S$, X_M^S, and X_C^S are mole fractions of the solvent aggregate, pure solvents MeOH and $CHCl_3$ in the solvation sphere of the probe molecule, respectively and E_{TM}, E_{TC}, and E_{TMC_2} are the transition energies of solvatochromic probe molecule in pure solvent MeOH, $CHCl_3$ and solvent aggregate MC_2. The present hypothetical model gave a good idea for the synergetic mixtures where values of E_T of mixtures E_{TMC_2} are found to be lower than E_T values of pure solvent. The variation of E_T of C480 as a function of mole fraction of methanol has been fitted with equation 3.24 and is shown in Fig. 3.14. The *m* model gives a more appropriate fitting to the experimental result and also a reasonable explanation of the MeOH-$CHCl_3$ binary solvent mixture properties. The *m* value provides the number of solvent molecules in microsphere of solvation shell of the probe molecule affecting its transition energy. The formation of solvent aggregates in the solvation sphere induces large deviation in polarity (i.e., E_{TMC_2} = 71.9) as compared to bulk counterparts (E_{TM} =73.3 and E_{TC} = 73.9). In the fitting, the value of $f_{MC_2/C}$ is found to be 1.061 where as $f_{M/c}$ is 0.454. This clearly indicate the synergistic behavior of solvation. The result attributes that the strong H-bonding network between hydrogen donor and hydrogen acceptor solvent guided more polar environment in binary solvent system.

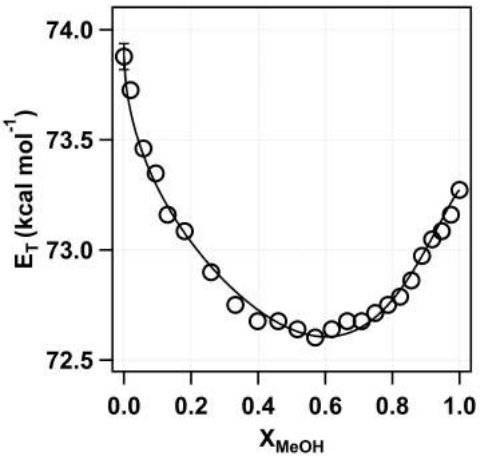

Fig. 3.14

Plot of molar transition energy of C480 plotted as a function of MeOH mole fraction in MeOH-$CHCl_3$ binary mixture. The solid line is the fitting following equation 3.24.

(b) Solvent Exchange Model for MeOH-DCM Binary Solvent Mixture

The solvation behavior of the MeOH-DCM binary solvent mixture towards a solvatochromic probe molecule in the solvation sphere has been analyzed by the 1:1 solvent exchange model (see in chapter 2). A solvent exchange model considers the existence of two solvent exchange equilibria exists between the solvatochromic probe (P) and being solvated by all three different entities ca. more polar solvent MeOH (M), less polar solvent DCM (D) and the hydrogen bonded complex between M and D (i.e. MD). From the ^{1}H-NMR analysis, it has been found that on an average one MeOH molecule is communicating with 1.33 DCM molecules. Assuming 1:1 association, the two proposed equilibria can be written as

$$P(D)_m + mM \leftrightharpoons P(M)_m + mD \tag{3.25}$$

$$P(D)_m + \frac{m}{2}M \leftrightharpoons P(MD)_m + \frac{m}{2}D \tag{3.26}$$

The equilibrium constants of the earlier two processes can be written as

$$f_{M/D} = \frac{X_M^S/X_D^S}{\sqrt{(X_M^0/X_D^0)^m}} \tag{3.27}$$

$$f_{MD/D} = \frac{X_{MD}^S/X_D^S}{\sqrt{(X_{MD}^0/X_D^0)^m}} \tag{3.28}$$

where, $f_{M/D}$ is a measure of the solvatochromic molecule to be more preferentially solvated by MeOH than DCM, while $f_{MD/D}$ quantified the efficacy of the solvatochromic molecule to be synergistically solvated by solvent aggregate rather than the pure solvent counterparts and X_M^S, X_D^S and X_{MD}^S are respectively the mole fractions of MeOH, DCM, and hydrogen bonded complex in the solvation microsphere of probe molecule, whereas X_M^0 and X_D^0 are mole fractions of two pure solvent counterparts in the bulk with the relation

$$\begin{aligned} X_D^0 + X_M^0 &= X_D^S + X_M^S + X_{MD}^S \\ &= 1 \end{aligned} \tag{3.29}$$

The E_T value of the mixed solvent system can be expressed as

$$\begin{aligned} E_T = {} & E_{TD} \\ & + \left[\frac{(E_{TM} - E_{TD})(X_M^0)^m f_{M/D} + (E_{TMD} - E_{TD})(X_M^0)^{m/2}(1 - X_M^0)^{m/2} f_{MD/D}}{(1 - X_M^0)^m + (X_M^0)^m f_{M/D} + (X_M^0)^{m/2}(1 - X_M^0)^{m/2} f_{MD/D}} \right] \end{aligned} \tag{3.30}$$

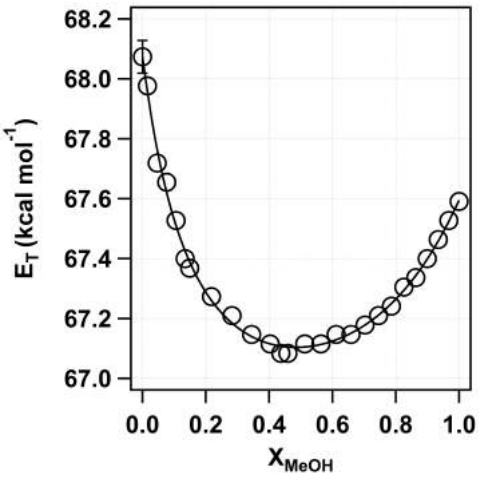

Fig. 3.15

Plot of molar transition energy of C153 plotted against mole fraction of MeOH in MeOH-DCM binary mixture. The solid line is the fitting by equation 3.30.

where, E_{TM}, E_{TD} and E_{TMD} are the molar transition energies of C153 in MeOH, DCM and MeOH-DCM binary solvent mixture respectively. The m value in present model suggests the number of solvent molecules in microsphere of solvation shell of the probe molecule affecting its transition energy. The equation has been used to fit the molar transition energy of C153 in MeOH-DCM binary solvent mixture as a function of MeOH mole fraction as

shown in Fig. 3.15. In present study, the proposed model gave a good idea for the synergetic solvation where value of m is found to be 2.0. The formation of solvent aggregates in the solvation sphere induces large deviation in polarity (estimated E_{TMD} = 58.50) as compared to bulk counterparts (E_{TM} = 67.59 and E_{TD} = 68.07). In the analysis, the value of $f_{MD/D}$ is found to be 7.7 whereas $f_{M/D}$ is found to be 2.2. The observed high value of synergistic parameter (3.5 times more than the preferential parameter) clearly indicates the predominant synergistic behavior of solvation. The result attributes that the H-bonding network between the hydrogen bond donor and the hydrogen bond acceptor solvent accomplish a more polar environment in the binary solvent system.

(c) Solvent Exchange Model for *t*-BuOH-DCM Binary Solvent Mixture

The synergistic behavior of *t*-BuOH-DCM binary solvent mixture towards a solvatochromic probe molecule generates nonlinear characteristics in the molar transition energy (E_T) which results from solvent micro-heterogeneity, i.e. where combined component of mixed solvent prefers to solvate a solvatochromic probe molecule compared to anyone component of binary solvent. The nature of solvation behavior has been examined by solvent exchange model. The interaction between the two pair solvents composite evolves micro-domain complex species, which was inferred by proton NMR analytical study. This study clearly proposed that there exists the possibility of solvation of the probe molecule by micro-domain complex species of ratio 1:1.12. The solvent exchange model assumes two solvent exchange (1:1) equilibria persists between the solvatochromic probe (P) and three distinguishable entities ca. more polar solvent *t*-BuOH (B), less polar solvent DCM (D) and the hydrogen bonded complex species between B and D (i.e. BD). The two proposed equilibria of 1:1 complex species can be written as

$$P(D)_m + mB \leftrightharpoons P(B)_m + mD \tag{3.31}$$

$$P(D)_m + \frac{m}{2}B \leftrightharpoons P(BD)_m + \frac{m}{2}D \tag{3.32}$$

The equilibrium constants of the earlier two processes can be written as

$$f_{B/D} = \frac{X_B^S/X_D^S}{\sqrt{(X_B^0/X_D^0)^m}} \tag{3.33}$$

$$f_{BD/D} = \frac{X^S_{BD}/X^S_D}{\sqrt{(X^0_{BD}/X^0_D)^m}} \tag{3.34}$$

where, $f_{B/D}$ is a measure of the probe to be more preferentially solvated by *t*-BuOH than DCM, while $f_{BD/D}$ quantified the efficacy of the indicator to be synergistically solvated by solvent aggregate rather than the pure solvent and X^S_B, X^S_D and X^S_{BD} are respectively the mole fractions of *t*-BuOH, DCM, and hydrogen bonded complex in the solvation micro-domain of probe molecule, whereas X^0_M and X^0_D are mole fractions of two pure solvents in the relation as

$$\begin{aligned} X^0_D + X^0_B &= X^S_D + X^S_B + X^S_{BD} \\ &= 1 \end{aligned} \tag{3.35}$$

The E_T value of the mixed solvent system can be expressed as

$$\begin{aligned} E_T = {} & E_{TD} \\ & + \left[\frac{(E_{TB} - E_{TD})(X^0_B)^m f_{B/D} + (E_{TBD} - E_{TD})(X^0_B)^{m/2}(1 - X^0_B)^{m/2} f_{BD/D}}{(1 - X^0_B)^m + (X^0_B)^m f_{B/D} + (X^0_B)^{m/2}(1 - X^0_B)^{m/2} f_{BD/D}} \right] \end{aligned} \tag{3.36}$$

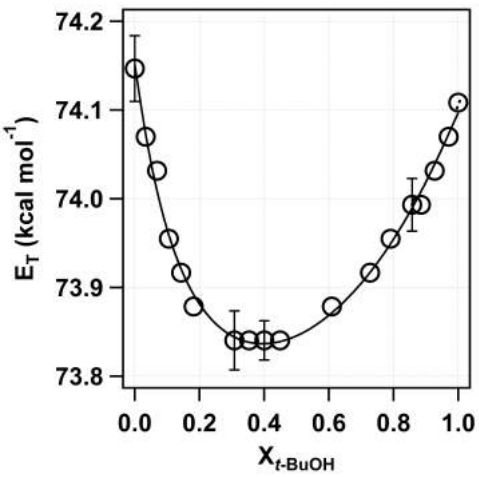

Fig. 3.16

Plot of molar transition energy of C480 plotted against mole fraction of *t*-BuOH in *t*-BuOH-DCM binary mixture. The fitting equation 3.36 is symbolized by solid line.

where, E_{TB}, E_{TD} and E_{TBD} are the molar transition energies of C480 in *t*-BuOH, DCM and *t*-BuOH-DCM binary solvent mixture respectively, and m value suggests the number of solvent molecules in micro-domain of solvation shell of the probe molecule and is found to be 2. The equation has been used to fit the molar transition energy of C480 in *t*-BuOH-DCM

binary solvent mixture as a function of *t*-BuOH mole fraction as shown in Fig. 3.16. The formation of solvent aggregates in the solvation sphere impetus large deviation in polarity (estimated E_{TBD} = 67.861) compare to pure solvents (E_{TB} = 73.991 and E_{TD} = 74.151). In the analysis, the value of $f_{BD/D}$ is found to be 6.5 whereas $f_{B/D}$ is found to be 2.9, which clearly indicates the predominant synergistic behavior of solvation. The result attributes that the specific interaction (i.e. weak H-bonding network between hydrogen bond donor and hydrogen bond acceptor solvent) accomplishes a more polar environment in binary solvent system.

3.2.5 Fluorescence Quenching in MeOH-$CHCl_3$ Binary Solvent Mixture

The presence of quencher can affect the lifetime of fluorophore molecules either through static interactions or through dynamic pathways.[199] Static quenching is a consequence of complexation between fluorophore and quencher molecules, while as dynamic quenching is limited by the diffusion of quencher molecules and thus being a function of solvent property like hydrogen bonding. To know quantitatively the extent of interactions prevailing in the binary solvent mixture of MeOH and $CHCl_3$, the fluorescence quenching study of C480 by 1,2-phenylenediamine (PDA) was done. The dynamic nature of quenching was experimentally observed by measuring the effect of quencher on the lifetime of C480, whose concentration was kept at $\sim$5 μM and the concentration of PDA was varied from 0 to 10 mM in Fig. 3.17a. The observed rates of quenching as a function of mole fraction of MeOH in MeOH-$CHCl_3$ binary mixture were plotted as shown in Fig. 3.17b. In pure $CHCl_3$ the observed value of quenching rate constant is found to be 1.5879 M^{-1}. As the proportion of MeOH in the MeOH-$CHCl_3$ binary mixture increases, the rate constant of quenching first decreased until X_{MeOH} = 0.45, where the deviation from ideality is observed to be maximum (see, Fig. 3.17c) and then increased. In pure MeOH the value of quenching rate constant is found to be 3.13 M^{-1}. As mentioned above, the rate of dynamic quenching is affected by the interaction of quencher with the solvent molecules. In other words, the greater extent of interaction between molecules of binary mixture, the greater restriction they will impose on the movement of quencher toward the fluorophore and hence will retard the rate of quenching. The large deviation in quenching constant observed for $\sim$0.45 mol fraction of MeOH-$CHCl_3$ binary mixture inferences the maximum restriction posed on the diffusion of quencher molecules toward the fluorophore and thus comprehends the existence of stronger hydrogen bonding between MeOH and $CHCl_3$ molecules corresponding to this mole fraction.

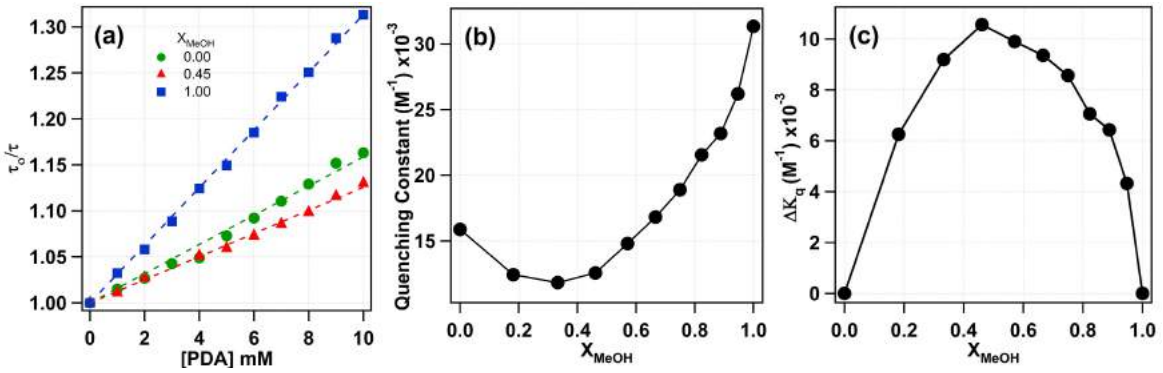

Fig. 3.17

(a) Stern-Volmer plots of C480 with 1,2-phenylenediamime used as a quencher in bulk MeOH, bulk $CHCl_3$ and ~ 0.45 mole fractions of MeOH in MeOH-$CHCl_3$ binary mixture. (b) Plot showing variation of fluorescence quenching constant (k_q) with respect to the mole fraction of MeOH in MeOH-$CHCl_3$ binary mixture. (c) The difference of the experimental value of quenching constant and the ideal value showing maximum deviation for ~ 0.45 mole fraction of MeOH in MeOH-$CHCl_3$ binary mixture.

This observation supports the existence of stronger MeOH-$CHCl_3$ intermolecular interactions observed through UV-vis spectroscopy, ^{1}H-NMR and refractivity measurements.

3.3 Conclusion

UV-vis absorption spectroscopy using solvatochromic probe molecules, molar refractivity and proton-NMR measurements were pursued to explore the structure and solvation behaviour of binary solvent mixture. A strong synergistic solvation was observed for the mixtures of hydrogen bond donating (e.g., chloroform, dichloromethane) and accepting solvent (e.g., alcohols like methanol, *tert*-butanol) pairs, which causes solvatochromic probe molecules to sense increased polarity compared to the bulk counterparts. Such strong synergism was not observed when chloroform or dichloromethane was replaced by carbon tetrachloride. The origin of the strong synergism was explained in terms of solvent-solvent interactions as evidenced from probe dependence, molar refractivity, proton NMR measurements, and solvent exchange model. The solvation behavior of binary mixture shows strong probe dependence with no synergism observed when *p*-nitroaniline was taken as the solvatochromic probe, which is ascribed to the higher ground state dipole moment of *p*-nitroaniline (8.8 D) relative to C480 (6.3 D). Surprisingly, the synergistic signature is no longer observed for solvatochromic probe in binary mixture employing fluorescence measurements, which is substantiated by higher excited state dipole moment. Such strongly perturbed systems (due

to high dipole moment) do not allow persistence of hydrogen bonding network, resulting in preferential solvation instead of synergism. The analysis of proton-NMR data corresponding to chloroform and methanol protons suggest the structure of binary solvent mixture through the existence of about two hydrogen bonds per methanol molecule and single hydrogen bond for each chloroform molecule. However, the solvent structure of other two binary solvent systems persists in ca. 1:1 stoichiometric ratio as infered from ^{1}H-NMR analysis. Diffusion controlled dynamic quenching of C480 fluorescence by 1,2-phenylenediamine in the MeOH-$CHCl_3$ binary solvent mixture also suggested the presence of strong H-bonding network.

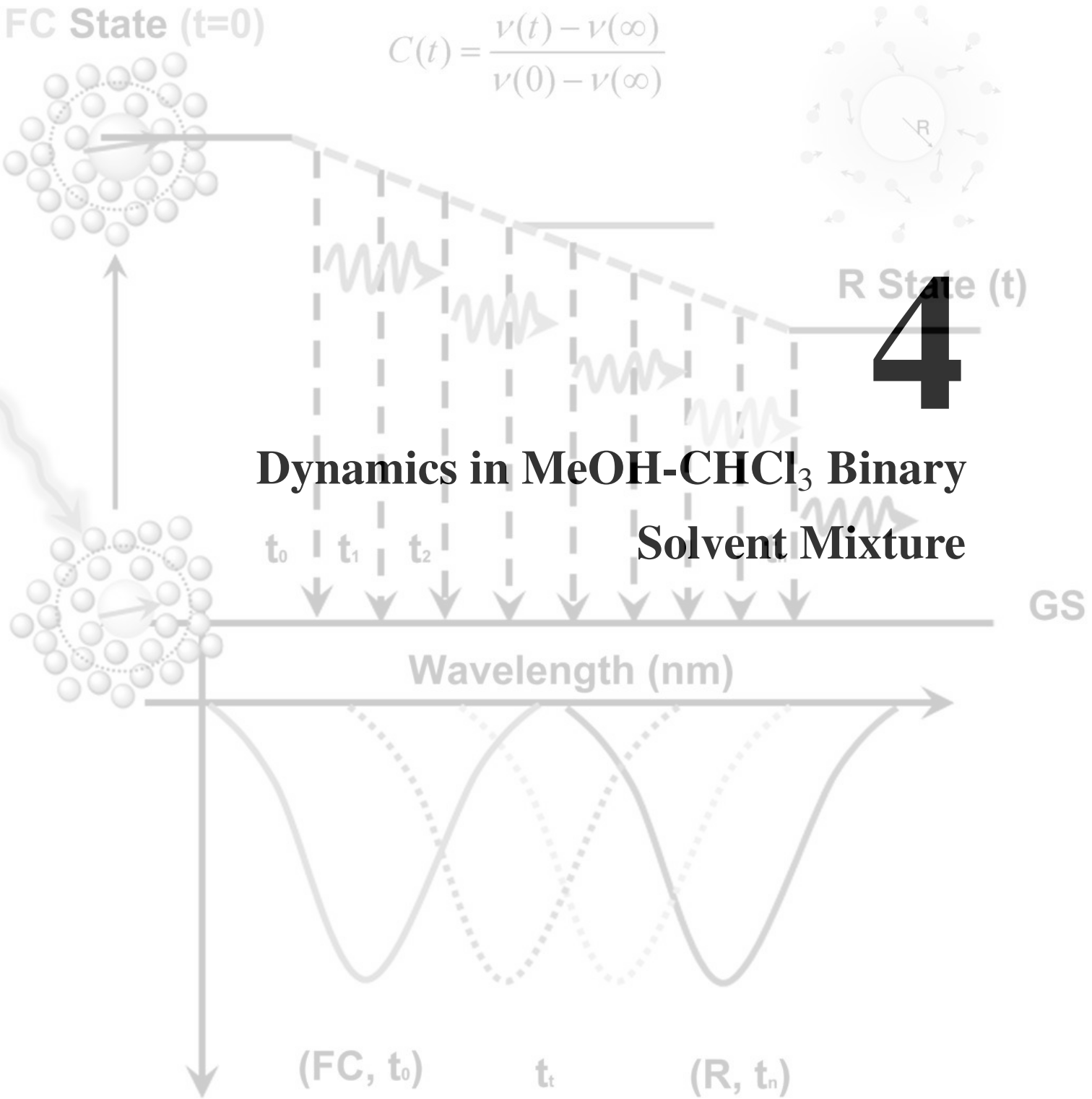

4

Dynamics in MeOH-$CHCl_3$ Binary Solvent Mixture

[1]*Femtosecond transient absorption pump-probe technique is used to measure the solvation dynamics of pure methanol (MeOH), chloroform ($CHCl_3$), and different mole fraction of MeOH in MeOH-$CHCl_3$ binary solvent mixture. The appearance of synergistic solvation behavior in the steady state absorption measurement is explained on account of solvent-solvent interactions through extended hydrogen-bonding network. This appeared synergistic behavior is the only cause for the slow solvation dynamics in solvent mixed system and found to be lower at $X_{MeOH} = 0.45$ in binary mixture. This certify the probe molecule in such intermolecular association among solvent system will experience unique solvation shell, which may responsible for slow solvent dynamics in mixture compare to pure solvents. The solvation data are provided better insight of effect of binary solvent system. Disappearance of such synergistic behavior in the excited state of the Pyran dye displays the weak nature of the intermolecular interaction present in binary solvent mixture.*

[1]Submitted in *J. Phys. Chem.*

4.1 Introduction

The importance of binary solvent mixtures in chemical, physical and biochemical processes have been extensively discussed in literature.[200–209] The physical properties of mixed solvents modify the pathways of chemical transformations through altering the energies of participating reactant species, and also the solvent dependent characteristics of an intermediate state decides the type of the product to be formed during a chemical reaction.[200,203,205,206] The features of the mixed solvent which decide the course of the reaction and subsequently the rates of transformations are the dynamical response of the solvent and the local structure of the solvent molecules participating in the formation of solvation shell. Revealing such dynamical response of the mixed solvent system has been a challenge in the past,[209–220] however, lately a lot of attention has been devoted to establish the role of solvation in chemical and biochemical reactions.[200–209] The dynamical characteristics of one solution phase can thus enhance or retard the rate and yield of a chemical transformation as compared to another solution phase depending on the dynamical response and the local structure of the solvent system.[209–212,221–226] In essence, the dynamical features of a solvent systems at the molecular level determines the rate of fluctuations of solvent molecules, which subsequently decides how rapidly and instantaneously solvent molecules respond to an external perturbation.[209–212] The timescale of the solvent response will thus depend on the rate of breakage of initial solvent structure and the re-establishment of a new one. As a result, the existence of various interactions among the solvent molecules and the structural evolution of an interactive solvent system are the significant factors which will anticipate the overall solvation dynamics and the rate of intermolecular energy flow.[209–212,227,228]

The mode of solvation of solvatochromic molecules have been widely investigated by various ultrafast techniques such as femtosecond or picosecond time-resolved fluorescence spectroscopy,[213,215,217,218,220,229–232] femtosecond pump-probe spectroscopy,[204,210–212] 2D-IR spectroscopy,[204] dielectric relaxation spectroscopy[213] and ^{1}H NOESY spectroscopy.[233,234] Additionally, lot of work has also been carried out using simulation studies[204,215,235–238] and ab-initio calculations[213,219,236]. Fayer and co-workers[204] have measured the solvation dynamics of phenol-OD in pure and mixed solvents by ultrafast 2D-IR and IR pump-probe techniques. They have noticed a difference in the slow dynamics for pure solvents and their mixture, which was ascribed to the different nature of first solvent shell (around solute) in solvents of different compositions and was also justified by MD simulations. Recently, Zhang *et al.*[213] have tested mixture of ionic liquid and water by

dielectric and ultrafast time resolved fluorescence techniques and examined the utility of dielectric solvation model. They found that the solvent response functions predicted by dielectric continuum model are similar to the spectral response function measured with coumarin-153. The only difference they observed is that the measured spectral response functions is ~ 7 fold slower than as predicted by dielectric model.[213] Agmon *et al.*[219] discussed the dynamics of preferential solvation by introducing the translational diffusion origin of preferential solvation, which is essentially an extension of Smoluchowski model.

In practice, many interactive mixed solvent systems induce shift in steady state spectra of the solvatochromic molecule, and this shift continues with increase in concentration of more polar solvent in the binary solvent mixture.[239–244] In other words, when solvatochromic molecules are solvated preferably by the more polar solvent molecules, this selective solvation is termed as preferential solvation. Some interactive solvent mixtures on the other hand, induce large shift in the steady state spectra as compared to the bulk counterpart, and the observed larger shift is caused by the solvation of probe molecules with combined components of solvent in binary mixture. Therefore, this non selective solvation is named as synergism. In chapter 3, we have noticed synergetic behaviour in MeOH–$CHCl_3$[23], MeOH–DCM, and *t*-BuOH-DCM binary solvent mixtures and has been studied by spectroscopic techniques, 1H-NMR analysis, electron-transfer dynamics, and is also justified by analytical modeling.[23] It was proposed that the existence of weak hydrogen bonded network between hydrogen bond accepting (e.g. MeOH, *t*-BuOH) and donating (e.g. $CHCl_3$, DCM) solvent is mainly responsible for the observed synergism. The miscibility of alcohols in such weakly interactive solvents leads to distinct hydrogen bonding networking, and hence may present a different solvent response. However, to the best of our knowledge, solvation dynamics in MeOH–$CHCl_3$ binary solvent mixture has not been pursued. In the present study, we address the dynamical characteristics of MeOH–$CHCl_3$ binary solvent mixtures through femtosecond pump-probe measurements.

4.2 Results and Discussion

4.2.1 Steady State Absorption and Emission Spectra in MeOH-$CHCl_3$ Binary Solvent Mixture

The steady state absorption and fluorescence spectra of 4-(dicyanomethylene)-2-methyl-6-(4-dimethylaminostyryl)-*4H*-pyran (Pyran, Fig. 4.1) dye were recorded in various proportions

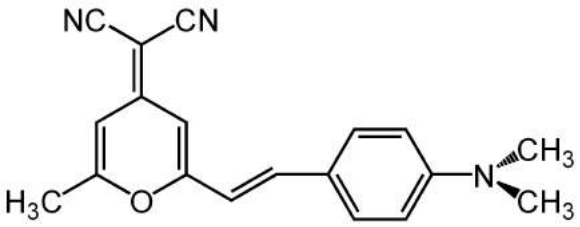

Fig. 4.1

Molecular structure of 4-(dicyanomethylene)-2-methyl-6-(4-dimethylaminostyryl)-*4H*-pyran used in this study.

of MeOH in MeOH-$CHCl_3$ binary solvent mixtures. Fig. 4.2a and 4.2b shows the absorption and fluorescence spectra of Pyran dye in different compositions of MeOH-$CHCl_3$ mixtures. The absorption maximum of Pyran dye in neat MeOH and $CHCl_3$ are at 466.6 nm and 469.2 nm respectively. In the solvent mixture of 0.10 mole fraction of MeOH, the absorption maximum changes to 471.4 nm. As the mole fraction of MeOH in MeOH-$CHCl_3$ solvent mixture increases from 0.10 to 0.45, the absorption maximum of Pyran dye exhibits a monotonous red shift from 471.4 to 475.3 nm. Further increase in mole fraction of MeOH cause a hypsochromic shift of the absorption maximum from 474.8 (0.5 X_{MeOH}) to 470 nm (0.9 X_{MeOH}). The variation of absorption maximum of Pyran dye as a function of X_{MeOH} is shown in Fig. 4.1a. It clearly shows that the absorption maxima of Pyran dye significantly depends on the composition of solvent mixture. In order to depict the stabilization of Pyran dye in the corresponding binary mixture, the concept of molar electronic transition energy E_T $(kcal\ mol^{-1})$ was used, whose relationship with absorption maximum (λ_{max}) is given by;[23,245–247]

$$E_T = \frac{28591}{\lambda_{max}}\ (kcal\ mol^{-1}) \tag{4.1}$$

For an ideal mixture, one expects that any equilibrium property in a binary liquid (e.g. solvation energy, composition etc.) is a weighted average of that in the two solvents. Thus in an ideal case, where all solvent-solvent interactions are assumed to be same, the dye is characterized by maximum value of molar electronic transition energy given by[23,247,248]

$$E_T(ideal) = X_{S_1}E_{T(S_1)} + X_{S_2}E_{T(S_2)} \tag{4.2}$$

where, X_{S_1} and X_{S_2} are mole fractions of solvent 1 and solvent 2 respectively and $E_{T(S_1)}$ and $E_{T(S_1)}$ are E_T values of a dye or indicator solute in pure solvents 1 and 2. This equation corresponds to the ideal behaviour of binary solvent mixture, and the variation of E_T as a

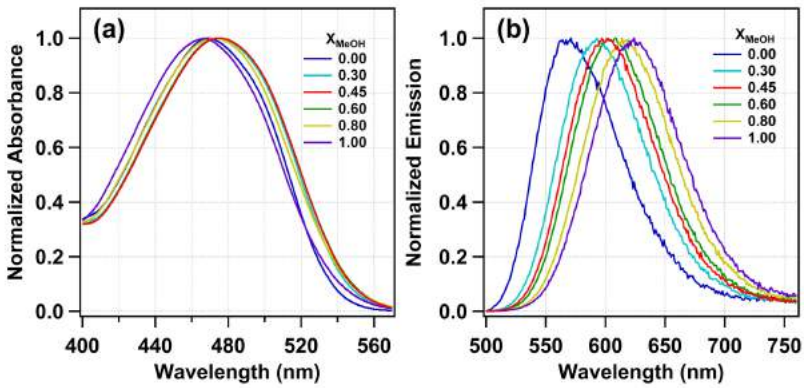

Fig. 4.2

(a) Normalized absorption and (b) emission spectra of Pyran dye in a different composition of MeOH (X_{MeOH} = 0.00, 0.30, 0.45, 0.60, 0.80, 1.00) in MeOH-$CHCl_3$ mixtures. The excitation wavelength of emission spectra was set at 450 nm.

function of mole fraction of any component should always be linear. However, in practice, the variation is barely linear, which points towards the existence of some specific and selective interactions between the dye molecule and one of the components of the solvent mixture, which is termed as preferential solvation. Apart from this, the deviation from the ideal behaviour may also appear from the interaction of combined solvent counterparts in the binary solvent mixture, exhibiting a synergistic effect. In terms of molar transition energy, E_T, which provides the direct measure of stabilization energy on account of solvation, the variation is expressed as a function of X_{MeOH} in MeOH-$CHCl_3$ binary mixture (see in Fig. 4.3a). It is shown that, maximum stabilization in terms of solvation is obtained at ca. 0.45 mole fraction of MeOH, after deducting the ideal behaviour of the dye in the binary mixture as per equation 4.2 (see in Fig. 4.3c). The efficient solvation imposed by the mixed solvent system inferences towards the prevalence of mutual solvation around the solvatochromic probe molecule and such a phenomenon is recognized as synergism.[23] This certifies that the MeOH-$CHCl_3$ solvent mixture exhibits a different solvation behaviour as compared to either of the pure solvents, and its mutual interaction appears to be stronger than the pure bulk counterparts. However, such peculiar variation was not observed in emission maximum of Pyran dye in MeOH-$CHCl_3$ solvent mixtures, rather it displays a monotonous red shift from 567.5 to 623.5 nm (see Fig. 4.2b and 4.3b).

In chapter 3, the appearance of similar features in MeOH-$CHCl_3$ solvent mixture by using different types of probe molecules (coumarin dyes and 4-AP dye) vividly suggested the

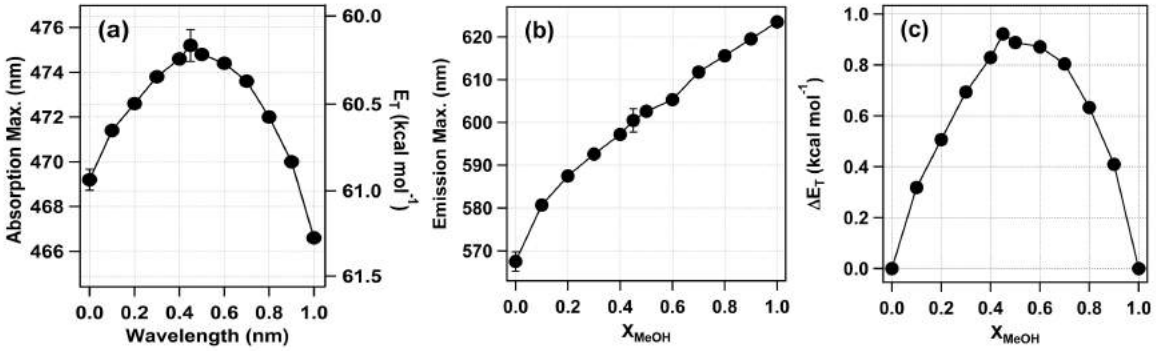

Fig. 4.3

(a) The variation of absorption maximum and molar electronic energy E_T, (b) the peak position of emission spectra of Pyran dye in MeOH-$CHCl_3$ binary solvent mixture as a function of the mole fraction of polar solvent *i.e.* X_{MeOH} and (c) the difference in molar electronic transition energy of Pyran dye in different composition of MeOH-$CHCl_3$ binary solvent mixture as a function of mole fraction of MeOH in MeOH-$CHCl_3$ solvent mixture.

existence of higher polar environment in mixed solvent mixture. This inherently facilitates distinct synergistic solvation behaviour as compared to pure solvents. However, the observed synergistic solvation disappears in the excited state. It was proposed that the disappearance of synergism in the excited state is most probably because of the perturbations induced in the solvation shell on behalf of large dipole moment in the excited states, resulting in breakage of the solvent structure. This disturbance guides selective solvation of probe molecules by more polar component of binary solvent mixture. In the present situation, since the excited state dipole moment of Pyran dye is very large, μ_e = 26.3 D,[249] the interactive solvent structure no longer remains intact and as a result no synergism is observed in the excited state. On the contrary, the magnitude of ground state dipole moment (μ_g = 5.6 D)[249] is not sufficient enough to make any perturbation in the structure of solvent mixture and hence synergistic solvation prevails. Thus, the degree of synergistic solvation directly depends on the magnitude of dipole moment of dye molecule used, and strength of the H-bonding network between interactive solvents present in solvent mixture. To establish the above proposition of efficient solvation provided by the solvent mixture as compared to the pure solvents, solvation dynamics study was undertaken to find the solvation times of pure solvents and the solvent mixture. Femtosecond transient absorption measurements of Pyran dye were pursued to track the time evolution of stimulated emission band.

4.2.2 Solvation Dynamics Study in MeOH-$CHCl_3$ Solvent Mixture

The time resolved difference absorbance ($\triangle A$) spectra of Pyran dye in different proportions of MeOH in MeOH-$CHCl_3$ mixture were measured by femtosecond transient absorption technique over a wavenumber range of 13000–22000 cm^{-1}. Fig. 4.4 shows the difference absorption spectra ($\triangle A$) of Pyran dye in neat MeOH (4.4a), neat $CHCl_3$ (4.4b), 0.45 X_{MeOH} (4.4c), 0.70 X_{MeOH} (4.4d), and 0.20 X_{MeOH} (4.4e). In each plot, a difference spectrum

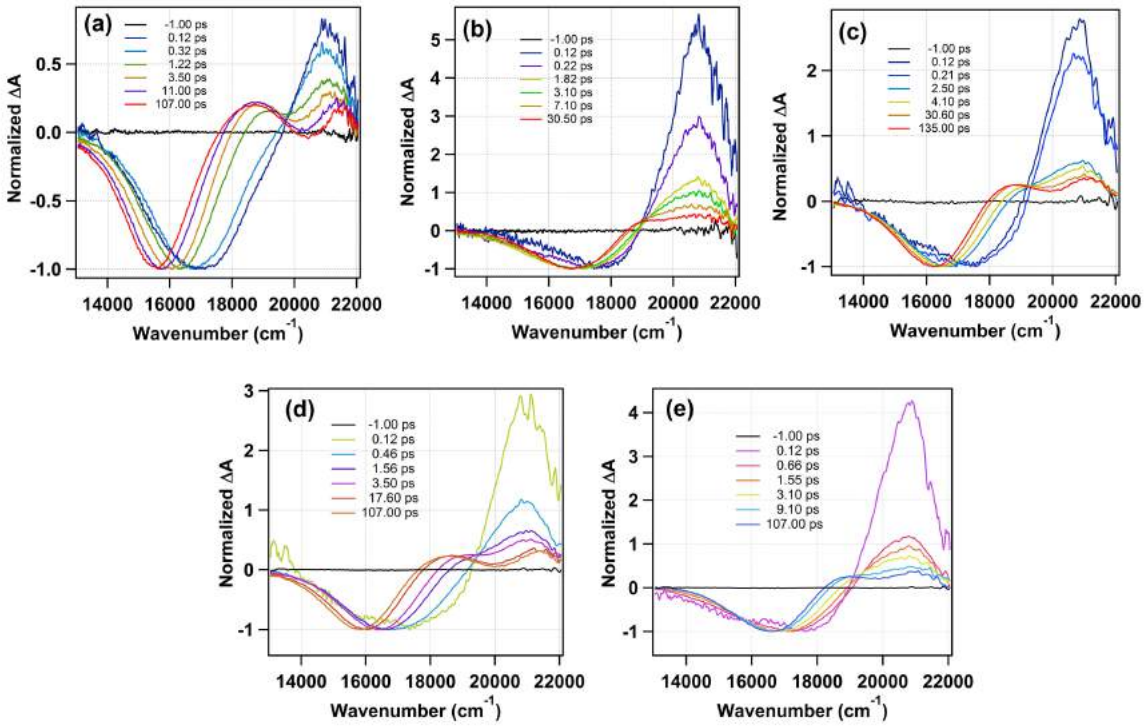

Fig. 4.4

Time resolved or Transient absorbance spectra of Pyran dye (excitation wavelength is 400 nm) in (a) pure MeOH, (b) pure $CHCl_3$, (c) X_{MeOH} = 0.45, (d) X_{MeOH} = 0.70, and (e) X_{MeOH} = 0.20 in MeOH-$CHCl_3$ at different time periods. The black solid line represents spectrum before pump pulse or time zero.

corresponding to negative delay time between the pump and the probe beams is shown as a reference (black). In all situations, within the current spectral window, two processes can be observed; excited state absorption (ESA) and stimulated emission (SE). The detailed solvent dependent transient absorption signal assignment of Pyran dye has already been reported in the literature.[250–252] Briefly, in MeOH the time evolution of transient absorption signals suggest the existence of two states in the excited state of Pyran (Fig. 4.4a). The locally

excited (LE) state is characterized by the ESA signal (20000-22000 cm^{-1}) with a broad SE signal (14000-19000 cm^{-1}). Within a picosecond, a new ESA signal appears on the lower wave number side with a maximum at ca. 19000 cm^{-1} and is assigned to the charge transfer (CT) state.[250–252] The stimulated emission signal occurs from both the locally excited state and the charge transfer state in polar solvents, while as in non-polar solvents ($CHCl_3$), the SE is from LE state only (no ESA from CT state is observed in transient absorption spectra of Pyran in $CHCl_3$). Instead of revealing the solvent dependent excited state dynamics in detail, the evolution of SE signal as a function of solvent mixture will be discussed here. More importantly, this procedure signifies the use of transient absorption in deducing the solvation dynamics. In essence, instead of constructing the time-resolved spectra as in fluorescence spectroscopy, transient absorption can give the raw time resolved emission spectra (in case the SE signal is prominent and is not overlapping with other transient absorption signals), such that no reconstruction is required. It will be effective to remove any ambiguity caused during the fitting of the fluorescence transients and can report features like time dependent broadening of the emission spectra exactly. To get the exact SE peak position, each $\triangle A$ spectrum was fitted by a log-normal function in the SE spectral region.

In MeOH, the first distinct SE signal can be identified at 120 fs and the shape of the subsequent SE signals at higher times infers that there is no overlapping of the other transient signals in the region of emission maximum. The SE signal at 120 fs is primarily from the LE state ($\nu_{max} = 17023$ cm^{-1}) and with advancement in time, a contribution from CT states also appears and finally the SE signal occurs exclusively from the CT state (Fig. 4.4a). With time, there is a continuous shift in the SE maximum towards the lower wave number and this accounts for the time-dependent dynamics Stokes shift of the excited state (TDSS). Initially, the dynamic Stokes shift is very rapid and then it slows down till 107 ps ($\nu_{max} = 15550$ cm^{-1}) in methanol. In $CHCl_3$ (Fig. 4.4b), as mentioned above, the SE signal occurs predominantly from the LE state and thus the observed dynamic Stokes shift is essentially because of the solvation of the LE state. In $CHCl_3$, the first distinct SE signal can be observed at around 120 fs ($\nu_{max} = 17750$ cm^{-1}) followed by a continuous shift towards the lower wave number till it attains steadiness at ca. 30 ps ($\nu_{max} = 16730$ cm^{-1}) (Fig. 4.3b). In 0.45 X_{MeOH} (Fig. 4.4c) in the MeOH-$CHCl_3$ solvent mixture, the evolution of transient absorption signals with time suggests initial decay of LE state into the CT state. The SE signal occurs from both the LE and the CT state, with first distinct signal observed at 120 fs ($\nu_{max} = 17284$ cm^{-1}). There is an initial fast evolution followed by slow dynamic Stokes shift which appears to

reach steadiness at ca. 135 ps ($\nu_{max} = 16230\ cm^{-1}$).

To extract information from the time-dependent variation of SE signal of the transient absorption spectra, solvation correlation function $C(t)$ was plotted from the equation given below.[250–258]

$$C(t) = \frac{\nu(t) - \nu(\infty)}{\nu(0) - \nu(\infty)} \tag{4.3}$$

where $\nu(0)$, $\nu(t)$, and $\nu(\infty)$ are respectively the peak wave number of the SE band at time zero, at intermediate times, and at infinity. The correlation function $C(t)$ of Pyran dye in pure methanol, pure chloroform and various proportions of MeOH in MeOH-$CHCl_3$ solvent mixture is shown is Fig. 4.5

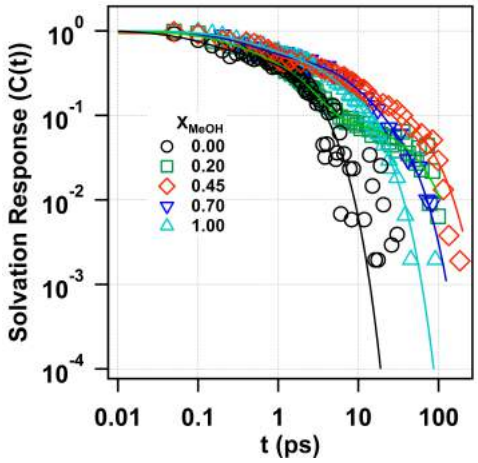

Fig. 4.5

The solvation response function $C(t)$ of Pyran dye in MeOH-CHCl3 binary solvent mixture at different mole fraction of MeOH (X_{MeOH} = 0.00, 0.20, 0.45, 0.70, 1.00). The symbols $\circ, \square, \diamondsuit, \triangledown$, and $\triangle$ are corresponding to X_{MeOH} = 0.00, 0.20, 0.45, 0.70, and 1.00, which denote the experimental value of $C(t)$ and the corresponding solid line represents the best fitted exponential decay.

The correlation function of Pyran in each solvent is either fitted bi-exponentially or tri-exponentially (see Table 4.1). From the fitting parameters, the average solvation time ($< \tau_s >$) was obtained. The $< \tau_s >$ in pure MeOH is found to be 4.32 ps, in pure $CHCl_3$, it is 1.32 ps, while as in 0.45 X_{MeOH}, the average solvation time is found to be 12.03 ps. The list of average solvation time in all the pure solvents and various proportions of solvent mixtures is shown in Table 4.1 and the variation is shown in Fig. 4.6. As can be observed, the 0.45 X_{MeOH} offers considerably slower solvation of the excited state than either of the counterparts. This result is in concordance with the variation of steady state absorption maximum, wherein

$\mathbf{X}_{MeOH}$	τ_1 **(ps)**	τ_2 **(ps)**	τ_3 **(ps)**	b_1	b_2	b_3	a_0 **(cm^{-1})**	a_∞ **(cm^{-1})**	**<τ_s>** **(ps)**	**%C(t) missed**
0.00	2.17	0.10	-	0.59	0.41	-	17750	16726	1.32	30.52
0.20	0.22	1.59	47.47	0.35	0.56	0.09	17696	16602	5.24	24.25
0.45	0.53	7.33	53.47	0.53	0.29	0.18	17416	16186	12.03	29.49
0.70	0.37	6.02	23.93	0.45	0.35	0.20	17314	15793	7.06	31.14
1.00	0.40	3.41	10.94	0.37	0.36	0.27	17022	15554	4.32	46.89

Table 4.1

The relevant parameter of solvent response functions of MeOH-$CHCl_3$ at room temperature. The average relaxation time $< \tau_s >$ is calculated by $\sum_i b_i \tau_i$. The solvation responses function $C(t) = \sum_i b_i \, exp(-t/\tau_i)$ with $\tilde{\nu}(t) = (a_0 - a_\infty)C(t) + a_\infty$.

the absorption maximum is red shifted in 0.45 X_{MeOH} compared to either of the pure solvents. The possible reason of the slower solvation offered by 0.45 X_{MeOH} may be due to the rigid solvent cage, which restricts itself from undergoing immediate reshuffling once the molecule is promoted to the excited state. In other words, in the ground state of Pyran the solvent cage will be having some arrangements around the molecule, and once the molecule is promoted to excited state by irradiation, immediate charge redistribution will require a

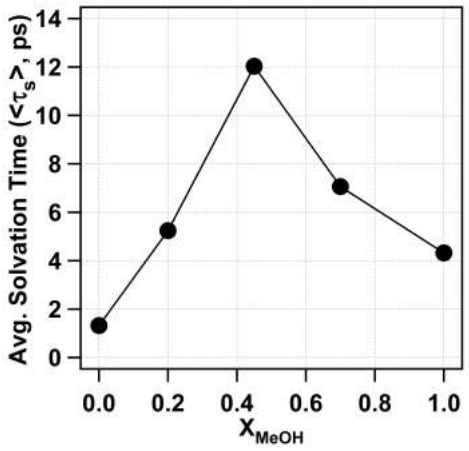

Fig. 4.6

The variation of average solvation time as a function of mole function of MeOH in MeOH-$CHCl_3$ binary solvent mixture.

simultaneous change in the structure of the solvent cage. The time scale of restructuring of the solvent cage decides the solvation time, and it depends on how fast the solvent molecule within the cage break their old arrangement and re-establish new interactions as per the requirement of the excited state. Slower solvation will essentially mean that the solvent

molecules within the solvation shell are kept intact by means of intermolecular interactions and hence respond slowly to the changing dipole moment of the Pyran in excited state. This emphasizes on the existence of extended networking through weak hydrogen bond formation between MeOH and $CHCl_3$ in the binary solvent mixtures. Consequently, one can expect that the binary solvent mixture is well organized compare to the bulk solvent counterparts and maximum organization prevails at X_{MeOH} = 0.45. These experimental results clearly suggest the significant role of enhancement in polarity and extended weak hydrogen bonding network (which has been established previously in chapter 3) in MeOH-$CHCl_3$ binary solvent mixture in deciding the dynamics of the solvation. Present solvation studies support the proposition of enhanced intermolecular hydrogen bonding interactions and polarity of binary solvent mixture, and hence the synergism.

However, initial part of solvation dynamics is missed even in present femtosecond setup of time resolution 120 fs. The magnitude of missed solvation time is calculated by using the Fee-Maroncelli method.[256–258] The emission frequency at zero time, $\nu^p_{em}(0)$, can be determined in a polar medium by using following formula as,

$$\nu^p_{em}(0) = \nu^p_{abs} - (\nu^{np}_{abs} - \nu^{np}_{em}) \tag{4.4}$$

where ν^{np}_{abs}, and ν^{np}_{em} represent the steady state frequencies of absorption and emission, respectively, of Pyran dye in non-polar solvent (in present study, cyclohexane). Hence, the percentage of solvation escaped, are calculated by using following equation,

$$\textbf{\% of solvation missed} = \left[1 - \frac{\nu_{abs}(0) - \nu_{abs}(\infty)}{\nu_{em}(0) - \nu_{abs}(\infty)}\right] * 100 \tag{4.5}$$

where all terms have usual meaning as described before. The magnitude of percentage of solvation missed in different mole fraction of MeOH in MeOH-$CHCl_3$ mixtures has been listed in Table 4.1. Aside this, it is readily observed that the decay of $C(t)$ exhibits comprisable slow dynamics at X_{MeOH} = 0.45 in mixture. This is considerably slower in comparison to the solvation dynamics in pure MeOH and $CHCl_3$ solvent. In other words, the average solvation time of Pyran dye in X_{MeOH} = 0.45 in MeOH-$CHCl_3$ mixture displays higher magnitude of about 12.03 ps compare to other mole fraction of MeOH mixtures and pure respective solvent (i.e. MeOH and $CHCl_3$).

4.3 Conclusion

In the present work, we have re-established the synergism in in MeOH-$CHCl_3$ binary solvent mixture using solvatochromic probe molecules 4-(dicyanomethylene)-2-methyl-6-(4-dimethylaminostyryl)-*4H*-pyran (Pyran) using femtosecond transient absorption spectroscopy

and also filled the gap between the ground state and excited state response. The unique mixed solvent environment arises to higher degree of solvent stabilization energy by achieving lower E_T value compared to the bulk counter parts and the position of maximum is to be found at near X_{MeOH} = 0.45 similar as proposed in earlier chapter. Following femtosecond transient absorption study, it has been inferred that the intermolecular association among solvent molecules is responsible for slow solvent dynamics in mixture rather than pure solvents and achieved slower solvent dynamics at point where E_T shift is observed highest, termed as synergistic effect. Overall interactions present within the MeOH and $CHCl_3$ binary solvent mixture furnishes a clear evidence of solvent aggregation interplay aspect of weak hydrogen bonding. The peculiar feature (higher polarity, and weak hydrogen bonding) and inherent complexity prepared a clear necessity for further theoretical ground as well as molecular dynamics and ab initio quantum chemical studies, which will brought more transparent picture about the system in future.

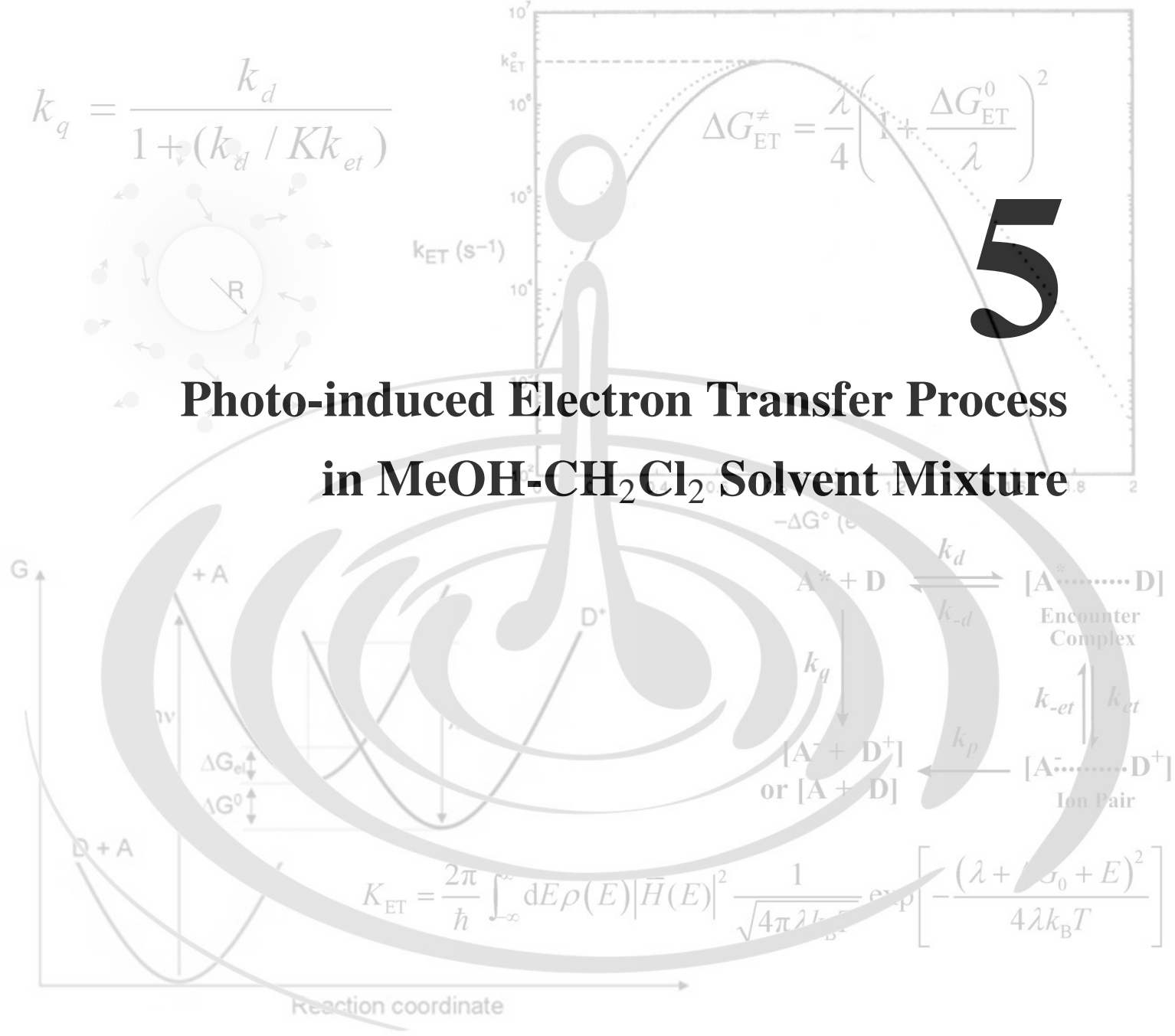

5

Photo-induced Electron Transfer Process in MeOH-CH_2Cl_2 Solvent Mixture

[1]*The intriguing feature of synergistic solvation behavior of methanol (MeOH) and dichloromethane (DCM) binary solvent mixture has been studied by bimolecular photo-induced electron transfer (PET) process between a donor and an acceptor molecule. The appearance of synergistic solvation behavior in the steady state absorption measurement is explained on account of solvent-solvent interactions through extended hydrogen-bonding network, which is in accordance with* ^{1}*H-NMR study, molar refractivity measurement and solvent exchange model rationalized up to the hilt in chapter 3.* ^{1}*H-NMR analysis in chapter 3 indicates the existence of MeOH-DCM cluster in stoichiometric ratio of 1:1.33. The solvent exchange model has been used to find the efficacy of synergistic nature and the polarity of the mixed solvent system. The synergistic solvation parameter is found to be 3.5 times larger compared to the preferential solvation parameter. Here, the proposition of extended hydrogen-bonding network was further authenticated by measuring the rate of bimolecular PET reaction and the solvent reorganization energy of binary solvent mixtures. The slowest rate of electron transfer and highest value of solvent reorganization energy (at the Marcus inversion point) have been observed for* $X_{MeOH} = 0.40$*, which furnishes highest synergistic effect and provides distinct environment from the pure solvent cases.*

[1]Submitted in *J. Chem. Phys.*

5.1 Introduction

The symptomatic electron transfer (ET) process between a donor and an acceptor, and its dependence on the local environment have drawn a widespread interest in the past several decades because of its importance in many fundamental chemical processes and reactions.[259–278] The increasing rate of electron transfer reaction with their exergonicity (-△G) has been known for a long time.[263,266,267,272,274,277] Historically, in 1956, Marcus proposed the decrease of rate of ET reaction after a certain limit of the reaction exergonicity (system dependent) leading to the appearance of the inverted region.[259,260,263] Followed by this, the existence of inverted region has been established experimentally by several research groups with suitable donor-acceptor pairs in different environments and systems.[261–269] According to Marcus theory, the rate of ET (k_{et}) is given by[266,267,271,273,276–278]

$$k_{et} = \frac{4\pi^2}{h}\frac{V_{el}^2}{2\pi\lambda k_B T} exp\left[-\frac{\triangle G^*}{k_B T}\right] \tag{5.1}$$

where, λ is the total reorganization energy, which is the sum of intramolecular and solvent reorganization energy ($\lambda = \lambda_{in} + \lambda_s$). V_{el}, k_B, T and $\triangle G^*$ are respectively the electronic coupling parameter that determines the extent of overlap between electronic wave functions of the reactant and the product, Boltzmann constant, absolute temperature and free energy of activation for ET reaction. $\triangle G^*$ is related to λ and free energy of the reaction ($\triangle G^0$) as[267,273]

$$\triangle G^* = \frac{(\triangle G^0 + \lambda)^2}{4\lambda} \tag{5.2}$$

According to Marcus theory, ET rate will increase exponentially with decrease in free energy of the reaction ($\triangle G^0$) under the condition of ($-\triangle G^0 < \lambda$) and start decreasing when $-\triangle G^0$ value just overcomes λ ($i.e. -\triangle G^0 > \lambda$), with the highest value of rate of ET (k_{et}) at ($\lambda = \triangle G^0$) which is known as the inversion point. At the inversion point the rate of ET become highest and it also estimates the extent of total reorganization energy (λ) of the system. Over the past few decades the evidence of Marcus inverted region has been observed in both homogenous and heterogeneous mediums like liquid-liquid interface,[265] micelle,[266,271,272,275] cyclodextrin,[267] reverse micelle,[270] ionic liquid,[268,269,271] vesicles,[274] etc. Sun *et al.*[265] investigated the ET reaction at a non-polarized ITIES (interface between two immiscible electrolyte solution) and asserted the existence of inverted region in terms of the rate constant of a second order ET reaction. Das *et al.*[271] have examined the role of diffusion and reorganization energy on the appearance of Marcus inverted region in

neat ionic liquid and ionic liquid mixed micelles. Lately, Kumbhakar *et al.*[272] have shown that the relative propensity of ET rate is responsible for the solvent reorganization energy and the arrival of inversion region varies with the nature and organization of the medium. They have confirmed that the position of inversion point is a very informative parameter about the nature of the medium. According to the figure of electron transfer reaction in solution phase (see Fig. 5.1), under the steady state approximation, the rate equation can be written as[260,276–278]

$$k_{et} = \frac{1}{K_A}\left[\frac{k_q k_d}{k_d - k_q}\right] \tag{5.3}$$

where, k_d, k_q, and K_A are respectively the diffusion controlled rate component, bimolecular quenching constant and diffusional equilibrium constant $\left(K_A = \frac{k_{et}}{k_{-et}}\right)$. Here k_{et} and k_{-et} are the rate of formation and dissociation of the encounter specie respectively.

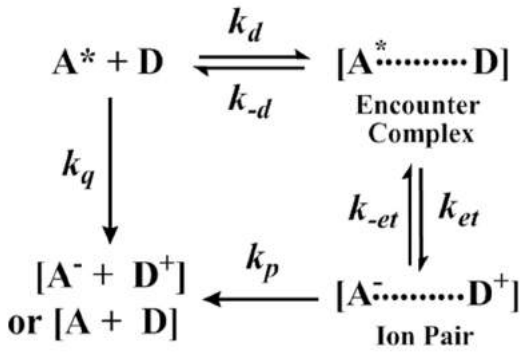

Fig. 5.1

Schematic representation of bimolecular electron transfer (ET) upon photoexcitation. Firstly, the acceptor in the excited state (A^*) forms an encounter complex ($A^* - - - D$) with the donor D, and this newly formed encounter complex undergoes electron transfer through ion pair ($A^- - - - D^+$) formation. The terms, k_d and k_{-d} are the diffusion rate constant for formation and dissociation of ($A^* - - - D$), k_{et} and k_{-et} are the forward and backward ET rate constants. The k_q is the fluorescence quenching constant of excited acceptor molecule A^*.

On the other hand, the binary solvent mixtures have attracted a lot of attention in the field of biology, chemistry and pharmaceuticals due to discrete behavior of solvent mixture compare to its bulk constituents.[279–291] The interactive solvents develops a unique environment in solution phase via specific interaction like hydrogen bonding or by nonspecific such as dipole-dipole, dipole-induced dipole interaction, etc.[291–296] Consequently, many

researches are being devoted to investigate the behavior of such interactions present in binary solvent systems.[284–295] The nature of solvation in binary solvent mixtures are often found to be preferential. The process where one counterpart of solvent mixture solvates the solute more predominately compared to the other is known as preferential solvation. Apart from preferential solvation, there is always some possibility of mutual interaction of solvent counterparts providing a completely distinct solvation environment which termed as synergistic solvation.[297,298] Recently, we have shown synergetic solvation behavior in MeOH-$CHCl_3$ binary solvent mixture by spectroscopic techniques and analytical modeling.[23] It has been proposed that the weak hydrogen bonded network between hydrogen bond accepting (e.g. MeOH) and hydrogen bond donating (e.g. $CHCl_3$) solvent is mainly responsible for the observed synergism, with an extended H-bonded network in the system. However, to the best of our knowledge the study of PET reaction in binary solvent mixture is not yet accomplished. In the present chapter, we explore the Marcus inverted region to ascertain strong evidence about the presence of H-bonding network in methanol (MeOH) – dichloromethane (DCM) binary solvent mixture, which also displays strong synergism. The interaction in MeOH-DCM binary solvent mixture has already been discussed in chapter 3 by means of electronic spectroscopy, ^{1}H-NMR study and analytical modeling.

5.2 Results and Discussion

5.2.1 Electron Transfer in MeOH-DCM Binary Mixture

^{1}H-NMR study along with solvent exchange model and steady state UV-visible absorption measurement suggests the possibility of extended networking between MeOH and DCM in their binary solvent mixtures by hydrogen bond formation. Consequently, one may expect that the organization of the binary solvent mixture is different than the bulk solvent counterparts and the maximum change should be observed in a mixture with $X_{MeOH} = 0.40$. Henceforth, the rate of an electron transfer process is expected to be most affected in binary mixture with $X_{MeOH} = 0.40$. This means, the rate depends on how loosely or tightly the solvation shell is associated around the reactant and product state. Under such circumstance, the PET process is highly sensitive to the solvent reorganization and barely has any contribution from the intramolecular reorganization.[276] Here we consider that contribution of intramolecular reorganization energy (λ_{in}) is negligible compared to the dominant solvent reorganization energy (λ_s). To investigate the dependence of the rate of electron transfer reaction (k_{et})

and solvent reorganization energy (λ_s) on different MeOH-DCM binary solvent mixtures of varying proportion, we have studied photo induced electron transfer (PET) between electron donors (DMA and DEA, see in Fig. 5.2) and acceptors (C30, C151, C152, C153 and C481, Fig. 5.3) molecules.

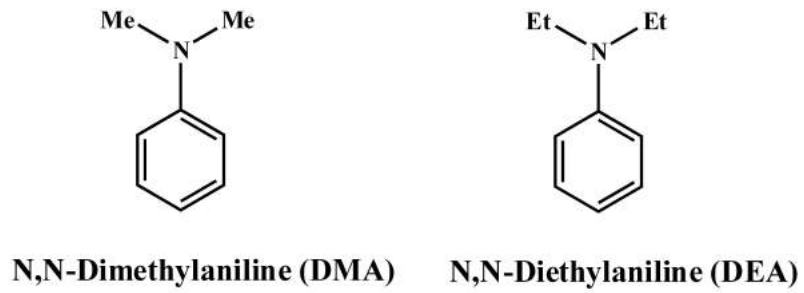

Fig. 5.2

Molecular structures of donor molecules used in the present study.

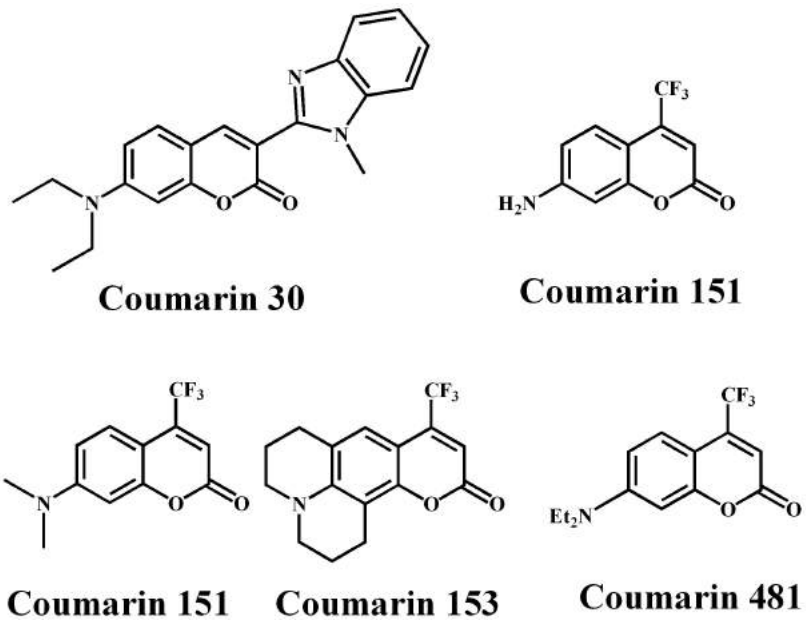

Fig. 5.3

Molecular structures of acceptor molecules used in this study.

First we studied the PET reactions in pure solvents namely methanol (MeOH), dichloromethane (DCM) and acetonitrile (ACN). The time resolved quenching constant was determined by Stern-Volmer equation as[4,272,274–276]

$$\begin{aligned}\frac{\tau_0}{\tau} &= 1 + K_{sv}[Q] \\ &= 1 + k_{q,TR}\tau_0[Q]\end{aligned} \tag{5.4}$$

where, τ_0 and τ are the fluorescence lifetimes of acceptor molecule in absence and presence of the quencher molecules, K_{sv} is the Stern-Volmer constant and [Q] is the donor concentration. The quenching constant ($k_{q,TR}$) values were determined by dividing Stern-Volmer constant (K_{sv}) with acceptor lifetime in absence of the quencher (τ_0), see fluorecence transient profiles of acceptors in presence and absence of donor molecules in Fig. 5.4. Stern-Volmer plot for all donor-acceptor pairs are found to be linear in nature (Fig. 5.5). The $\triangle G^0$ values has been calculated from Rehm-Weller equation neglecting the electronic repulsion parameter as[299]

$$\triangle G^0 = E^0_{D/D^+} - E^0_{A/A^-} - E_{00} \tag{5.5}$$

where, E^0_{D/D^+} and E^0_{A/A^-} are respectively the oxidation and reduction potential of donor and acceptor, which was measured by potentiostat cyclic voltametry, and E_{00} is the intersection of normalized absorption and emission spectra of the acceptor in respective solvents (see in Fig. 5.6).

According to Rehm and Weller, the rate constant of bimolecular electron transfer reaction increases with driving force up to a value that corresponds to that of the diffusion of the reactants, and remains diffusion limited even at driving forces where inversion is expected.[277,278,300] Till date, such slow reactions were observed only in the Marcus normal region and so far there has been no convincing experimental observation of the Marcus inverted region for bimolecular PET reactions in liquid solution.[268,269,276,277,300] In case of DCM and ACN we have observed similar dependence of rate of bimolecular PET reaction with the reaction exergonicity (Fig. 5.7b and 5.7c). Similar behavior was also observed by Nad *et al.*[276] in ACN. However, in case of PET reaction in MeOH, which has not been well reported in the literature, we have observed the decrease in rate of ET process after a certain exergonicity of the reaction (Fig. 5.7a), and thus observed the Marcus inverted region in pure liquid. In other words, it is evident from Fig. 5.7a that the value of $k_{q,TR}$ initially increases as $\triangle G^0$ becomes more negative and after reaching the maximum, it starts decreasing with higher negative value of $\triangle G^0$. Nevertheless, an opposite picture is found in the case of DCM and ACN, where the value of $k_{q,TR}$ increases as $\triangle G^0$ value gets more negative and finally remains almost constant at highly negative value of $\triangle G^0$.

On the other hand, the steady-state fluorescence properties of acceptor (C151, C153 and C481) have been measured on gradual increase of the concentration of donors in five

X_{MeOH}	Donor	Acceptor	E_{00} (eV)	τ_0 (ns)	$E(A/A^-)$ (V)	$E(D/D^+)$ (V)	$\triangle G^0$ (eV)	k_q x 10^8 (lit. mol^{-1} s^{-1})
	DMA	C153	2.60	4.29	-1.520	+0.675	-0.405	8.08
		C481	2.73	0.76	-1.520		-0.535	15.70
0.78		C151	2.87	5.50	-1.530		-0.665	13.80
	DEA	C153	2.60	4.29	-1.520	+0.580	-0.500	15.20
		C481	2.73	0.76	-1.520		-0.630	16.00
		C151	2.87	5.50	-1.530		-0.760	12.00
	DMA	C153	2.60	5.27	-1.495	+0.680	-0.425	7.60
		C481	2.74	1.21	-1.433		-0.627	13.30
0.61		C151	2.88	5.53	-1.532		-0.668	12.50
	DEA	C153	2.60	5.27	1.495	+0.573	-0.532	11.74
		C481	2.74	1.21	-1.433		-0.734	13.03
		C151	2.88	5.53	-1.532		-0.775	11.08
	DMA	C153	2.61	5.43	-1.514	+0.700	-0.396	6.31
		C481	2.75	2.13	-1.540		-0.510	10.20
0.40		C151	2.90	5.40	-1.470		-0.730	10.33
	DEA	C153	2.61	5.43	-1.514	+0.620	-0.476	6.96
		C481	2.75	2.13	-1.540		-0.590	9.88
		C151	2.90	5.40	-1.470		-0.810	9.06
	DMA	C153	2.62	5.75	-1.510	+0.700	-0.410	7.31
		C481	2.76	2.59	-1.530		-0.530	14.05
0.28		C151	2.91	5.42	-1.464		-0746	13.40
	DEA	C153	2.62	5.75	-1.510	+0.650	-0.460	6.93
		C481	2.76	2.59	-1.530		-0.580	13.45
		C151	2.91	5.42	-1.464		-0.796	10.32
	DMA	C153	2.63	5.87	-1.540	+0.690	-0.400	6.47
		C481	2.77	2.93	-1.580		-0.500	15.02
0.21		C151	2.92	5.35	-1.500		-0.730	11.58
	DEA	C153	2.63	5.87	-1.540	+0.680	-0.410	9.03
		C481	2.77	2.93	-1.580		-0.510	18.43
		C151	2.92	5.35	-1.500		-0.740	11.77

Table 5.1

Bimolecular quenching constant (k_q), and free energy changes ($\triangle G^0$) for ET reaction in different coumarin-amine pairs in MeOH-DCM binary solvents of different compositions.

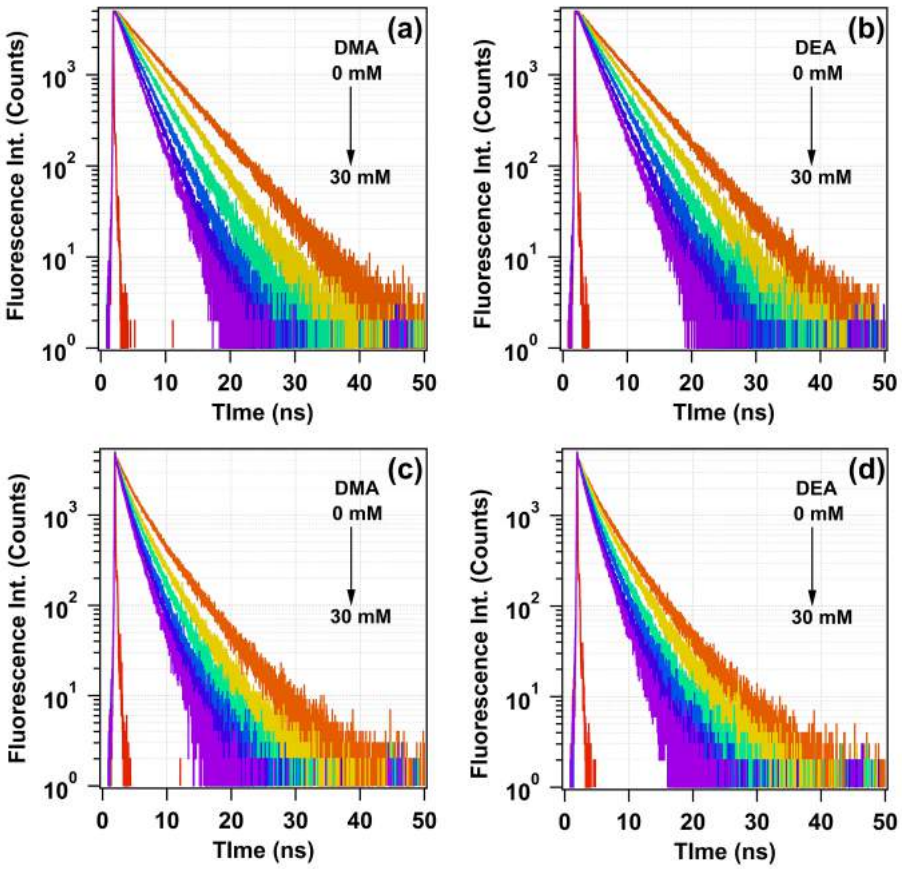

Fig. 5.4

Fluorescence transients of C151 (in (a) and (b)) and of C153 (in (c) and (d)) with the gradual addition of DMA and DEA in methanol (MeOH).

different MeOH-DCM binary solvent mixtures (ca. X_{MeOH} = 0.78, 0.61, 0.40, 0.28, 0.21). It has been found that the fluorescence intensity of coumarin dyes quenched in different extent in different binary solvent mixtures without affecting the shape of either the absorption or the emission spectra. The quenching constant was determined by Stern-Volmer equation as[4]

$$\begin{aligned} \frac{I_0}{I} &= 1 + K_{sv}[Q] \\ &= 1 + k_q \tau_0 [Q] \end{aligned} \tag{5.6}$$

where, I_0 and I are the fluorescence intensities of acceptor molecule in absence and presence of the donor molecules, and other terms have been discussed earlier (emission spectrum of C153 at different conc. of DEA in $X_{MeOH} = 0.40$ is represented in Fig. 5.8). A representative Stern-Volmer plots in $X_{MeOH} = 0.40$ of MeOH-DCM binary solvent mixture,

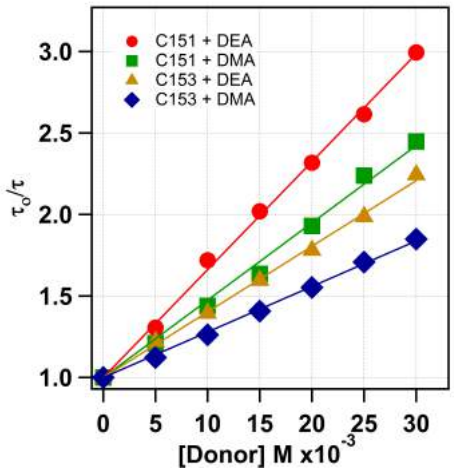

Fig. 5.5

Stern-Volmer plots for $\frac{\tau_0}{\tau}$ vs donors concentration (DEA and DMA) of coumarin dyes in MeOH.

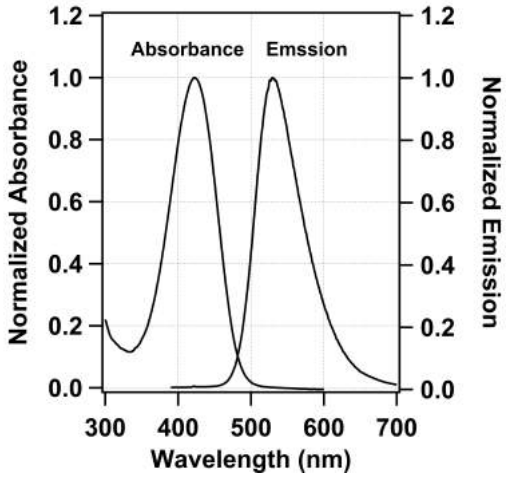

Fig. 5.6

E_{00} of C153 of $X_{MeOH} = 0.40$ in MeOH-DCM binary mixture.

with three different acceptor molecules (C151, C153, and C481) are shown in Fig. 5.9. The rate of bimolecular quenching constant (k_q) for different donor acceptor pairs in different solvent mixtures have been tabulated in Table 5.1 and depicted in Fig. 5.10. Upon fitting the data by equation 5.1, the inversion point was calculated ($\lambda = -\triangle G_0$), which estimate the maximum value of the rate (k_q^{max}) along with the solvent reorganization energy (λ_s) for a particular binary solvent mixture and is shown in Fig. 5.11 and their values are summarized in Table 5.2. At $X_{MeOH} = 0.78$, the value of k_q^{max} is found to be 12.6 x10^9 $lit.mol^{-1}s^{-1}$ and λ_s is found to be 0.60 eV. Interestingly, on decreasing the proportion of MeOH in the binary

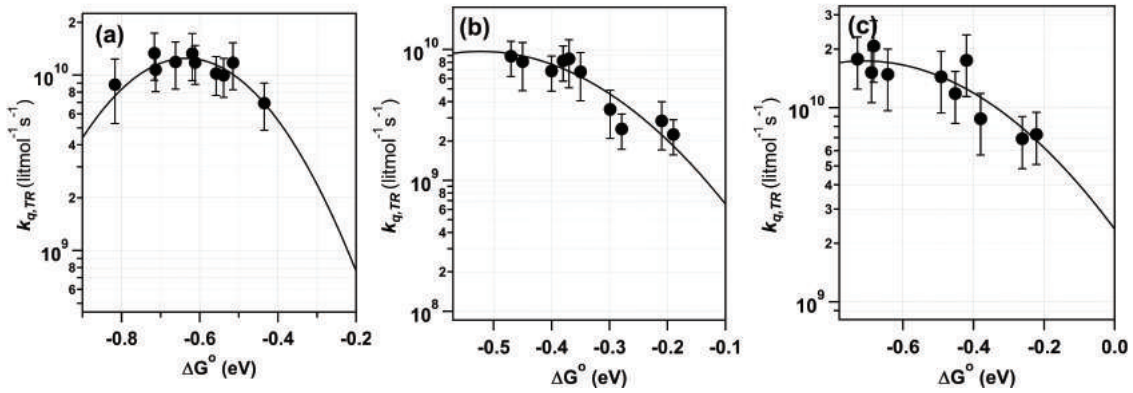

Fig. 5.7

Plot of $k_{q,TR}$ values from time resolved measurement vs. $\triangle G^0$ for the different coumarin-amine pairs in (a) MeOH, (b) DCM and (c) ACN. Experimental data were depicted by solid circles, and the solid line is the best fit to equation 5.1.

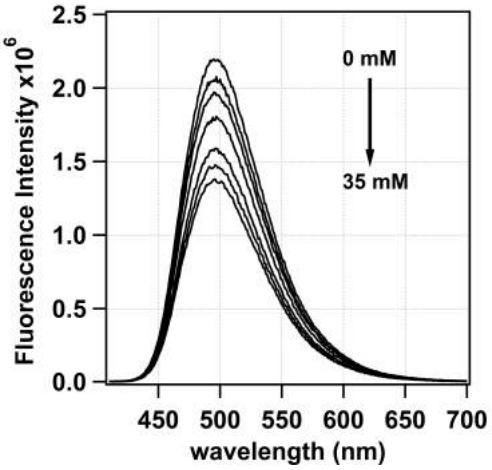

Fig. 5.8

Steady-state fluorescence quenching of C153 with gradual increase in concentration of DEA (used as a Donor) in binary mixture of $X_{MeOH} = 0.40$.

solvent mixture, the value of k_q^{max} first decreased and then again increased (Fig. 5.11a). On the other hand, the value of λ_s was found to behave inversely (Fig. 5.11b). The minimum value of k_q^{max} (8.7 x10^9 $lit.mol^{-1}s^{-1}$) with the maximum value of λ_s (0.66 eV) was observed for $X_{MeOH} = 0.40$, as already predicted from the observed highest synergistic effect. As λ_s weakly depends on the polarity of solvent, the dependence of λ_s on solvent mixture composition may be because of the enhanced H-bonding in binary solvent system. The observed slowest rate and high solvent reorganization energy thus supports our conclusion

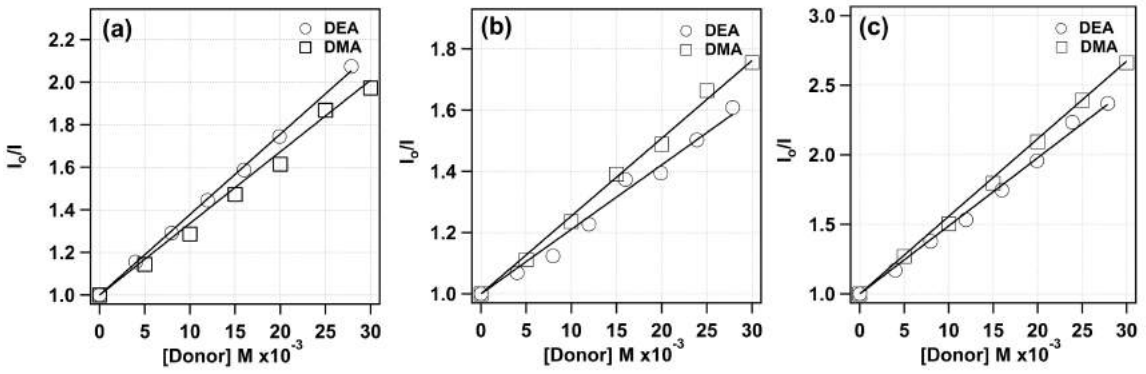

Fig. 5.9

Stern-Volmer plot for steady-state fluorescence quenching of (a) C153, (b) C481, (c) C151 using DMA and DEA as donor in MeOH-DCM binary solvent mixture with $X_{MeOH} = 0.40$.

of the extended H-bond network in the MeOH-DCM binary solvent mixture. Among the other mixtures, $X_{MeOH} = 0.78$ and $X_{MeOH} = 0.28$ have shown similar rate of quenching. Additionally, for $X_{MeOH} = 0.78$ and 0.21, it has been found that there is less possibility of extended networking from both absorption and proton NMR study and it was expected to get a higher rate and lower value of λ_s in this mixed solvent, which has also been confirmed from the PET study. Thus the present study demonstrates that intermolecular interaction plays an important role in the binary solvent mixtures to show a completely distinct behavior than the bulk counter parts, which is known as synergistic effect.

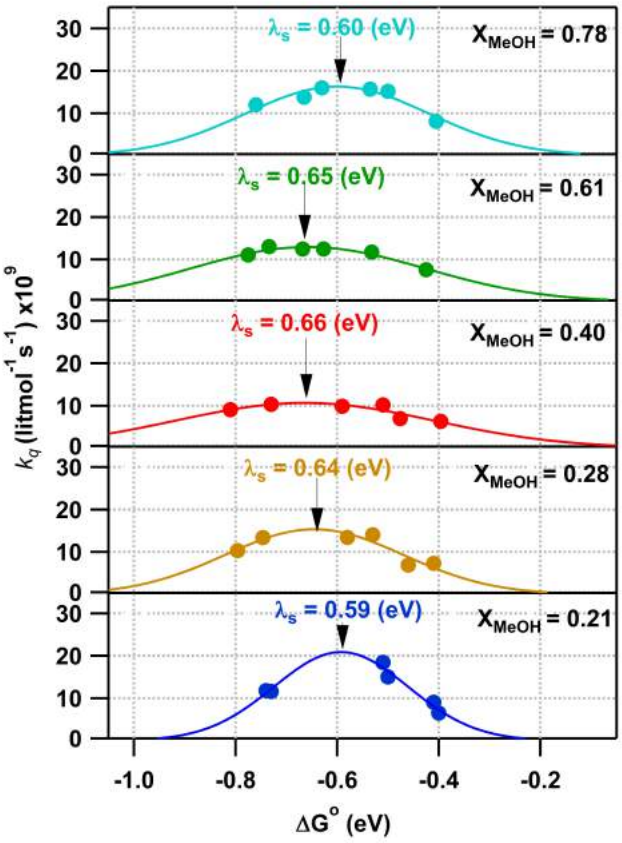

Fig. 5.10

k_q (solid circle) are plotted against the free energy deriving force ($\triangle G^0$) for different coumarin–aromatic amine pairs in MeOH-DCM binary solvents mixtures of different compositions. The solid lines are the best fit to equation 5.1.

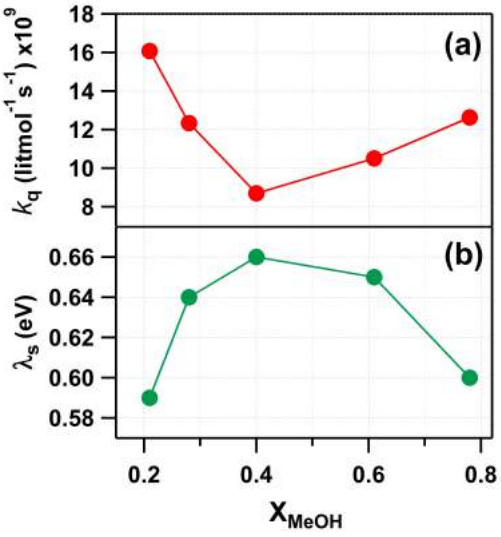

Fig. 5.11

(a) Plot of maximum observed rate (k_q^{max}) and (b) solvent reorganization energy (λ_s) at the inversion point for a particular MeOH-DCM binary solvent mixture against different compositions of MeOH.

$\mathbf{X}_{MeOH}$	**0.21**	**0.28**	**0.40**	**0.61**	**0.78**
$\mathbf{k}_q^{max}\mathbf{x10}^9$ ($\mathbf{lit.mol}^{-1}\mathbf{s}^{-1}$)	16.1	12.3	8.7	10.5	12.6
λ_s **(eV)**	0.59	0.64	0.66	0.65	0.60

Table 5.2

The maximum observed rate (k_q^{max}) and solvent reorganization energy (λ_s) at inversion point in MeOH-DCM binary solvents of different compositions.

5.3 Conclusion

A strong synergistic behavior has been observed in MeOH-DCM binary solvent mixture, which causes solvatochromic probe molecules to sense increased polarity compared to the bulk counterparts. The maximum synergistic effect has not only observed by means of UV-vis absorption spectroscopy using solvatochromic probe molecules, molar refractivity, ^{1}H-NMR measurements but also through PET reaction. The unique mixed solvent environment gives rise to higher degree of solvent reorganization energy and lower rate of PET reaction compared to the bulk counter parts. Also, it has been inferred that the intermolecular association is responsible for such synergistic effect.

6

Facile Reaction in *t*-BuOH-CH_2Cl_2 Binary Solvent Mixture

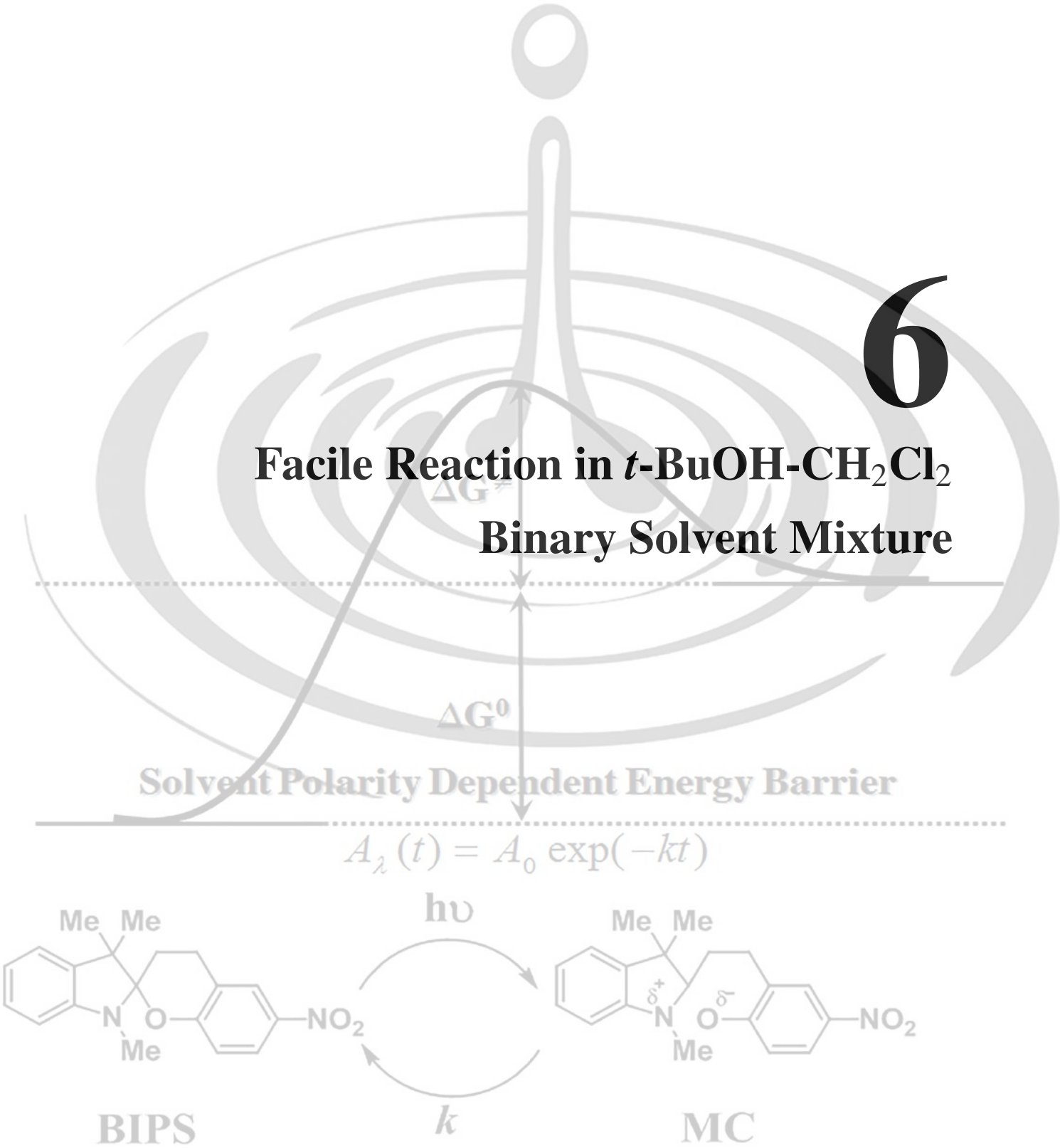

[1]*The synergetic behaviour in t-BuOH-DCM binary solvent mixture was studied by steady state UV-visible absorption measurement using solvatochromic probe which provides the evidence of solvent-solvent interactions led by weak hydrogen bonding, and has also been confirmed by proton NMR and solvent exchange analytical models in chapter 3. It points that intermolecular association and polarity of the binary solvent mixture must accelerate chemical reaction that goes through the polar transient state. The unique environment of solvent mixture is accountable for the lower rate of photo-decolourization of merocyanine and was explained in terms the extended intermolecular hydrogen bond networking. Additionally, we observed that the proportion of solvent pair at which maximum synergism is observed act as an ideal medium for the efficient solubilisation of TetMe-IBX reagent and the yield of oxidation reaction increased 4 times compared to in t-BuOH. Hence the binary solvent mixture may provide platform for a reaction to proceed at faster rates with a greater yield. Present study apparently established that intermolecular association plays deciding role in the binary solvent mixtures to show improvement in product yield and effect the rate of chemical processes, which is due to the synergistic solvation. This clearly is a new approach in the intensified concerns of green chemistry.*

[1]Submitted in *J. Phys. Chem.*

6.1 Introduction

Solvents play an indispensable role in controlling rate of almost every chemical and biological process.[301–307] The chemical and biological processes occurred in different solvents offer many advantages over solvent free phase reactions (like gas and solid phase), and provides thermodynamically and kinetically favourable conditions during the course of reaction, which effects on the rate of the reaction and modify the product yield.[301,303,307–310] The local solvation structure plays a crucial role in controlling the fate of the reaction in solution phase.[301,305–310] Different types of solute-solvent interactions such as solvophobic effect, hydrogen bond donor (HBD) interaction, hydrogen bond acceptor (HBA) interaction and dipolarity polarisability are generally involved.[301,303,310] However, it is not easy to resolve the contributions of those physical interactions, which are sufficiently strong enough to make significant change in the electronic environment of atoms present in reactants molecules. The majority of scientific groups have devoted their experiments[308–313] and theoretical calculation[314–317] to certify these factors, which effects the feasibility of chemical transformation. Despite, the versatile utility of single mediated solvent reaction has found limited scope and applications to assist reaction rate due to their poor physical tunability (like polarity, viscosity, diffusion constant, specific and non-specific interactions, and dielectric constant). This restricted tunabilty can be ended by switching single mediated solvent system to new environments like ionic liquid[317–321] confined medium[322–325] and solvent mixtures.[326–332] Controlling the rate of reaction under these media become the primary motivation of several groups in recent decades.[321,324,326,328,330] Lately, Yoshizawa *et al.*[324] revealed the intermolecular [2+2] photoaddition reaction of acenphthylene and 5-ethoxynaphthoquione in self-assembled coordination nanocage. This isolated microenvironment of self assembled nanocage control regio- and stereochemistry of product. In the last few years, the chemistry involved in ionic liquids has received remarkable significance due to their different physicochemical properties, and is considered as an alternative substitute to replace organic solvent in many chemical processes. Kumar *et al.*[321] observed the Diels-Alder reaction of cyclopentadiene with methyl methacrylate in organic solvent and chloroaluminate ionic liquids. They found that chloroaluminate ionic liquids greatly influence the product percentage yield of Diels-Alder reaction and also the product ratio of endo:exo has been found improved in ionic liquids compared to organic solvents. Likewise, the distinct physical and chemical properties of mixed solvents have been extensively investigated along with advantages over chemical processes.[326–332] The physicochemical

properties of mixed solvent solution have shown often deviation from ideal behavior comes from Raoult's law. This non ideal behavior emerges in almost all mixed solvent, appears due to the specific/non-specific interaction amongst molecules present in solvent mixture, which is termed as either preferential or synergistic solvation.[329,333–336] The preferential solvation or selective solvation is a phenomena, where one component of solvent binary mixture solvates probe molecule predominately than other components. Besides selective solvation, the mutual interaction of both solvents in mixture solvated solute predominately compare to the individual counterpart of mixture. Such co-operative solvation is termed as synergism. Usually, an enhancement in solvent polarity of mixture is accompanied by a change in the rate of a chemical transformation, through low energy polar transition state. The polarity of solvent mixture will not only eventually control the rate of the reaction, but also likewise other physical parameters which decides direction of chemical equilibrium such as rate of keto-enol tautomerization,[331,332] and stereoselectivity.[326,328,330] Mancini *et al.*[329] observed the kinetics of 1-fluoro-2,4-nitrobenzene with morpholine and piperidine in several binary mixtures of polar aprotic H-bond accepting solvents like acetonitrile and chloroform or dichloromethane. This study has shown that the reaction rate is higher in binary solvent mixture compared to the corresponding pure solvents. Also, in the same sequence, Shinde *et al.*[318] certified the combined effect of two solvents-ionic liquid (IL) and tert-alcohol into the nucleophilic fluorination substitution of mesylate with CsF. This combined form of solvent mixture increased the yield of desire product, along with a remarkable reduction of other olefin by-product. They have interpreted the possibility of mixed solvent engineering for a specific reaction.

In chapter 3, the synergistic solvation behavior in *t*-BuOH-DCM binary solvent mixture and has been studied by spectroscopic techniques and was rationalized by analytical modeling. It has been proposed that the weak hydrogen bonded networks between hydrogen bond accepting and donating solvent are accountable for the observed synergistic behavior. Although significant attention has been paid to realize the substantial role of synergism in binary solvent mixture over the rate of a chemical reaction and chemical process, but it has not been well established explicitly. In this connection, we look here the appearance of synergism in *t*-BuOH-DCM binary solvent mixture by means of millisecond flash-photolysis study and also observe dramatic change in percentage conversion of reaction in this binary solvent mixture.

6.2 Results and Discussion

6.2.1 Photo-decolourization of BIPS-NO_2 in *t*-BuOH-DCM Binary Solvent Mixture

The proton NMR study along with solvent exchange model and steady state UV-visible absorption measurement intimates the possibility of intermolecular interactions through extended hydrogen bond network between *t*-BuOH and DCM in the binary solvent mixtures along with 1:1.12 proportionality (in chapter 3). Consequently, we can expect that the binary solvent mixture is better organized compared to the pure solvent systems and maximum organization is obtained in a mixture with X_{t-BuOH} = 0.40. Subsequently, the rate of decolourization of BIPS-NO_2 is expected to be lowest in binary mixture with X_{t-BuOH} = 0.40 as the formation of the transient species passes before ring closure takes place as depicted in Fig. 6.1. The process of decolourization before ring closure is considered to be

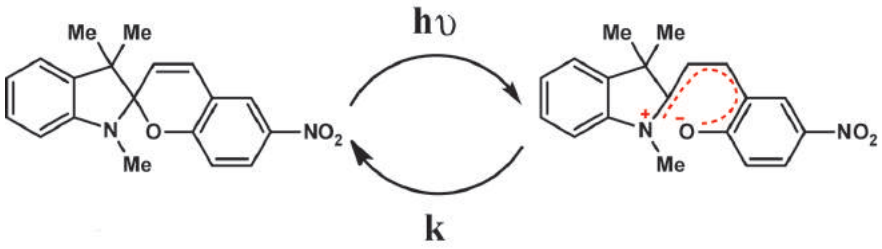

Fig. 6.1

A reversible photo-chromic reaction between BIPS-NO_2 (left) and merocyanine (MC, right).

sensitive towards the solvent polarity and is the rate determining step of the overall reaction process. Therefore, an increase in the polarity of *t*-BuOH-DCM binary solvent mixture cause slow down the rate of decolourization through stabilization of zwitterions species of BIPS and also leads to modification in the π bond order of the olefinic double bond.[337] In other words, fadedness of photo-mesocynine state (see in Fig. 6.1) is accomplishing by heterolytic ring formation C-O bond through transient species which follows the first order rate law.[337–340] The polarity of solvent mixture modifies the Gibbs free energy of fadedness process which alters the fading rate process.[337] In order to clearly know the polarity effect, we have performed millisecond flash photolysis in different composition of binary solvent mixture, the time dependent millisecond decay profile of photo-merocyanine as shown in Fig. 6.2a, where flash light is used to excite BIPS-NO_2 molecule to generate mesocyanine and 532 nm green laser beam is applied to measure the fading of photo-mesocyanine state.

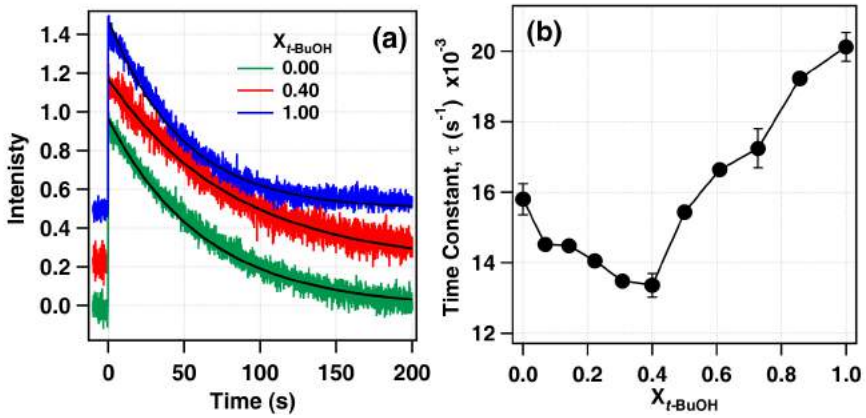

Fig. 6.2

(a) The representative absorption transients of BIPS-NO2 derivative in pure DCM, *t*-BuOH, and 0.40 mole fraction of *t*-BuOH in *t*-BuOH-DCM binary solvent mixture and their data are fitted solid black line by equation 2.2. (b) the rate mesocyanine as a function of mole fraction of *t*-BuOH in *t*-BuOH-DCM binary solvent mixture.

$\mathbf{X}_{t-BuOH}$	$\boldsymbol{k}$, 10^{-3} (s^{-1})
0.00	15.80
0.07	14.51
0.14	14.48
0.22	14.05
0.31	13.48
0.40	13.36
0.50	15.43
0.61	16.64
0.72	17.24
0.86	19.22
1.00	20.12

Table 6.1

The rate (k) of mesocyanine as a function of mole fraction of *t*-BuOH in *t*-BuOH-DCM binary solvent mixture.

The rate constants (k, s^{-1}), of fadedness process is measured in *t*-BuOH-DCM binary solvent mixtures with increasing proportion of *t*-BuOH in *t*-BuOH-DCM binary mixture. The mutual variation of rate constants, k (s^{-1}), of merocyanine as a function of mole fraction of *tert*-butyl alcohol (X_{t-BuOH}) in *t*-BuOH-DCM binary mixture is shown in Fig. 6.2b and all the values are tabulated in Table 6.1. This infers, s the polarity solvent mixture increased, consequently, the rate of fadedness decelerated. As a result, the lower rate observed in solvent mixture and found slowest at X_{t-BuOH} = 0.40 (k = 13.36 x10^{-3} s^{-1}) compared to

t-BuOH (k = 20.12 x10^{-3} s^{-1}), and DCM (k = 15.80 x10^{-3} s^{-1}). The experimental data clearly suggests the significant role of enhancement in polarity and extended weak hydrogen networks in *t*-BuOH-DCM binary solvent mixture which decelerates the rate of fadedness and has already been confirmed confirmed from ^{1}H NMR study along with solvent exchange model and steady state UV-visible absorption measurements. Present study clearly manifests that intermolecular interactions and polarity of binary solvent mixture play a crucial role to show an entire distinct behaviour from the bulk counter parts, which refers as a synergistic effect.

6.2.2 Green Chemistry approach in *t*-BuOH-DCM Binary Solvent Mixture

Many solvents and their mixtures play crucial role in the improvement of product yield, which has already been intensified approach in chemistry. we examine solvent polarity effect on the modified IBX (TetMe-IBX) which is used to commonly utilized in alcoholic oxidation which goes through polar intermediate state controlled by solvent polarity.[341] For such purpose, we preformed oxidation of coprostanol (see in Fig. 6.3) in the presence of modified

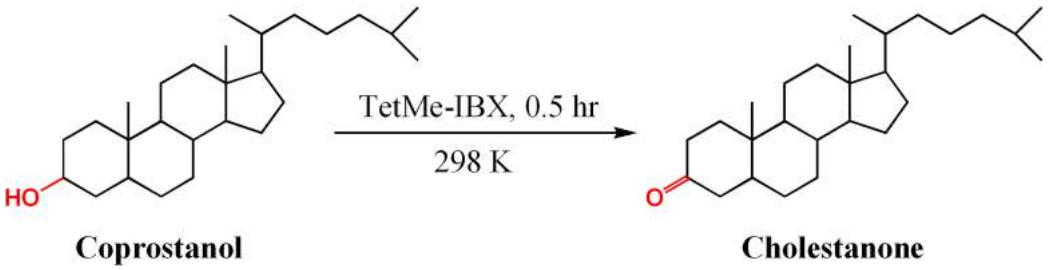

Fig. 6.3

Oxidation of Copraostanol with TetMe-IBX at 298 K.

IBX[341] (TetMe-IBX) in some composition of *t*-BuOH-DCM binary solvent mixture and their respective pure solvents.

The study of fadedness process along with proton NMR, solvent exchange analytical model and steady state UV-visible absorption measurement reckoned that the activation energy barrier for modified IBX is considered to be lowest at X_{t-BuOH} = 0.40 in binary solvent mixture. The percentage conversion of oxidised product (i.e. cholestanone) is found higher compared to pure solvents. The experimental data are shown in Fig. 6.4. The result infers that percentage conversion of cholestanone is found maximum (90

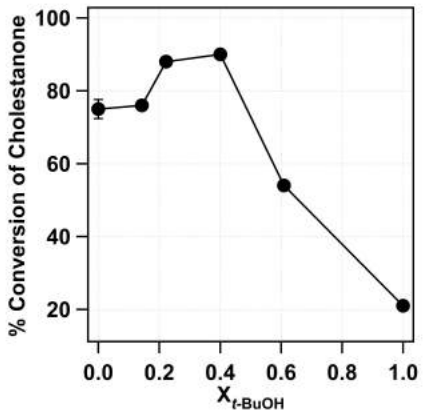

Fig. 6.4

Percentage conversion of cholestanone as a function of mole fraction of *t*-BuOH in *t*-BuOH-DCM binary solvent mixture.

6.3 Conclusion

The weak hydrogen bonded networks between hydrogen bond accepting and donating solvent are accountable for the observed synergistic behavior and also influences rate of chemical reaction, which goes mainly through the polar transient state. In other words, the unique mixed solvent environment causes the lower rate of decolourization of mesocyanine compared to the pure solvent system, and are explained in terms of the extended intermolecular hydrogen bond networking. This is facilitating the proper utilization of binary solvent in the green chemistry. Present study apparently established that intermolecular association plays deciding role in the binary solvent mixtures to show improvement in product yield and effect the rate of chemical reaction, which is a remark of synergistic effect.

7

Concluding Remarks & Future Outlook

This chapter summarizes the thesis, discusses its finding and contributions, points out the limitations of the present work, and also outlines direction for future outlook. All experimental results of photo-physical processes and their interpretations have been demonstrated relevance to the molecular interactions outlive in alcohol-chlorinated methane binary solvent mixtures and also reports the main cause of synergism. However, still many extensions of this present research deserves further consideration.

The present chapter is splitted into three parts. First part brings the thesis to a conclusion. Second presents a discussion of the contribution and limitations of the current work and the last part discusses the future outlook.

7.1 Conclusion of the Thesis chapters

In this thesis, we exmained the photo-physical responses like fluorescence quenching, solvation dynamics, photo-induced electron transfer (PET) and chemical kinetics, using steady state and time resolved spectroscopic methods along with a support from analtical models, which have been clearly evident the inherency of molecular interactions persist in alcohol-chlorinated methane binary solvent mixtures and evolves new composition of solvation nature in these binary solvent systems, termed “synergistic solvation”. Here, we conclude the final essence of all chapters in following steps.

7.1.1 Chapter 1

It describes the fundamental aspect of the role of solvation on solute molecule in liquid phase (both pure and mixed solvent cases). Generally, the effect of pure or mixed solvent on the electronic spectra of solute (or probe) molecule principally accounts solute/solvent nonspecific and specific interactions, comprising dipole/dipole, dipole-induced/dipole, dispersion interactions, and hydrogen bonding. Therefore, a major emphasis was given in this chapter to understand effect of different modes of solvation phenomenon at probe or solute molecule which undergoes electronic transition in mixed solvent systems.

7.1.2 Chapter 2

This chapter basically throws light on the different experimentals (i.e. steady state and time resolved spectroscopic) methods and analytical models which have been used to understand the appearance of distinguished solvation in binary solvent systems and their consequence on photo-physical processes.

7.1.3 Chapter 3

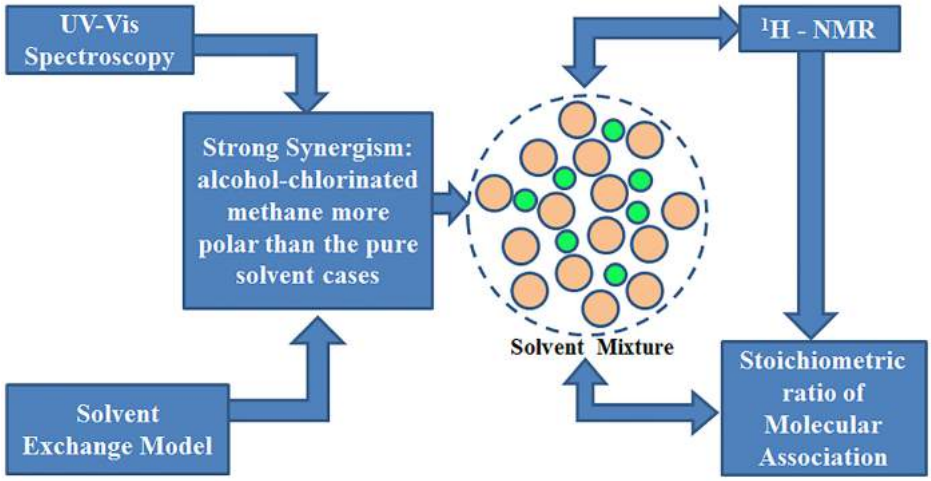

The ground state synergistic behavior of the solvent mixtures of hydrogen bond donating (e.g., chloroform, dichloromethane) and accepting solvents (e.g., alcohols like methanol, *tert*-butanol) pairs have been demonstrated the role of dipole moment of the solvated molecule. In other words, the solvation behavior of binary mixtures reveals strong probe dependence with no synergism observed when *p*-nitroaniline was taken as the solvatochromic probe, which is ascribed to the higher ground state dipole moment of *p*-nitroaniline (8.8 D) relative to C480 (6.3 D). Surprisingly, the synergistic signature is no longer observed for solvatochromic probe in binary mixture employing excited state measurements, which is substantiated by higher excited state dipole moment. Such strongly perturbed systems (due to high dipole moment) do not allow persistence of hydrogen bonding network, resulting in preferential solvation instead of synergism. The analysis of proton NMR of MeOH-$CHCl_3$ binary solvent mixture indicates the existence of MeOH-$CHCl_3$ network in the stoichiometric ratio of 1:2.15. A different stiochiometric ratio has been observed for MeOH-DCM (1:1.33) and *t*-BuOH-DCM (1:1.12). The solvent exchange model has been used to determine the feasibility of synergistic behavior and polarity parameter of the mixed solvent structure of alcohol-chlorinated methane binary solvent mixtures. Diffusion controlled dynamic quenching of C480 dye by 1,2-phenylenediamine in MeOH-$CHCl_3$ binary solvent mixtures suggested the existence of H-bonded network.

7.1.4 Chapter 4

Femtosecond Transient Absorption (FTA) has been elucidated the mechanism of solvation of 4-(dicyanomethylene)-2-methyl-6-(4-dimethylaminostyryl)-*4H*-pyran (Pyran dye)

in different composition of MeOH-$CHCl_3$ binary solvent mixture, which has been reported scarcely in the literature. The current study abundantly provides information about the intermediary response between the ground state and excited state. The remarkable damping

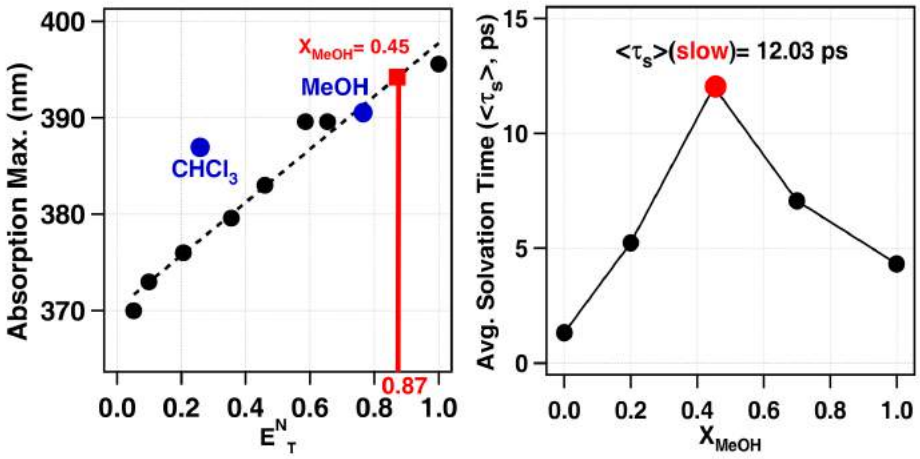

of solvation time of Pyran dye is possibly because of the slow diffusion of solvent molecules in the MeOH-$CHCl_3$ mixture-rich first solvation shell followed by hydrogen bond solvent-solvent rearrangements around the solute dipole. On the other side, the fast solvation of Pyran molecule occurs by the fast reorganization dynamics of pure solvent (i.e. Methanol and chloroform) around the solute dipole. Surprisingly, a noteworthy solvent polarity dependency in solvation dynamics was enucleated in the case of MeOH-$CHCl_3$ binary solvent and achieved slower solvent dynamics at the point where E_T shift is observed highest, termed as synergistic effect. The intermolecular association among solvent molecules (i.e. MeOH and $CHCl_3$) furnishes a clear evidence of slow solvent dynamics in mixture rather than pure solvents.

7.1.5 Chapter 5

Appearance of ground state synergism in MeOH-DCM binary solvent mixture in chapter 3 is illustrated in the terms of solvent-solvent interactions via UV-vis absorption, ^{1}H-NMR study, molar refractivity measurement and solvent exchange model. Following the study of photo-induced electron transfer (PET) reaction in MeOH-DCM binary solvent mixture deems that intermolecular solvent association is amenable for ground state synergistic effect in the MeOH-DCM mixture. A slow solvation in mixed solvent environment provides higher degree of reorganization of reactant molecules before PET. At particular mole fraction of MeOH ($X_{MeOH} = 0.40$) in MeOH-DCM solvent mixture, we measured the lowest rate of PET (k_{et})

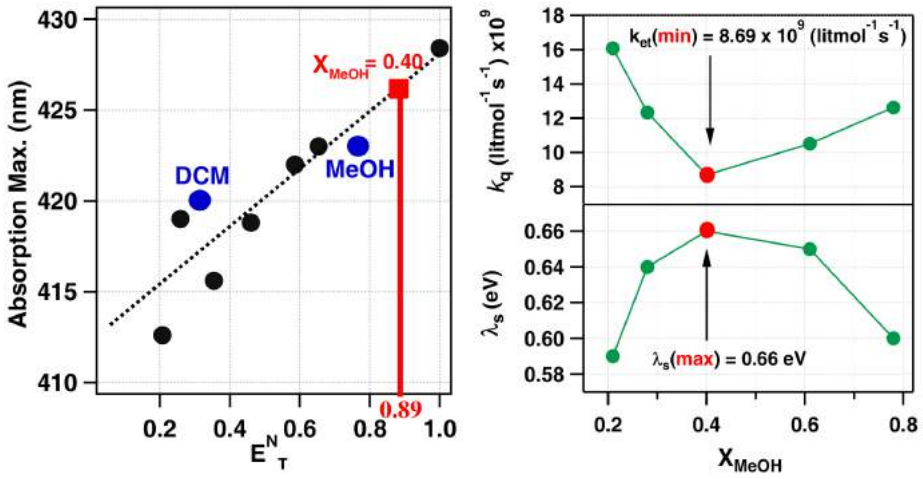

with highest reorganization energy (λ_s), as anticipated from the observed highest synergistic effect. Ultimately, it concludes that the presence of extended hydrogen-bonding network structure in the binary solvent system interposes slowing down of the rate of diffusion of reactant molecules which prevent the formation of encounter complex and hereof lowers the rate of PET process.

7.1.6 Chapter 6

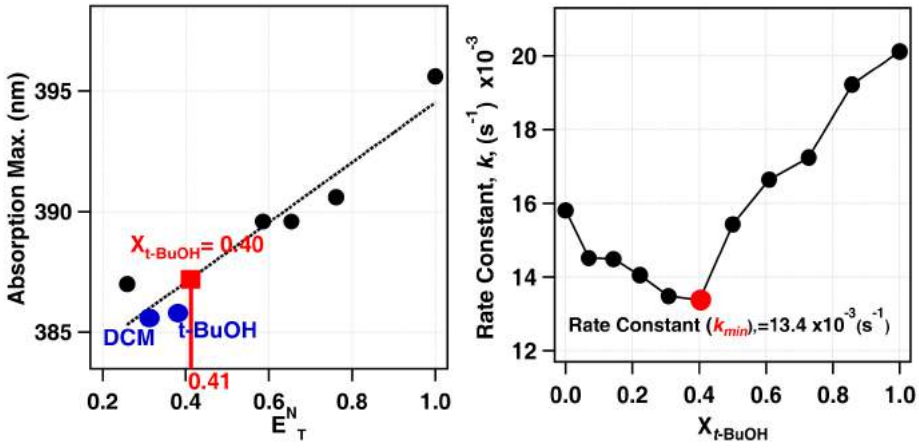

A noticable ground state synergetic nature in *t*-BuOH-DCM bianry solvent mixture was observed in UV-visible absorption study through solvachromic probe and molecular association of mixed solvent molecules was ratified by proton NMR study. Also, the feasibility of the synergistic nature of mixed solvent system has been verified by solvent exchange model. An idea of inherency of intermolecular association and polarity of the binary solvent mixture employ either speed up or slow down the chemical reaction that

progress through the polar transient state. The unique mixed solvent environment enforces slowing down the rate constant of photodecolourization of merocyanine compound compared to the pure solvent case. Also this solvent mixture acts as an ideal medium for the efficient solubilization of TetMe-IBX reagent and increases the yield of oxidation reaction 4 times as compared to that in *t*-BuOH. Hence, the binary solvent mixtures may provide platform for reactions to proceed at faster rates with higher yields. Finally, we take above evidences as a greener approach in chemistry.

7.2 Discussion

7.2.1 Contributions of Thesis

This thesis contributes to develop the elementary idea of behavior of alchohol-chlorinated methane binary solvent mixtures and also determines the fate of solvation behavior in mixed solvent system, by using steady state and time resolved spectroscopic methods along with a support from analyitcal studies. All experimental and analyitcal studies can be used to exclusively on all of these solvent mixture sytems to reveal especially the sysnergistic nature, which are otherwise unable to probe in excited state study. An occurrence of photo-physical processes in these binary solvent system infer a primarily and vivid knowledge about the of solvent molecular accociation in term of synergism. At the application point of view, this study also reports a higher product formation yield when the medium of the reaction was chosen as the mixed solvent compared to neat solvent. We take this idea as a greener approach in chemistry.

7.2.2 Limitations of Thesis

This study is not cover the features about the mechanistic pathway of hydroden bond dissociation and reformation dynamics in alcohol-chlorinated methane mixtures, and also has not the explored the molecular level picture of intermolecular interaction persist in the binary solvent mixture. As well, it requires theoretical background, molecular dynamics and ab initio quantum chemical studies, which will be brought more transparent picture about sturcture or networking of binary solvent systems.

7.3 Future outlook

While this thesis has demonstrated the fundamental idea of nature of solvation phenomenon in binary solvation and also provides potential application in green chemistry area, many opportuniities for extending the scope of this thesis still remains. This section presents some of these outlooks.

1. Inspite of comprehensive studies in this thesis, the clear evidence of solvation structure or intermolecular networking of binary solvent mixture has not been reported. For complete understanding about the molecular intractions or associations, it essentially requires various spectroscopic techniques (i.e. Dielectric relaxation, THz, Raman and near infrared (NIR) spectrascopic techniques) which not even covers the entire region of frequency domain, but also provides appropriate information of solvent structure of binary system used in this thesis work. In other words, dielectric relaxation, Raman and NIR spectroscopic techniques could identified the existence of synergistic solvation structure held together by weak intersolvent interactions.
2. In this thesis, we discussed the static nature of H-bonding network in alcohol-chlorinated methane binary solvent mixtures, which leads higher polarity in the mixed solvent compared to pure solvent cases. However, the understanding of hydrogen bond dynamics in such binary solvent systems is outwaiting and will help to better perceive the mechanistic pathway of hydrogen bond dissociation and reformation dynamics. The ultrafast infrared pump-probe spectroscopy is an excellently and suitable technique to watch hydrogen-bonds formation and breakage in real time domain. Also taking the advantage of laser pulse polarization, it is possible to examine rotational dynamics of -OH with chlorinated methanes and -OH with other alcohols molecules in real time.

References

[1] R. F. Barrow, Derek A. Long, and D. J. Millen. *Molecular Spectroscopy*. The Royal Society of Chemistry, 1974.

[2] N. J. Turro, V. Ramamurthy, and J. C. Scaiano. *Modern Molecular Photochemistry of Organic Molecules*. University Science Books, U.S., 2010.

[3] V. M. Agranovich and R. M. Hochstrasser. *Spectroscopy and excitation dynamics of condensed molecular systems*. North-Holland Pub., North-Holland Pub. Co., Amsterdam, 1983.

[4] J. R. Lakowicz. *Principles of Fluorescence Spectroscopy*. Springer, Singapore, 2007.

[5] P. Carmona, R. Navarro, and A. Hernanz. *Spectroscopy of Biological Molecules: Modern Trends: Modern Trends*. Springer, Netherlands, 1997.

[6] A. K. Downing. *Protein NMR Techniques*. Humana Press, Oxford, 2nd ed. edition, 2004.

[7] O. Svelto, S. De Silvestri, and G. Denardo. *Ultrafast Processes in Spectroscopy*. Springer, New York, 2nd ed. edition, 1996.

[8] B. D. Bartolo and O. Forte. *Frontiers of Optical Spectroscopy: Investigating Extreme Physical Conditions with Advanced optical Techniques*. Kluwer Academic, Netherland, 2005.

[9] A. M. Kelley. *Condensed-Phase Molecular Spectroscopy and Photophysics*. John Wiley & Sons, New Jersey, 2013.

[10] A. Lau, W. Werncke, and F. Siebert. *Time-Resolved Vibrational Spectroscopy VI: Springer Proceedings in Physics*. Springer, Berlin Heidelberg, 1995.

[11] J. D. Simon. *Ultrafast Dynamics of Chemical Systems*. Kluwer Academic, Netherland, 1994.

[12] M. D. Fayer. *Ultrafast Infrared and Raman Spectroscopy*. CRC Press, USA, 2001.

[13] Nathan P. Wells, Matthew J. McGrath, J. Ilja Siepmann, David F. Underwood, and David A. Blank. *J. Phys. Chem. A*, 112:2511, 2008.

[14] Arthur E. Bragg, Godwin U. Kanu, and Benjamin J. Schwartz. *J. Phys. Chem. Lett.*, 2:2797, 2011.

[15] T. Takamuku, A. Nakamizo, M. Tabata, K. Yoshida, T. Yamaguchi, and T. Otomo. *J. Mol. Liq.*, 103:143, 2003.

[16] Daniel T. Bowron, John L. Finney, and Alan K. Soper. *J. Phys. Chem. B*, 110:20235, 2006.

[17] J. Hao, H. Cheng, P. Butler, L. Zhang, and C. C. Han. *J. Chem. Phys.*, 132:154902, 2010.

[18] W. Marbach, A. N. Asaad, and P. Krebs. *J. Phys. Chem. A*, 103:28, 1999.

[19] S. Mukherjee, K. Sahu, D. Roy, S. K. Mondal, and K. Bhattacharyya. *Chem. Phys. Lett.*, 384:128, 2004.

[20] T. Molotsky and D. Huppert. *J. Phys. Chem. A*, 107:8449, 2003.

[21] Z. Li, H. Cheng, J. Li, J. Hao, L. Zhang, B. Hammouda, and C. C. Han. *J. Phys. Chem. B*, 115:7887, 2011.

[22] C. Yang, W. Li, and C. Wu. *J. Phys. Chem. B*, 108:11866, 2004.

[23] S. Gupta, S. Rafiq, M.k Kundu, and P. Sen. *J. Phys. Chem. B*, 116:1345, 2012.

[24] S. Sarkar, S. Mandal, C. Ghatak, V. G. Rao, S. Ghosh, and N. Sarkar. *J. Phys. Chem. B*, 116:1335, 2012.

[25] R. Naejus, D. Lemordant, R. Coudert, and P. Willmann. *J. Chem. Thermodyn.*, 29:1503, 1997.

[26] W. Akihiro, Y. Hassan, A. C.and Yoshitaka, and K. Yoshimichi. *J. Chem. Soc., Faraday Trans.*, 94:369, 1998.

[27] G. P. Dubey and K. Kumar. *Thermochim. Acta*, 524:7, 2011.

[28] H. C. Van Ness. *Industrial & amp; Engineering Chemistry*, 59:33, 1967.

[29] P. Pirilä-Honkanen. *J. Solution Chem.*, 25:555, 1996.

[30] V. Brandani and J. M. Prausnitz. *PNAS*, 79:5103, 1982.

[31] W. Linert. *Highlights In Solute-Solvent Interactions*. Springer Vienna, 2002.

[32] H. G. Harris and J. M. Prausnitz. *AlChE J.*, 14:737–740, 1968.

[33] V. K. Sharma, S. Bhagour, S. Solanki, and A. Rohilla. *Journal of Chemical & amp; Engineering Data*, 58:1939, 2013.

[34] P. R. Naidu and V. R. Krishnan. *J. Phys. Soc. Jpn.*, 20:1554, 1965.

[35] A. V. Anantaraman. *Can. J. Chem.*, 64:46, 1986.

[36] M. Radhamma, K. Siva Kumar, and M. Rao. *Phys. Chem. Liq.*, 42:597, 2004.

[37] S. L. Oswal, M. M. Maisuria, and R. L. Gardas. *J. Mol. Liq.*, 108:199, 2003.

[38] Berg, W. Rolf, Hansen, Susanne Brunsgaard, Shapiro, A. Alexander, Stenby, and H. Erling. *Appl. Spectrosc.*, 61:367, 2007.

[39] S. Trivedi and S. Pandey. *J. Phys. Chem. B*, 115:7405, 2011.

[40] Ana M. Navarro, B. García, S. Ibeas, F. J. Hoyuelos, I. A. Peñacoba, and J. M. Leal. *J. Phys. Chem. B*, 117:11765, 2013.

[41] G. C. A. M. Mooij, S. W. De Leeuw, B. Smit, and C. P. Williams. *J. Chem. Phys.*, 97, 1992.

[42] H. Liu, K. L. Sale, B. A. Simmons, and S. Singh. *J. Phys. Chem. B*, 115:10251, 2011.

[43] A. Yoshimori, T. J. F. Day, and G. N. Patey. *J. Chem. Phys.*, 109:3222, 1998.

[44] M. H. Rausch, J. Lehmann, A. Leipertz, and A. P. Froba. *Phys. Chem. Chem. Phys.*, page 9525, 2011.

[45] M. Józefowicz. *Chem. Phys.*, 383:19, 2011.

[46] C. Moon, G. S. Pawley, and J. Crain. *Mol. Phys.*, 99:2037, 2001.

[47] S. Daschakraborty and B. Ranjit. *J. Phys. Chem. B*, 115:4011, 2011.

[48] S. Mandal, S. Ghosh, C. Banerjee, J. Kuchlyan, and N. Sarkar. *J. Phys. Chem. B*, 117:12212, 2013.

[49] M. I. Cabaço, Y. Danten, M. Besnard, Y. Guissani, and B. Guillot. *J. Phys. Chem. B*, 102:10712, 1998.

[50] Y. Marcus. *Solvent Mixtures: Properties and Selective Solvation*. Taylor and Francis, USA, 2002.

[51] Y. Marcus. *Introduction to liquid state chemistry*. Wiley-interscience publication. Wiley, UK, 1977.

[52] Y. Marcus. *The properties of solvents*. Wiley, UK, 1998.

[53] A. Ben-Naim. *J. Phys. Chem.*, 82:792, 1978.

[54] A. BenNaim and Y. Marcus. *J. Chem. Phys.*, 81:2016, 1984.

[55] A. Ben-Naim. *J. Solution Chem.*, 30:475, 2001.

[56] A. Ben-Naim. *Solvation Thermodynamics*. Springer, New York, 1987.

[57] B. Bagchi. *Molecular Relaxation in Liquids*. Oxford University Press, USA, 2012.

[58] B. Mennucci and R. Cammi. *Continuum Solvation Models in Chemical Physics: From Theory to Applications*. Wiley, UK, 2008.

[59] F. Hirata. *Molecular Theory of Solvation*. Springer, USA, 2003.

[60] O. Tapia and J. Bertrán. *Solvent Effects and Chemical Reactivity*. Springer, USA, 2003.

[61] C. Reichardt and T. Welton. *Solvents and Solvent Effects in Organic Chemistry*. Wiley, Germany, 2011.

[62] C. J. Cramer and D. G. Truhlar. *Acc. Chem. Res.*, 41:760, 2008.

[63] J. Li, T. Zhu, C. J. Cramer, and D. G. Truhlar. *J. Phys. Chem. A*, 104:2178, 2000.

[64] A. Papazyan and A. Warshel. *J. Phys. Chem. B*, 102:5348, 1998.

[65] W. L. Jorgensen. *Chemtracts-Organic Chemistry*, 4:91, 1991.

[66] J. M. Martínez, R. R. Pappalardo, and E. S. Marcos. *J. Phys. Chem. A*, 101:4444, 1997.

[67] F. J. Luque and M. Orozco. *J. Phys. Chem. B*, 101:5573, 1997.

[68] G. P. Das and D. S. Dudis. *J. Phys. Chem. A*, 104:4767, 2000.

[69] S. M. Bachrach. *Computational Organic Chemistry*. Wiley, 2007.

[70] N. Mataga and T. Kubota. *Molecular interactions and electronic spectra*. M. Dekker, New York, 1970.

[71] S. E. Sheppard. *Rev. Mod. Phys.*, 14:303, 1942.

[72] Noel S. Bayliss. *J. Chem. Phys.*, 18, 1950.

[73] N. S. Bayliss and E. G. McRae. *J. Chem. Phys.*, 58:1002, 1954.

[74] E. G. McRae. *J. Phys. Chem.*, 61:562, 1957.

[75] N. Mataga, Y. Kaifu, and M. Koizumi. *Bull. Chem. Soc. Jpn.*, 28:690, 1955.

[76] N. Mataga, Y. Kaifu, and M. Koizumi. *Bull. Chem. Soc. Jpn.*, 29:465, 1956.

[77] W. W. Robertson, A. D. King, and O. E. Weigang. *J. Chem. Phys.*, 35:464, 1961.

[78] E. Lippert. *Z. Naturforsch*, 10a:541, 1955.

[79] T. Kubota and M. Yamakawa. *Bull. Chem. Soc. Jpn.*, 35:555, 1962.

[80] P. W. Atkins and J. De Paula. *Atkins' Physical Chemistry*. Number vol. 1. Oxford University Press, 2002.

[81] E. B. Smith. *Basic Chemical Thermodynamics*. Imperial College Press, Singapore, 2004.

[82] I. M. Klotz and R. M. Rosenberg. *Chemical Thermodynamics: Basic Concepts and Methods*. Wiley, New Jersey, 2008.

[83] D. A. McQuarrie and J. D. Simon. *Molecular Thermodynamics*. University Science Books, USA, 1999.

[84] G. F. Liptrot, J. J. Thompson, and G. R. Walker. *Modern Physical Chemistry*. CollinsEducational, 1982.

[85] J. A. V. Butler. *J. Am. Chem. Soc.*, 47:117, 1925.

[86] G. N. Lewis. *J. Am. Chem. Soc.*, 28:766, 1906.

[87] H. H. Gilmann and P. Gross. *J. Am. Chem. Soc.*, 60:1525, 1938.

[88] W. D. Bancroft and H. L. Davis. *J. Phys. Chem.*, 33:361, 1928.

[89] S. E. Wood. *J. Am. Chem. Soc.*, 59:1510, 1937.

[90] G. Calingaert and L. B. Hitchcock. *J. Am. Chem. Soc.*, 49:750, 1927.

[91] M. H. Abraham, P. L. Grellier, J. L. M. Abboud, R. M. Doherty, and R. W. Taft. *Can. J. Chem.*, 66:2673, 1988.

[92] N. B. Chapman and J. Shorter. *Advances in linear free energy relationships*. Plenum Press, New York, 1972.

[93] R. M. C. Goncalves, Ana M. N. Simoes, and L. M. P. C. Albuquerque. *J. Chem. Soc., Perkin Trans. 2*, page 1379, 1990.

[94] K. Medda, P. Chatterjee, A. K. Chandra, and S. Bagchi. *J. Chem. Soc., Perkin Trans. 2*, page 343, 1992.

[95] A. Maitra and S. Bagchi. *J. Mol. Liq.*, 137:131, 2008.

[96] P. P. Singh, B. R. Sharma, and K. S. Sidhu. *Can. J. Chem.*, 57:387, 1979.

[97] M. Tkadlecova, V. Dohnal, and M. Costas. *Phys. Chem. Chem. Phys.*, 1:1479, 1999.

[98] Anna M. Crabtree and J. F. O'Brien. *Journal of Chemical & amp; Engineering Data*, 36:140, 1991.

[99] M. Rezaei-Sameti, H. Iloukhani, and M. Rakhshi. *Russ. J. Phys. Chem. A*, 84:2023–2032, 2010.

[100] A. V. Orchilles, P. J. Miguel, E. Vercher, and A. Martinez-Andreu. *Journal of Chemical & amp; Engineering Data*, 55:1209, 2010.

[101] M. C. R. Symons and V. K. Thomas. *J. Chem. Soc., Faraday Trans. 1*, 77:1883, 1981.

[102] Izhack Oref. *J. Chem. Soc., Faraday Trans. 1*, 82:1289, 1986.

[103] M. A. Wendt, Meiler, J., F. Weinhold, and T. C. Farrar. *Mol. Phys.*, 93:145, 1998.

[104] R. Buchner and J. Barthel. *J. Mol. Liq.*, 52:131, 1992.

[105] N. E. Levinger, P. H. Davis, and M. D. Fayer. *J. Chem. Phys.*, 115:9352, 2001.

[106] K. J. Gaffney, P. H. Davis, I. R. Piletic, N. E. Levinger, and M. D. Fayer. *J. Phys. Chem. A*, 106:12012, 2002.

[107] I. R. Piletic, K. J. Gaffney, and M. D. Fayer. *J. Chem. Phys.*, 119:423, 2003.

[108] A.S.R. Koti and N. Periasamy. *J. Fluoresc.*, 10:177, 2000.

[109] J. Harnes, M. Abu-samha, H. Bergersen, M. Winkler, A. Lindblad, L. J. Saethre, O. Bjorneholm, and K. J. Borve. *New J. Chem.*, 35:2564, 2011.

[110] I. Bhattacharyya, P. Kumar, and D. Goswami. *J. Phys. Chem. B*, 115:262, 2011.

[111] R. Gratias and H. Kessler. *J. Phys. Chem. B*, 102:2027, 1998.

[112] K. Bloch and C. P. Lawrence. *J. Phys. Chem. B*, 114:293, 2010.

[113] A. D. Vladimir, G. T. Oleg, and Yu. S. Ignat. *J. Mol. Liq.*, 121:127, 2005.

[114] P.G. Ashmore, T.M. Sugden, and F.S. Dainton. *Photochemistry and Reaction Kinetics*. Cambridge University Press, Cambridge, 2010.

[115] R. G. W. Norrish and G. Porter. *Nature*, 164:658–658, 1949.

[116] G. Porter. *Proc. Roy. Soc. (London) Ser. A*, 200:254, 1950.

[117] G. Porter. *Discussions Faraday Soc.*, 9:60, 1950.

[118] T. E. Meyer, M. Rivera, F. A. Walker, M. R. Mauk, A. G. Mauk, M. A. Cusanovich, and G. Tollin. *Biochemistry*, 32:622, 1993.

[119] A. K. Bhattacharyya, T. E. Meyer, M. A. Cusanovich, and G. Tollin. *Biochemistry*, 26:758, 1987.

[120] M. C. Walker and G. Tollin. *Biochemistry*, 30:5546, 1991.

[121] B. Alpert, R. Banerjee, and L. Lindqvist. *Proc Natl Acad Sci.*, 71:558, 1974.

[122] D. V. O'Connor and D. Phillips. *Time-Correlated Single Photon Counting*. Academic Press, New York, 1984.

[123] W. Becker. *Advanced Time-Correlated Single Photon Counting Techniques*. Springer, 2005.

[124] N. V. Tkachenko. *Optical Spectroscopy: Methods and Instrumentations*. Elsevier Science, 2006.

[125] J. R. Lakowicz. *Principles of Fluorescence Spectroscopy*. Springer, 2007.

[126] G. R. Fleming. *Chemical Applications of Ultrafast Spectroscopy*. Oxford University Press, New York, 1986.

[127] P. R. Bevington and D. K. Robinson. *Data Reduction and Error Analysis for the Physical Sciences*. McGraw-Hill Higher Education. McGraw-Hill, 2003.

[128] A. Douhal and J. Santamaria. *Femtochemistry and Femtobiology: Ultrafast Dynamics in Molecular Science*. World Scientific, 2002.

[129] A. H. Zewail. *Femtochemistry: Ultrafast Dynamics of the Chemical Bond*. World Scientific, 1994.

[130] E. Schreiber. *Femtosecond Real-Time Spectroscopy of Small Molecules and Clusters*. Springer, UK, 2014.

[131] A. H. Zewail. *J. Phys. Chem.*, 104:5693; and reference therein, 2000.

[132] J. Manz and L. Wöste. *Femtosecond Chemistry*. Number v. 1. Wiley, 1995.

[133] T. Arlt, S. Schmidt, W. Kaiser, M. Lauterwasser, C.; Meyer, H. Scheer, and W. Zinth. *Proc. Natl. Acad. Sci.*, 90:794, 1993.

[134] J. T. M. Kennis, A. Y. Shkuropatov, I. H. M. Van Stokkum, P. Gast, A. J. Hoff, V. A. Shuvalov, and T. J. Aartsma. *Biochemistry*, 36:16231, 1997.

[135] S. Mukamel. *Principles of Nonlinear Optical Spectroscopy*. Oxford University Press, New York, 1999.

[136] R. Berera, R. V. Grondelle, and J. T. M. Kennis. *Photosynth. Res.*, 101:105, 2009.

[137] M. Lorenc, M. Ziolek, R. Naskrecki, J. Karolczak, J. Kubicki, and A. Maciejewski. *Appl. Phys. B*, 74:13, 2002.

[138] S. Gupta, S. Rafiq, M. Kundu, and P. Sen. *J. Phys. Chem. B*, 116:1345, 2012.

[139] M. Roses, C. Rafols, J. Ortega, and E. Bosch. *J. Chem. Soc. Perkin Trans. 2*, page 1607, 1995.

[140] R. Skwierczynski and K. Connors. *J. Chem. Soc. Perkin Trans. 2*, page 467, 1994.

[141] E. Bosch, M. Roses, K. Herodes, I. Leito, I. Koppel, and V. Taal. *J. Phys. Org. Chem.*, 9:403, 1996.

[142] J. Ortega, C. Rafols, E. Bosch, and M. Roses. *J. Chem. Soc. Perkin Trans. 2*, page 1497, 1996.

[143] K. Bhattacharayya. *Chem. Com.*, 25:2848, 2008.

[144] S. Basu, D. R. Vutukuri, and S. Thaymanavan. *J. Am. Chem. Soc.*, 127:16794, 2005.

[145] G. M. Sando, K. Dahl, and J. C. Owrutsky. *J. Phys. Chem. B*, 111:4901, 2007.

[146] M. Shannigrahi, R. Pramanik, and S. Bagchi. *Spectrochim. Acta A Mol. Biomol. Spectrosc.*, 59:2921, 2003.

[147] S. Dixit, J. Crain, W. C. K. Poon, J. L. Finney, and A. K. Soper. *Nature*, 416:829, 2002.

[148] H. A. R. Gazi and R. Biswas. *J. Phys. Chem. A*, 115:2445, 2011.

[149] J. Catalan, C. Diaz, and F. Garcia-Blanco. *J. Org. Chem.*, 65:9226, 2000.

[150] S. Mukherjee, K. Sahu, D. Roy, S. K. Mondal, and K. Bhattacharyya. *Chem. Phy. Lett.*, 128:133, 2004.

[151] D. Banerjee, A. K. Laha, and S. J. Bagchi. *Photochem. Photobiol. A: Chem.*, 85:153, 1995.

[152] N. Ray and S. Bagchi. *J. Phys. Chem. A*, 109:142, 2005.

[153] A. Maitra and S. Bagchi. *J. Phys. Chem. B*, 112:2056, 2008.

[154] V. Ramakrishnan, A. Sarua, M. Kuball, and A. F. Abdullah. *J. Raman Spectrosc.*, 40:921, 2009.

[155] P. L. Silva, E. L. Bastos, and A. E. Secoud. *J. Phys. Chem. B*, 111:6173, 2007.

[156] M. Roses, C. Rafols, J. Ortega, and E. Bosch. *J. Chem. Soc. Perkin Trans. 2*, page 1607, 1995.

[157] R. Skwierczynski and K. Connors. *J. Chem. Soc. Perkin Trans. 2*, page 467, 1994.

[158] E. Bosch, M. Roses, K. Herodes, I. Leito, and V. Taal. *J. Phys. Org. Chem.*, 9:403, 1996.

[159] J. Ortega, C. Rafols, E. Bosch, and M. Roses. *J. Chem. Soc. Perkin Trans. 2*, page 1497, 1996.

[160] A. Maitra and S. Bagchi. *J. Mol. Liq.*, 137:131, 2008.

[161] B.R. Gayathri, J. R. Mannekutla, and S. R. Inamdar. *J. mol. Struc.*, 889:383, 2008.

[162] H. Salari, M. Khodadabi-Moghaddam, A. R. Hariffi-Mood, and M. R. Gholami. *J. Phys. Chem. B*, 114:9586, 2010.

[163] A. K. Laha, P. K. Das, and S. Bagchi. *J. Phys. Chem. A*, 106:3230, 2002.

[164] M. J. Kamlet and R.W. Taft. *J. Am. Chem. Soc.*, 98:377, 1976.

[165] M. J. Kamlet, J. L. M. Abboud, M. H. Abraham, and R. W. Taft. *J. Org. Chem.*, 48:2877, 1983.

[166] P. M. E. Mancini, A. Terenzani, C. Adam, and L. R. Vottero. *J. Phys. Org. Chem.*, 12:430, 1999.

[167] Y. Marcus. *J. Chem. Soc. Perkin Trans. 2*, page 1015, 1994.

[168] T. Bevilaqua, T. F. Goncalves, C. G. Venturini, and V. G. Machado. *Spectrochim. Acta A: Mol. Biomol. Spectrosc.*, 65:535, 2006.

[169] P. M. E. Mancini, A. Terenzani, C. Adam, A. C. Perez, and L. R. Vottero. *J. Phys. Org. Chem.*, 12:207, 1999.

[170] P. M. E. Mancini, A. Terenzani, C. Adam, and L. R. Vottero. *J. Phys. Org. Chem.*, 10:849, 1997.

[171] A. C. Perez and P. M. E. Mancini. *J. Phys. Org. Chem.*, 22:197, 2005.

[172] Christian Reichardt. *Solute-Solvent Interactions; Edited by J. F. Coetzee and C. D. Ritchie*, volume 9. Hüthig & Wepf Verlag, 1970.

[173] V. Dohnal and M. Tkadlecova. *J. Phys. Chem. B*, 106:12307, 2002.

[174] J. Klingenfus and P. Palmas. *Phys. Chem. Chem. Phys.*, 13:10661, 2011.

[175] M. Tkadlecova, J. Havlicek, and V. Dohnal. *Can. J. Chem.*, 73:1406, 1995.

[176] M. Tkadlecova, V. Dohnal, and M. Costas. *Phys. Chem. Chem. Phys.*, 1:1479, 1999.

[177] S. S. Yadava and N. Yadav. *Can. J. Chem. Eng.*, 89:576, 2011.

[178] M. Iglesias, B. Orge, and J. Tojo. *J. Chem. Eng. Data*, 41:218, 1996.

[179] P. P. Singh, B. R. Sharma, and K. S. Sidhu. *Can. J. Chem.*, 57:387, 1979.

[180] M. Bauer, A. Rollberg, A. Barth, and S. Spange. *Eur. J. Org. Chem.*, page 4475, 2008.

[181] P. M. E. Mancini, A. Terenzani, C. Adam, A. C. Perez, and L. R. Vottero. *J. Phys. Org. Chem.*, 12:713, 1999.

[182] D. Seth, S. Sarkar, R. Pramanik, C. Ghatak, P. Setua, and N. Sarkar. *J. Phys. Chem. B*, 113:6826, 2009.

[183] J. G. Dawber and S. Etemad. *J. Chem. Soc. Faraday Trans.*, 86:3725, 1990.

[184] S. Banerjee, S. Roy, and B. Bagchi. *J. Phys. Chem. B*, 114:12875, 2010.

[185] N. R. Dhumal. *Spectrochim. Aceta A*, 79:654, 2011.

[186] S. Y. Bae and B. R. Arnold. *J. Phys. Org. Chem.*, 17:187, 2004.

[187] R. Gratias and H. Kessler. *J. Phys. Chem. B*, 102:2027, 1998.

[188] V. A. Durov, O. G. Tereshin, and I. Y. Shilov. *J. Mol. Liquids.*, 121:127, 2005.

[189] S. Prabhakar and H. Z. weingartner. *Phys. Chem. Neue. Folge.*, 137:1, 1983.

[190] I. Bhattacharyya, P. Kumar, and D. Goswami. *J. Phys. Chem. B*, 115:262, 2011.

[191] C. Reichardt. *Chem. Rev.*, 94:2319, 1994.

[192] C. Reichardt. *Chem. Soc. Rev.*, 21:147, 1992.

[193] V. Kuznetsova, P. Morozova, Bazyl O. K., and B. V. Korolev. *Rus. Phys. J.*, 43:608, 2000.

[194] J. Y. Choi, E. J. Park, S. H. Chang, and T. J. Kang. *Bull. Korean Chem. Soc.*, 30:1452, 2009.

[195] M. Meyer and J. C. Mialocq. *Opt. Commun.*, 64:264, 1987.

[196] M. Sajadi, T. Obernhuber, S. A. Kovalenko, M. Mosquera, B. Dick, and N. P. Ernsting. *J. Phys. Chem. A*, 113:44, 2009.

[197] S. Glasstone and D. Lewis. *Textbook of Physical Chemistry*. McMillan, 1976.

[198] C. F. Jumper, M. T. Emerson, and B. B. Howard. *J. Chem. Phys.*, 35:1911, 1961.

[199] J. R. Lakowicz. *Principles of Fluorescence Spectroscopy*. Springer, Singapore, 2007.

[200] S. S. Shinde, B. S. Lee, and D. Y. Chi. *Org. Lett.*, 10:733, 2008.

[201] A. Kumar and S. S. Pawar. *J. Org. Chem.*, 72:8111, 2007.

[202] N. D. Khupse and A. Kumar. *J. Phys. Chem . A*, 115:10211, 2011.

[203] J. B. Hyne. *J. Am. Chem. Soc.*, 82:5129, 1960.

[204] K. Kwak, S. Park, and M. D. Fayer. *PNAS*, 104:14221, 2007.

[205] B. Wang, B. Han, T. Jiang, Z. Zhang, Y. Xie, W. Li, and W. Wu. *J. Phys. Chem. B*, 109:24203, 2005.

[206] T. Rispens and J. B. F. N. Engberts. *J. Phys. Org. Chem.*, 18:908, 2005.

[207] M. L. Damstrup, J. Abildskov, S. Kill, A. D. Jensen, F. V. Sparso, and X. Xu. *J. Agric. Food Chem.*, 54:7113, 2006.

[208] K. H. Tan and R. Lavrien. *J. Bio. Chem.*, 247:3278, 1972.

[209] I. Faidovich. *J. Bio. Chem.*, 241:3624, 1966.

[210] N. E. Levinger, P. H. Davis, and M. D. Fayer. *J. Chem. Phys.*, 115:9352, 2001.

[211] I. R. Piletic, K. J. Gaffney, and M. D. Fayer. *J. Chem. Phys.*, 119:423, 2003.

[212] K. J. Gaffney, P. H. Davis, I. R. Piletic, N. E. Levinger, and M. D. Fayer. *J. Phys. Chem. A*, 106:12012, 2002.

[213] X. X. Zhang, M. Liang, J. Hunger, R. Buchner, and M. Maroncelli. *J. Phys. Chem. B*, 117:15356, 2013.

[214] J. Hunger, T. Sonnleitner, L. Liu, R. Buchner, M. Bonn, and H. J. Bakker. *J. Phys. Chem. Lett.*, 3:3034, 2012.

[215] D. Roy and M. Maroncelli. *J. Phys. Chem. B*, 116:5951, 2012.

[216] S. Chattoraj, R. Chowdhury, S. Ghosh, and K. Bhattacharya. *J. Chem. Phys.*, 138:214507, 2013.

[217] S. Mukherjee, K. Sahu, D. Roy, S. K. Mondal, and K. Bhattacharyya. *Chem. Phys. Lett.*, 384:128, 2004.

[218] T. Molotsky and D. Huppert. *J. Phys. Chem. A*, 107:8449, 2003.

[219] N. Agmon. *J. Phys. Chem. A*, 106:7256, 2002.

[220] A. Paul and A. Samanta. *J. Phys. Chem. B*, 112:947, 2008.

[221] D. Chandler. *J. Chem. Phys.*, 68:2959, 1978.

[222] R. F. Grote and J. T. Hynes. *J. Chem. Phys.*, 73:2715, 1980.

[223] H. Frauenfelder and P. G. Wolynes.

[224] B. Bagchi and G. R. Fleming. *J. Phys. Chem.*, 94:9, 1990.

[225] G. A. Voth and R. M. Hochstrasser. *J. Phys. Chem.*, 100:13034, 1996.

[226] M. Karplus. *J. Phys. Chem. B*, 104:11, 2000.

[227] P. Schuster, G. Zundel, and C. Sandorfy. *The Hydrogen Bond. Recent Developments in Theory and Experiments*. North-Holland: Amsterdam, 1976.

[228] O. Herni-Rousseau and P. Blaise. *Adv. Chem. Phys.*, 103:1, 1998.

[229] W. Jarzeba, G. C. Walker, A. E. Johnson, and P. F. Barbara. *Chem. Phys.*, 152:57, 1991.

[230] J. K. Gardecki and M. Maroncelli. *Chem. Phys. Letts.*, 301:571, 1999.

[231] F. Cichos, A. Willert, U. Rempel, and C. V. Borczyskowski. *J. Phys. Chem. A*, 101:8179, 1997.

[232] K. Sahu, S. K. Mondal, D. Roy, R. Karmakar, and K. Bhattacharyya. *J. Photochem. Photobio. A*, 172:180, 2005.

[233] A. Bagno, G. Scorrano, and S. Stiz. *J. Am. Chem. Soc.*, 119:2299, 1997.

[234] A. Bagno, M. Campulla, M. Pirana, G. Scorrano, and S. Stiz. *Chem. Eur. J.*, 5:1291, 1999.

[235] R. Gratias and H. Kessler. *J. Phys. Chem. B*, 102:2027, 1998.

[236] V. A. Durov, O. G. Tereshin, and I. Y. Shilov. *J. Mol. Liquids.*, 121:127, 2005.

[237] B. Bagchi. *Annu. Rev. Phys. Chem.*, 40:115, 1989.

[238] J. Rodriguez, M. D. Elola, and D. Laria. *J. Phys. Chem. B*, 113:12744, 2009.

[239] J. J. Paghaleh, A. R. Harifi-Mood, and M. R. Gholami. *J. Phys. Org. Chem.*, 24:1095, 2011.

[240] Y. Marcus. *J. Phys. Org. Chem.*, 25:1072, 2012.

[241] H. Salari, M. Khodadabi-Moghaddam, A. R. Hariffi-Mood, and M. R. Gholami. *J. Phys. Chem. B*, 114:9586, 2010.

[242] Y. Marcus. *J. Mol. Liq.*, 158:23, 2011.

[243] A. Sarkar, S. Trivedi, G. A. Baker, and S. Pandey. *J. Phys. Chem. B*, 112:14927, 2008.

[244] S. Trivedi, S. Pandey, S. N. Baker, G. A. Baker, and S. Pandey. *J. Phys. Chem. B*, 116:1360, 2012.

[245] C. Reichardt. *Chem. Rev.*, 94:2319, 1994.

[246] C. Reichardt. *Chem. Soc. Rev.*, 21:147, 1992.

[247] A. K. Laha, P. K. Das, and S. Bagchi. *J. Phys. Chem. A*, 106:3230, 2002.

[248] A. Maitra and S. Bagchi. *J. Phys. Chem. B*, 112:9847, 2008.

[249] M. Meyer and J. C. Mialocq. *Opt. Commun.*, 64:264, 1987.

[250] M. Glasbeek and H. Zhang. *Chem. Rev.*, 104:1929, 2004.

[251] P. Meulen, H. Zhang, A. M. Jonkman, and M. Glasbeek. *J. Phys. Chem.*, 100:5367, 1996.

[252] T. Gustavsson, G. Baldacchino, J. C. Mialocq, and S. A Pommeret. *Chem. Phys. Letts.*, 236:587, 1995.

[253] M. L. Horng, J. A. Gardecki, A. Papazyan, and M. Maroncelli. *J. Phys. Chem.*, 99:17311, 1995.

[254] W. Lu, J. Kim, W. Qiu, and D. Zhong. *Chem. Phys. Letts.*, 388:120, 2004.

[255] M. Sajadi, M. Weinberger, H. A. Wagenknecht, and N. P. Ernsting. *Phys. Chem. Chem. Phys.*, 13:17768, 2011.

[256] A. Adhikari, K. Sahu, S. Dey, S. Ghosh, U. Mandal, and K. Bhattacharyya. *J. Phys. Chem. B*, 111:12809, 2007.

[257] M. Maroncelli and G. R. Fleming. *J. Chem. Phys.*, 86:6221, 1987.

[258] R. S. Fee and M. Maroncelli. *Chem. Phys.*, 183:235, 1994.

[259] R. A. Marcus. *J. Chem. Phys.*, 24:966, 1956.

[260] R. A. Marcus. *Biochimica et Biophysica Acta*, 811:265, 1985.

[261] Miller J.R., L.T. Calcaterra, and G.L. Closs. *J. Am. Chem. Soc.*, 106:3047, 1984.

[262] G. L. Closs and J. R. Miller. *Science*, 240:440, 1988.

[263] R. A. Marcus. *J. Phys. Chem.*, 93:3078, 1989.

[264] T. B. Truong. *J. Phys. Chem.*, 88:3906, 1984.

[265] P. Sun, F. Li, Y. Chen, M. Zhang, Z. Zhang, Z. Gao, and Y. Shao. *J. Am. Chem. Soc.*, 125:9600, 2003.

[266] M. Kumbhakar, S. Nath, T. Mukherjee, and H. Pal. *J. Chem. Phys.*, 122:84512, 2005.

[267] S. Ghosh, S. K. Mondal, K. Sahu, and K. Bhattacharyya. *J. Phys. Chem. A*, 110:13139, 2006.

[268] S. Sarkar, R. Pramanik, D. Seth, P. Setua, and N. Sarkar. *Chem. Phys. Lett.*, 477:102, 2009.

[269] S. Sarkar, S. Mandal, C. Ghatak, V. G. Rao, S. Ghosh, and N. Sarkar. *J. Phys. Chem. B*, 116:1335, 2012.

[270] A. Chakraborty, D. Seth, D. Chakrabarty, P. Hazra, and N. Sarkar. *Chem. Phys. Lett.*, 405:10, 2005.

[271] A. K. Das, T. Mondal, S. S. Mojumdar, and K. Bhattacharyya. *J. Phys. Chem. B*, 115:4680, 2011.

[272] M. Kumbhakar, S. Dey, P. K. Singh, S. Nath, A. K. Satpati, R. Ganguly, . V. K. Aswal, and H. Pal. *J. Phys. Chem. B*, 115:1638, 2011.

[273] U. Mandal, S. Ghosh, S. Dey, A. Adhikari, and K. Bhattacharyya. *J. Chem. Phys.*, 128:164505, 2008.

[274] S. D. Choudhury, M. Kumbhakar, S. Nath, and H. Pal. *J. Chem. Phys.*, 127:194901, 2007.

[275] A. K. Satpati, M. Kumbhakar, S. Nath, and H. Pal. *J. Phys. Chem. B*, 111:7550, 2007.

[276] S. Nad and H. Pal. *J. Phys. Chem. A*, 104:673, 2000.

[277] C. Turro, J. M. Zaleski, Y. M. Karabatsos, and D. G. Nocera. *J. Am. Chem. Soc.*, 118:6060, 1996.

[278] M. A. Smitha, E. Prasad, and K. P. Gopidas. *J. Am. Chem. Soc.*, 123:1159, 2001.

[279] G. G. Fortunato, P. M. Mancini, M. V. Bravo, and C. G. Adam. *J. Phys. Chem. B*, 114:11804, 2010.

[280] S. N. Timasheff. *PNAS , ,*, 99:9721, 2002.

[281] F. Spinozzi, M. G. Ortore, R. Sinibaldi, P. Mariani, A. Esposito, S. Cinelli, and G. Onori. *J. Chem. Phys.*, 129:35101, 2008.

[282] P. Wang, J. Gong, B. Wang, and J. Zhang, M.and Wang. *J. Chem. Eng. Data*, 54:162, 2009.

[283] A. J. Gharamaleki, M. B. Jalali, and W. E. Acree Jr. *Inter. J. Pharma.*, 166:205, 1998.

[284] S. Dixit, J. Crain, W. C. K. Poon, J. L. Finney, and A. K. Soper. *Nature*, 416:829, 2002.

[285] J. J. Paghaleh, A. R. Harifi-Mood, and M. R. Gholami. *J. Phys. Org. Chem.*, 24:1065, 2011.

[286] J. Catalan, C. Diaz, and F. Garcia-Blanco. *J. Org. Chem.*, 65:9226, 2000.

[287] S. Mukherjee, K. Sahu, D. Roy, S. K. Mondal, and K. Bhattacharyya. *Chem. Phys. Lett.*, 384:128, 2004.

[288] D. Banerjee, A. K. Laha, and S. Bagchi. *J. Photochem. Photobiol. A: Chem.*, 85:153, 1995.

[289] N. Ray and S. Bagchi. *J. Phys. Chem. A*, 109:142, 2005.

[290] S. Trivedi, S. Pandey, S. N. Baker, G. A. Baker, and S. Pandey. *J. Phys. Chem. B*, 116:1360, 2012.

[291] Y. Marcus. *J. Phys. Org. Chem.*, 25:1072, 2012.

[292] H. Salari, M. Khodadabi-Moghaddam, A. R. Hariffi-Mood, and M. R. Gholami. *J. Phys. Chem. B*, 114:9586, 2010.

[293] P. L. Silva, E. L. Bastos, and O. A. E. Seoud. *J. Phys. Chem. B*, 111:6173, 2007.

[294] M. Roses, C. Rafols, J. Ortega, and E. Bosch. *J. Chem. Soc. Perkin Trans. 2*, page 1607, 1995.

[295] Y. Marcus. *J. Mol. Liq.*, 158:23, 2011.

[296] B.R. Gayathri, J. R. Mannekutla, and S. R. Inamdar. *J. mol. Struc.*, 889:383, 2008.

[297] P. M. E. Mancini, A. Terenzani, C. Adam, and L. R. Vottero. *J. Phys. Org. Chem.*, 12:430, 1999.

[298] S. Gupta, S. Rafiq, M. Kundu, and P. Sen. *J. Phys. Chem. B*, 116:1345, 2012.

[299] D. Rehm and A. Weller. *Isr. J. Chem.*, 8:259, 1970.

[300] N. J. Turro, V. Ramamurthy, and J. C. Scaiano. *Modern Molecular Photochemistry of Organic Molecules*. University Science Books, Sausalito California, 2010.

[301] J. Parker. *Chem. Rev.*, 69:1, 1969.

[302] R. Radhakrishnan, C. E. Costello, and H. G. Khorana. *J. Am. Chem. Soc.*, 104:3990, 1982.

[303] K. Dernbecher and G. Gauglitz. *J. Chem. Phys.*, 97:3245, 1992.

[304] F. Proutiere, F.and Schoenebeck. *Angew. Chem. Int. Ed.*, 50:8192, 2011.

[305] A. M. Klibanov. *Nature*, 409:241, 2001.

[306] N. J. O'Reilly and E. Magner. *Phys. Chem. Chem. Phys.*, 13:5304, 2011.

[307] F. Terradas, M. T. Henry, P. A. Fitzpatrick, and A. M. Klibanov. *J. Am. Chem. Soc.*, 104:3990, 1993.

[308] F. Gao, D. Boyles, R. Sullivan, R. N. R. Compton, and M. Pagni. *J. Org. Chem.*, 67:9361, 2002.

[309] J. B. Jaquith, J. Guan, S. Wang, and S. Collins. *Organomrtallics*, 14:1081, 1995.

[310] C. Cativiela, J. I. Garcia, J. Gil, R. M. Martinez, J. A. Mayoral, L. Salvatella, J. S. Urieta, A. M. Mainar, and M. H. Abraham. *J. Chem. Soc., Perkin Trans. 2*, 14:653, 1997.

[311] D.J. Adams, P. J. Dyson, and S. J. Tavener. *Chemistry in Alternative Reaction Media*. John Wiley & Sons, Ltd., 2004.

[312] S. A. Hart, C. O. Trindle, and F. A. Etzkorn. *Org. Lett.*, 3:1789, 2001.

[313] Y. Mei, D. J. Averill, and M. J. Allen. *J. Org. Chem.*, 77:5624, 2012.

[314] T. Mori and S. Kato. *J. Phys. Chem. A*, 113:6158, 2009.

[315] B. J. Gertner, R. M. Whitnell, K. R. Wilson, and J. T. Hynes. *J. Am. Chem. Soc.*, 113:74, 1991.

[316] M. H. M. Olsson and A. Warshel. *J. Am. Chem. Soc.*, 126:15167, 2004.

[317] H. Ai Yu and M. Karplus. *J. Am. Chem. Soc.*, 112:5706, 1990.

[318] S. S. Shinde, B. S. Lee, and D. Y. Chi. *Org. Lett.*, 10:733, 2008.

[319] N. D. Khupse and A. Kumar. *J. Phys. Chem.*, 115:10211, 2011.

[320] A. Kumar and S. S. Pawar. *J. Org. Chem.*, 72:8111, 2007.

[321] A. Kumar and S. S. Pawar. *J. Org. Chem.*, 69:1419, 2004.

[322] C. H. Turner, J. K. Brennan, J. K.and Johnson, and K. E. Gubbins. *J. Chem. Phys.*, 116:2138, 2002.

[323] M. D. Halls and H. B. Schlegel. *J. Phys. Chem. B*, 106:1921, 2002.

[324] M. Yoshizawa, Y. Takeyama, T. Okano, and M. Fujita. *J. Am. Chem. Soc.*, 125:3243, 2003.

[325] M. D. Johnson, B. B. Lorenz, P. C. Wilkins, B. G. Lemons, B. Baruah, N. Lamborn, M. Stahla, P. B. Chatterjee, D. T. Richens, and D. C. Crans. *Inorg. Chem.*, 51:2757, 2012.

[326] X. F. Li, M. H. Zong, and G. L. Zhao. *Appl. Microbiol Biotechnol*, 88:57, 2010.

[327] T. Rispens and J. B. F. N. Engberts. *J. Phys. Org. Chem.*, 18:908, 2005.

[328] S. M. Sieburth and K. F. McGee. *Org. Lett.*, 1:1775, 1999.

[329] P. M. E. Mancini, A. Terenzani, C. Adam, and L. R. Vottero. *J. Phys. Org. Chem.*, 12:430, 1999.

[330] M. Zhong, I. Nowak, and M. J. Robins. *J. Org. Chem.*, 71:7773, 2006.

[331] G. Siani, G. Angelini, P. D. Maria, A. Fintana, and M. Pierini. *Org. Biomol. Chem.*, 6:4236, 2008.

[332] E. Iglesias. *New J. Chem.*, 29:625, 2005.

[333] S. Gupta, S. Rafiq, M. Kundu, and P. Sen. *J. Phys. Chem. B*, 116:1345, 2012.

[334] Y. Marcus. *J. Phys. Org. Chem.*, 25:1072, 2012.

[335] Y. Marcus. *J. Mol. Liq.*, 158:23, 2011.

[336] G. G. Fortunato, P. M. Mancini, M. V. Bravo, and C. G. Adam. *J. Phys. Chem. B*, 114:11804, 2010.

[337] X. Song, J. Zhou, Y. Li, and Y. Tang. *J. Photochem. Photobiology. A*, 92:99, 1995.

[338] R. Byrne, K. J. Fraser, E. Izgorodina, D. R. MacFarlane, M. Forsyth, and D. Diamond. *Phys. Chem. Chem. Phys.*, 10:5919, 2008.

[339] V. I. Minkin. *Chem. Rev.*, 104:2751, 2004.

[340] H. Gorner. *Phys. Chem. Chem. Phys.*, 3:416, 2001.

[341] J. N. Moorthy, K. Senapati, K. N. Parida, S. Jhulki, K. Sooraj, and N. N. Nair. *J. Org. Chem.*, 76:9593, 2011.

List of Publications

1 "Origin of Strong Synergism in Weakly Perturbed Binary Solvent System: A Case Study of Primary Alcohols and Chlorinated Methanes"
Shradhey Gupta[1], Shahnawaz Rafiq, Mainak Kundu and Pratik Sen, *J. Phys. Chem. B.* **2012**, *116*, 1346.

2 "Evidence of Intermolecular Hydrogen Bond Network in Methanol-Dichloromethane Synergistic Binary Solvent Mixture"
Shradhey Gupta[2], Arghya Chakraborty and Pratik Sen, Submitted in *J. Chem. Phys.*.

3 "An Unique Solvation Dynamics in MeOH-$CHCl_3$ Solvent Mixture: A case of Synergistic Solvation"
Shradhey Gupta[3], Shahnawaz rafiq and Pratik Sen, Submitted in *J. Phys. Chem.*.

4 "Greener Approach with Mixed Solvent Chemistry through Synergistic Solvation"
Shradhey Gupta[4], Puspal Mukherjee, Sunil Kumar Patel and Pratik Sen, Submitted in *J. Phys. Chem.*.

5 "An Understanding of Intermolecular Interactions in Binary Methanol-Chlorinated Methane mixtures through Dielectric Relaxation, THz, Raman and NIR Spectroscopy"
Shradhey Gupta, Keisuke Tominaga and Pratik Sen, Manuscript under preparation.

6 "Spectroscopic Investigation of ZnO Nanoparticle Size & Shape Controlled by using EtOH-BzOH Binary Solvent Mixture "
Shradhey Gupta, Puspal Mukherjee, Bhaswati Sengupta and Pratik Sen, Manuscript under preparation.

[1]Included in thesis
[2]Included in thesis
[3]Included in thesis
[4]Included in thesis

7 "Ramping of pH across the Water Pool of a Reverse Micelle"
Puspal Mukherjee, **Shradhey Gupta**, Shahnawaz Rafiq, Rajeev Yadav, Jayraj Raval and Pratik Sen, Submitted in *J. Phys. Chem.*.

8 "Highly Selective ppm Level Visual Detection of Fe^{3+} in Aqueous Solution"
Vaisakh Mohan K., Md. Serajul Haque Faizi, **Shradhey Gupta** and Pratik Sen, Submitted in *Sens. Actuators, B*.